

WL-TR-96-4019

DEVELOPMENT OF BALL BEARING DYNAMIC
ANALYSIS METHODS INCLUDING LIFE PREDICTION
METHODS FOR CERAMIC OR METAL BEARINGS



CRAWFORD MEEKS
BRIAN MURPHY
LONG TRAN

AVCON - ADVANCED CONTROLS TECHNOLOGY, INC
5210 LEWIS ROAD
AGOURA HILLS CA 91301

APRIL 1994

INTERIM REPORT FOR MARCH 1992 to APRIL 1994

APPROVED FOR PUBLIC RELEASE; DISTRIBUTION IS UNLIMITED

MATERIALS DIRECTORATE
WRIGHT LABORATORY
AIR FORCE MATERIEL COMMAND
WRIGHT PATTERSON AFB OH 45433-7734


19960620 159


NOTICE


When government drawings, specifications, or other data are used for any purpose other than in connection with a definitely related government procurement operation, the United States Government thereby incurs no responsibility nor any obligation whatsoever; and the fact that the government may have formulated, furnished, or in any way supplied the said drawings, specifications, or other data, is not to be regarded by implication or otherwise as in any manner licensing the holder or any other person or corporation, or conveying any rights or permission to manufacture, use, or sell any patented invention that may in any way be related thereto.

This report is releasable to the National Technical Information Service (NTIS). At NTIS, it will be available to the general public, including foreign nations.

This technical report has been reviewed and is approved for publication.


KARL R. MECKLENBURG, Project Engineer
Nonstructural Materials Branch
Nonmetallic Materials Division


KENT J. EISENTRAUT, Chief
Nonstructural Materials Branch
Nonmetallic Materials Division


CHARLES E. BROWNING, Chief
Nonmetallic Materials Division
Materials Directorate

If your address has changed, if you wish to be removed from our mailing list, or if the addressee is no longer employed by your organization, please notify WL/MLBT, Bldg 654, 2941 P Street, Suite 1, Wright-Patterson AFB OH 45433-7750 to help maintain a current mailing list.

Copies of this report should not be returned unless return is required by security considerations, contractual obligations, or notice on a specific document.

REPORT DOCUMENTATION PAGE

Form Approved
OMB No. 0704-0188

Public reporting burden for this collection of information is estimated to average 1 hour per response, including the time for reviewing instructions, searching existing data sources, gathering and maintaining the data needed, and completing and reviewing the collection of information. Send comments regarding this burden estimate or any other aspect of this collection of information, including suggestions for reducing this burden, to Washington Headquarters Services, Directorate for Information Operations and Reports, 1215 Jefferson Davis Highway, Suite 1204, Arlington, VA 22202-4302, and to the Office of Management and Budget, Paperwork Reduction Project (0704-0188), Washington, DC 20503.

| | | | | | |
|--|--|---|-----------------------------------|---|--|
| 1. AGENCY USE ONLY (Leave blank) | | 2. REPORT DATE APR 1994 | | 3. REPORT TYPE AND DATES COVERED INTERIM 03/01/92--04/01/94 | |
| 4. TITLE AND SUBTITLE DEVELOPMENT OF BALL BEARING DYNAMIC ANALYSIS METHODS INCLUDING LIFE PREDICTION METHODS FOR CERAMIC OR METAL BEARINGS | | | | 5. FUNDING NUMBERS C F33615-92-C-5908 PE 62712 PR 8355 TA 00 WU 04 | |
| 6. AUTHOR(S) CRAWFORD MEEKS BRIAN MURPHY LONG TRAN | | | | | |
| 7. PERFORMING ORGANIZATION NAME(S) AND ADDRESS(ES) AVCON - ADVANCED CONTROLS TECHNOLOGY, INC. 5210 LEWIS ROAD AGOURA HILLS CA 91301 | | | | 8. PERFORMING ORGANIZATION REPORT NUMBER AV9310 | |
| 9. SPONSORING/MONITORING AGENCY NAME(S) AND ADDRESS(ES) MATERIALS DIRECTORATE WRIGHT LABORATORY AIR FORCE MATERIEL COMMAN WRIGHT-PATTERSON AFB OH 45433-7734 | | | | 10. SPONSORING/MONITORING AGENCY REPORT NUMBER WL-TR-96-4019 | |
| 11. SUPPLEMENTARY NOTES | | | | | |
| 12a. DISTRIBUTION/AVAILABILITY STATEMENT APPROVED FOR PUBLIC RELEASE: DISTRIBUTION IS UNLIMITED. | | | | 12b. DISTRIBUTION CODE | |
| 13. ABSTRACT (Maximum 200 words) An analytical ball bearing dynamics model was developed that rigorously models all of the significant kinematics, structural and dynamic effects. The model can analyze bearings of any material combination for the races, ball and ball cage. This model analyzes the stresses and deflections of the loaded elements due to (1) preload, (2) external axial, radial and moment loads, (3) centrifugal and gyroscopic ball loads. A rigorous six-degree-of-freedom model of ball cage motions was developed to analyze ball and cage dynamics. The ball cage equations of motion were written in a rotating coordinate system, which greatly simplifies the equations, resulting in a highly efficient, but rigorous, model of bearing dynamics. A computer program was developed, incorporating the above model and algorithms to solve the multiple simultaneous quasi-static ball-to-race load equations using modified Newton-Raphson methods. The Lawrence Livermore Ode numerical integration package (LSODA) is also employed for integration of the dynamic equations of motion. This method assures convergence, while controlling the accuracy of the calculations as a function of computer run time and automatically selects the appropriate integration method of stiff and non-stiff of collision contact conditions. The program analyzes ball and cage motions in time domains and predicts wear life, fatigue life, lubricant film effects, ball-to-cage forces, torque noise and many other bearing parameters. | | | | | |
| 14. SUBJECT TERMS BALL BEARING DYNAMIC ANALYSIS PROGRAM CAGE DYNAMICS, LIFE PREDICTION WEAR PREDICTION | | | | 15. NUMBER OF PAGES 172 | |
| | | | | 16. PRICE CODE | |
| 17. SECURITY CLASSIFICATION OF REPORT UNCLASSIFIED | 18. SECURITY CLASSIFICATION OF THIS PAGE UNCLASSIFIED | 19. SECURITY CLASSIFICATION OF ABSTRACT UNCLASSIFIED | 20. LIMITATION OF ABSTRACT SAR | | |

TABLE OF CONTENTS

| | Page |
|--|------|
| 1. INTRODUCTION AND SUMMARY----- | 1 |
| 2. INTRODUCTION - BASDREL COMPUTER PROGRAM----- | 4 |
| 2.1 BACKGROUND----- | 4 |
| 2.2 SCOPE----- | 6 |
| 3. PROGRAM OPERATION----- | 6 |
| 3.1 Computer Hardware/Operating System----- | 6 |
| 3.2 Backing Up Your Program Disk----- | 7 |
| 3.3 Installing BASDREL on Your Hard Disk----- | 7 |
| 3.4 Starting The Program----- | 8 |
| 3.5 Input Field Selection and Navigation----- | 8 |
| 3.5.1 Text Field----- | 9 |
| 3.5.2 List Field----- | 9 |
| 3.6 Pull Down Menu System----- | 9 |
| 3.6.1 FILE Menu----- | 9 |
| 3.6.2 EDIT Menu----- | 11 |
| 3.6.3 VIEW Menu----- | 11 |
| 3.6.4 RUN Menu----- | 14 |
| 3.7 Parameter Input Dialog Boxes----- | 15 |
| 3.7.1 EDIT/DESIGN DATA Dialog Box----- | 16 |
| 3.7.2 EDIT/DESIGN PARAMETER Dialog Box----- | 20 |
| 3.7.3 EDIT/SHRINKAGE Dialog Box----- | 22 |
| 4. ANALYTICAL MODEL----- | 34 |
| 4.1 Load vs Deflection of Concentrated Contacts----- | 34 |
| 4.2 Normal Approach----- | 36 |
| 4.3 Working Contact Angle----- | 36 |
| 4.4 Ball Load Distribution and Working Contact Angle under Combined Loading Conditions----- | 37 |
| 4.5 Fatigue Life/Reliability----- | 37 |
| 4.5.1 Material Factor, A2----- | 40 |
| 4.5.2 Lubrication Factor, A3, and EHD Film Thickness----- | 40 |
| 4.6 Friction Torque----- | 43 |
| 4.6.1 Background----- | 43 |
| 4.6.2 Friction Torque----- | 44 |
| 4.7 Failure Modes of Ceramic Bearings----- | 55 |
| 5. SAMPLE PROBLEM----- | 56 |
| 5.1 OUTPUT FILE FOR SAMPLE PROBLEM----- | 57 |
| 6. REFERENCES - BASDREL PROGRAM----- | 64 |
| 7. INTRODUCTION - BABERDYN COMPUTER PROGRAM----- | 66 |
| 7.1 BACKGROUND----- | 66 |
| 7.2 GENERAL INFORMATION----- | 67 |
| 7.3 REASONS FOR DEVELOPMENT OF BABERDYN----- | 69 |
| 8. PROGRAM OPERATION----- | 71 |
| 8.1 Computer Hardware/Operating System----- | 72 |
| 8.2 Backing Up Your Program Disk----- | 72 |
| 8.3 Installing BABERDYN on Your Hard Disk----- | 72 |
| 8.4 Starting The Program----- | 73 |
| 8.5 Input Field Selection and Navigation----- | 74 |
| 8.5.1 Text Field----- | 74 |
| 8.5.2 List Field----- | 75 |

TABLE OF CONTENTS (con't)

| | Page |
|--|------|
| 8.6 Pull Down Menu System----- | 75 |
| 8.6.1 FILE Menu----- | 75 |
| 8.6.2 EDIT Menu----- | 76 |
| 8.6.3 RUN Menu----- | 77 |
| 8.7 Parameter Input Dialog Boxes----- | 78 |
| 8.7.1 EDIT/CAGE INPUTS Dialog Box----- | 78 |
| 8.7.2 EDIT/BEARING INPUTS Dialog Box----- | 81 |
| 8.7.3 EDIT/FRICTION & LUBRICANT Dialog Box----- | 84 |
| 8.7.4 EDIT/TRACTION DATA Dialog Box----- | 85 |
| 8.7.5 EDIT/CAGE POCKET GEOMETRY Dialog Box----- | 87 |
| 8.7.6 EDIT/BALL CONTACT PARAMETERS Dialog Box----- | 89 |
| 8.7.7 EDIT/OPERATING CONDITIONS Dialog Box----- | 90 |
| 8.7.8 EDIT/INTEGRATION PARAMETERS Dialog Box----- | 92 |
| 8.7.9 EDIT/BALL SLIP & SPIN Dialog Box----- | 94 |
| 9. DATA FILE FORMATS----- | 96 |
| 9.1 INPUT DATA FILE NOMENCLATURE----- | 96 |
| 9.2 SAMPLE INPUT DATA FILE----- | 99 |
| 9.3 OUTPUT DATA FILE FORMATS----- | 102 |
| 9.4 DESCRIPTION OF PRIMARY OUTPUT DATA FILE----- | 104 |
| 10. RUNNING THE BBDPLOT PROGRAM----- | 109 |
| 10.1 FRAME SELECTION----- | 111 |
| 10.2 NEXT----- | 111 |
| 10.3 PREVIOUS----- | 111 |
| 10.4 ZOOM----- | 112 |
| 10.5 FFT----- | 112 |
| 10.6 HCPY----- | 112 |
| 10.7 EXIT----- | 113 |
| 10.8 DATA----- | 113 |
| 10.9 HELP----- | 113 |
| 11. THEORETICAL MODEL----- | 114 |
| 11.1 NOMENCLATURE----- | 114 |
| 11.2 QUASI-STATIC BALL LOAD DEFLECTION ANALYSIS----- | 117 |
| 11.3 BALL-CAGE DYNAMICS----- | 118 |
| 11.3.1 Ball-To-Race Forces----- | 118 |
| 11.3.2 Ball and Ball-Cage Dynamics----- | 120 |
| 11.3.3 Collisions Between Balls and Cage----- | 122 |
| 11.3.4 Ball Guided Designs----- | 123 |
| 11.3.5 Race Guided Designs----- | 127 |
| 11.3.6 Viscous Forces on Ball Cage----- | 132 |
| 12. UTILIZATION AND INTERPRETATION OF RESULTS----- | 139 |
| 13. REFERENCES - BABERDYN PROGRAM----- | 145 |
| APPENDIX A - LUBRICANT PROPERTIES DATA BASE----- | 147 |
| A.1 Viscosity/Temperature Relationship----- | 149 |
| A.2 VISC Program----- | 149 |
| A.3 Viscosity-Pressure Coefficient----- | 150 |
| A.4 Additional References - Appendix A----- | 150 |
| APPENDIX B - McFRIC BALL/RACE TRACTION ANALYSIS PROGRAM----- | 151 |

LIST OF FIGURES

| Figure | | Page |
|--------|---|------|
| 1 | Ball Bearing Configurations That Can Be Analyzed by BASDREL----- | 4 |
| 2 | Load Application Diagram Showing Single DB Duplex Bearing----- | 5 |
| 3 | Quasi-Static and Dynamic Bearing Analysis Software System----- | 5 |
| 4 | Illustration of Some Ball Bearing Geometry Parameters----- | 16 |
| 5 | Illustration of Row Distance Parameter----- | 17 |
| 6 | Illustration of Applied Loads and Moments----- | 20 |
| 7 | Illustration of a Counterbored Raceway----- | 24 |
| 8 | Shaft and Housing are Modeled as a Series of Solid Circular Cylinders----- | 27 |
| 9 | General Model of Two Bodies of Compound Curvature Pressed Together-- | 35 |
| 10 | Lubrication Film Thickness Factor----- | 41 |
| 11 | Ball/Race Contact Area Under Load----- | 50 |
| 12 | Values of K_R for Race Curvature----- | 52 |
| 13 | Values of K_S for Race Curvature----- | 53 |
| 14 | Ball Bearing Analyzed by BABERDYN----- | 67 |
| 15 | Quasi-Static and Dynamic Bearing Analysis Software System----- | 68 |
| 16 | Some Bearing Design Geometry Parameters----- | 69 |
| 17 | Cage Dimensional Inputs----- | 79 |
| 18 | Illustration of Some Ball Bearing Geometry Parameters----- | 82 |
| 19 | Representative Traction Curve, for Illustration Only----- | 86 |
| 20 | Illustration of Ball Cage-to-Center Parameter Necessary for Ball Guided Cage Designs----- | 88 |
| 21 | Race Profile Imperfection Representation----- | 91 |
| 22 | Illustration of Some Ball Bearing Geometry Parameters----- | 99 |
| 23 | Illustration of Additional Bearing Geometry Parameters----- | 100 |
| 24 | Sample BBDPLOT Frame----- | 111 |
| 25 | Ball Bearing Slip Model (View Normal To Ball-Spin Axis)----- | 118 |
| 26 | Relationships of Coordinate Frame Systems----- | 121 |
| 27 | Ball-Guided Cage Pocket Cross Section----- | 122 |
| 28 | Race-Guided Cage Cross Section----- | 122 |
| 29 | Depiction of Gravitational Force Acting on Cage----- | 126 |
| 30 | Positions of Ball Center and Raceway Groove Curvature Centers at Angular Position With and Without Applied Load----- | 134 |
| 31 | BABERDYN Prediction of Cage Ball-Pocket Force Versus Time (Pocket No. 1)----- | 141 |
| 32 | Optimization of Ball Cage for Minimum Ball-Pocket Force----- | 142 |
| 33 | BABERDYN Prediction of Separator Ball-Pocket Wear Energy Dissipation Versus Time----- | 143 |
| 34 | Optimization of Ball Cage for Minimum Ball-Pocket Wear----- | 143 |

LIST OF TABLES

| Table | | Page |
|-------|--|------|
| 1 | Raceway and Ball Material Property Library----- | 19 |
| 2 | Housing/Shaft Cross Section Data Format----- | 27 |
| 3 | A_2 Factors----- | 40 |
| 4 | A_3 vs Lambda----- | 43 |
| 5 | Torque Coefficient (f_o) For Various Bearing Designs With Zero Load-- | 45 |
| 6 | Torque Coefficients (f_l) for Loaded Rolling Element Bearings of Various Types----- | 46 |
| 7 | Torque Factors for Lubrication Effects----- | 47 |
| 8 | System Specific Input Data for Sample Problem----- | 56 |
| 9 | Row Specific Input Data for Sample Problem----- | 57 |
| 10 | Synthetic Cage Material Properties----- | 81 |
| 11 | BBDPLOT Frames----- | 110 |
| 12 | Baseline Bearing Design Parameters----- | 140 |
| A-1 | Lubricant Properties Data Base----- | 148 |

FOREWORD

This document is an interim report covering the work performed under U. S. Air Force Systems Command Contract F33615-92-C-5908. The project was sponsored by the Materials Directorate, Wright Laboratory, Air Force Systems Command, Wright Patterson AFB OH 45433-7750. The Advanced Research Projects Agency (ARPA), Arlington VA, was the original source of the funding. The Air Force Project Engineer was Karl R. Mecklenburg of Wright Laboratory.

1. INTRODUCTION AND SUMMARY

Many advanced bearing applications now require understanding of dynamic effects, and classical quasi-static techniques of Jones¹, Harris², Palmgren³ and others are inadequate for *dynamic* analysis. Cage failures due to high pocket wear or destructive collision forces between the cage and balls or race lands, cage induced audio noise and structural vibration, and excessive torque, or torque noise, are examples of bearing performance characteristics that are significantly affected by *dynamics*. Premature race wear-out and ball damage in high speed bearings can also result from bearings that are not designed for *dynamic* effects. Ball-to-ball-cage interactions can induce excessive ball-to-race skidding and degraded performance, and can cause premature failure.

Dynamic analysis of ball bearings requires more sophisticated tools than those used in classical quasi-static analysis. Dynamic analysis requires solution of complex simultaneous equations to determine ball-to-race quasi-static loads, deflections, contact angles and then the use of these results in complete kinematic and dynamic models of the balls and ball cage. Solution of the dynamic equations of motion requires numerical integration techniques and moderate amounts of high speed computer time. Because this type of analysis can require a considerable number of calculations to achieve meaningful solutions, it is important that the computer program be designed with computational efficiency as a high priority along with rigor and accuracy.

This report summarizes the efforts to develop computerized tools for design, optimization, and life prediction of rolling element bearings utilizing new advanced wear resistant ceramic materials. AVCON has combined a number of previously developed programs for *metal* bearings into an integrated highly efficient tool for design of *ceramic* bearings. This effort has incorporated into these existing computer programs algorithms applicable to the unique

¹A.B. Jones, A General Theory for Elastically Constrained Ball and Radial Roller Bearings under Arbitrary Load and Speed Conditions, ASME Journal of Basic Engineering, pp. 309-320, June 1960

²T.A. Harris, Rolling Bearing Analysis, 1st ed., John Wiley & Sons, 1966, pp.203-241

³Arvid Palmgren, Ball and Roller Bearing Engineering, 3rd Ed., SKF Industries, Inc., 1959

material properties and characteristics of ceramics. Of particular importance are (1) stress fracture mechanics effects, (2) friction and traction contributions to race-to-ball stresses (and life) and ball train and ball-cage dynamics, and (3) the unique thermomechanical properties of all ceramic bearings as well as hybrid bearings using ceramic components and metal components together.

The integrated computer program utilizes advanced computational methods including Newton-Raphson algorithms, rotating polar coordinate frames for describing motion, vector notation, and advanced numerical integration methods by Runge-Kutta-Fehlberg. The Lawrence Livermore Ode numerical integration package (LSODA) is also employed for integration of the dynamic equations of motion. This method assures convergence, while controlling the accuracy of the calculations as a function of computer run time and automatically selects the appropriate integration method of stiff and non-stiff for collision contact conditions.

This sophisticated computer program has a "windows-like" graphical user interface (GUI) preprocessor to allow interactive processing of data. The GUI is user friendly, requiring only operator inputs of bearing geometry, material properties, and traction and friction characteristics. The output predictions include:

- ball-race slip, velocities, and accelerations
- continuous updating of a register that tracks the position of each ball
- load, stress and contact angle of each ball as a function of position in the ball train
- ball-cage position versus time as well as all transitional and angular positions, velocities and accelerations
- ball pocket collision forces as a function of time
- friction heating in various locations such as ball pockets and race land contact
- friction torque and torque noise as a function of time
- Fourier analysis of torque noise in frequency domain
- ball-race wear life
- cage wear life

- fatigue life of metal races or balls
- tensile stress analysis for predicting stress fracture life

This highly sophisticated set of computerized design tools will lead to a more rapid assimilation and utilization of new, wear resistant ceramic materials in bearing applications. This new set of analytical tools will aid in optimizing designs for the unique characteristics and properties of ceramic materials, such as modulus, stress fracture limits, thermal expansion rate, wear rate, and different ceramic-to-ceramic and ceramic-to-metal tribological interactions with both solid and liquid lubricants.

This report has been divided into two basic parts. The first part deals with BASDREL, the computer program for the determination of the stresses, deflections, stiffnesses, torques, and fatigue life of ball bearing pairs under the combined effects of pre-load, axial, radial, and moment loading. The second part deals with BABERDYN-II, the computer program for the determination of ball bearing life, torque level and torque noise, wear life, internal heating, audio noise, and general performance. The appearance of the two parts is similar, but the first portion presents the force determinations and the second portion presents the dynamic interactions.

The program has been examined by others and the reader/user is reminded that the program has a gravity vector. The basic bearing configuration for the program assumes that the shaft orientation is horizontal. Also, analyses of bearings for space applications may produce aberrations with the gravity vector.

2. INTRODUCTION - BASDREL COMPUTER PROGRAM

2.1. BACKGROUND

Determination of stresses, deflections, stiffnesses, torques, and fatigue life of ball bearing pairs under the combined effects of pre-load, axial, radial, and moment loading requires solution of complex simultaneous equations with multiple degrees of freedom. The only practical way for doing this is through the use of computers. The BASDREL ("Ball Bearing Stress Deflection Reliability and Life") computer program computes, for any arrangement of duplex pairs, the bearing stiffnesses, normal load of each ball, actual working contact angles, shoulder height required for each race land, torque, fatigue life and/or reliability for a specified life. Lubricant film thickness effects can also be computed, both for solid lubricated and liquid lubricated bearings. A new feature now available in BASDREL is the capability to analyze multi-bearing systems beyond basic duplex pairs. This new feature allows analysis of up to 10 bearings arbitrarily positioned along the same shaft.

This program is interactive and user friendly. The program makes extensive use of the mouse and pull down menus. On-line help is always available to assist the user in entering design data and running an analysis. Input data can be stored in permanent data files for later recall for design iterations. Stiffness and fatigue life data and all other portions of the program output can be selectively viewed on the screen in tabular form, saved to a disk file, or sent to a printer.

BASDREL is available in the IBM personal computer format and can be supplied on a standard 5¼ or 3½ inch floppy disk ready to run using MS-DOS or similar operating systems.

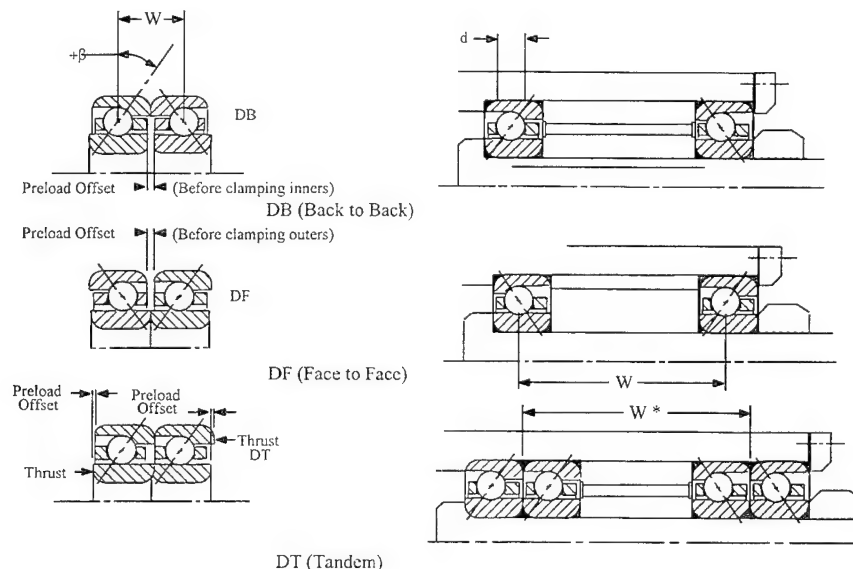


Figure 1. Ball Bearing Configurations That Can Be Analyzed by BASDREL.

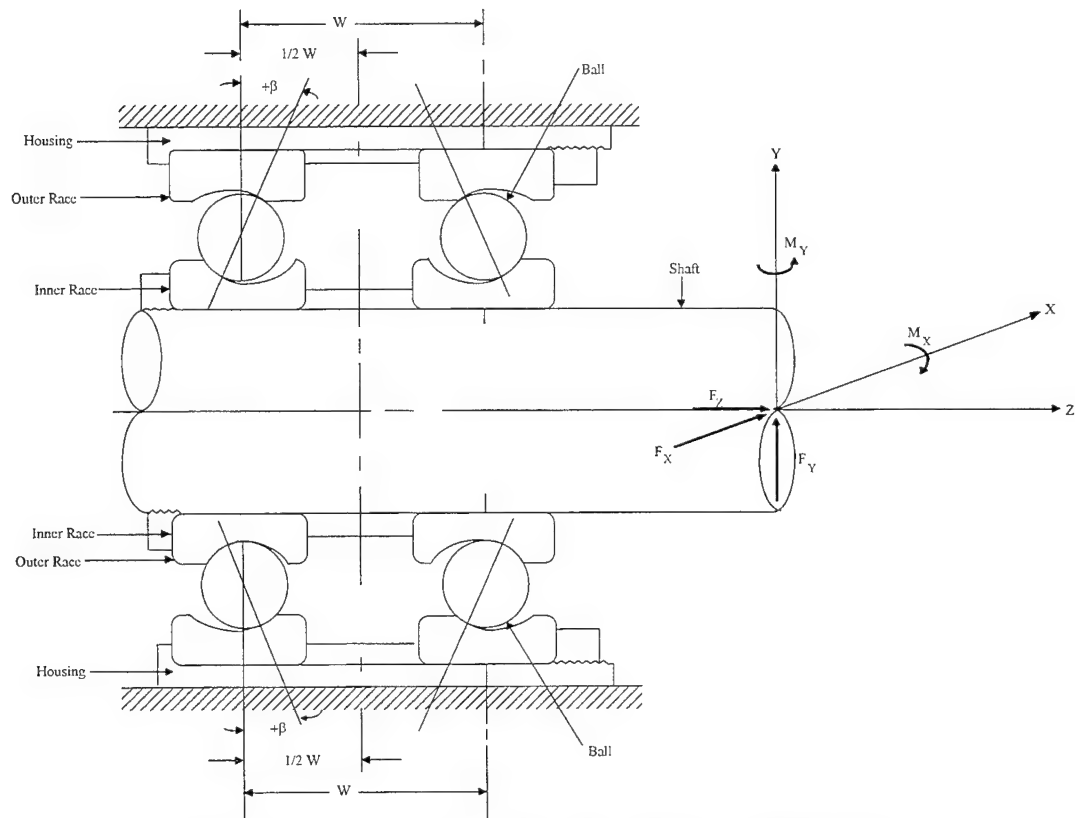


Figure 2. Load Application Diagram Showing Single DB Duplex Bearing.

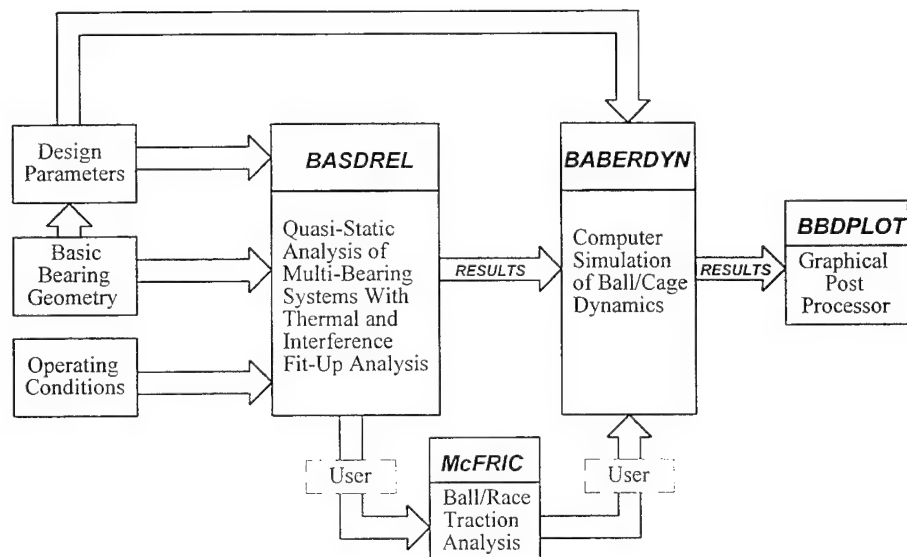


Figure 3. Quasi-Static and Dynamic Bearing Analysis Software System.

2.2. SCOPE

BASDREL (Ball Bearing Analysis of Stresses, Deflections, Reliability, and Life) computes, for any arrangement of up to ten bearings, the bearing stresses and deflections of every ball-to-race contact, stiffness, normal load, and actual working contact angle of each ball, shoulder height required for each race land, torque, EHD film thickness, fatigue life, and/or reliability for a specified life time. Lubrication film thickness effects for solid lubricants and viscous effects of liquid lubricants can also be computed.

BASDREL has a friendly intuitive Graphical User Interface (GUI) which makes extensive use of the mouse and pull down menus. Input data can be stored in permanent data files and can easily be recalled for later design iterations. Stiffness and fatigue life data are presented in tabular form for plotting using your own plotting routines. Stiffness data are saved in standard ASCII format and can be called by data base and plotting programs.

The algorithms in BASDREL are based on the work of A.B. Jones^[1], A. Palmgren, G. Lundberg^[3,4], E. Bamberger^[7], and the author C.R. Meeks.

3. PROGRAM OPERATION

The GUI makes full use of the mouse and keyboard to make it easy to enter your bearing design data and control all actions of the program. The GUI also has on-line help which explains the inputs and calculation options. BASDREL can save your input data to a disk file for later recall permitting easy design iteration studies. BASDREL output is in groups of tables which can be selectively viewed on the screen, saved to a file, or sent to a printer. The file form of output permits easy plotting of results using your own choice of plotting software or spreadsheet program. BASDREL also has a handy Auto Run feature which takes you through the natural series of steps involved in entering input, performing calculations, and viewing or saving results.

3.1. Computer Hardware/Operating System

To run BASDREL (PC) you need:

- ☐ An IBM PC/286/386/486 or PS/2, with at least 512K of memory available.
- ☐ At least one high density floppy drive.
- ☐ An EGA or VGA monitor.
- ☐ An MS-DOS 3.30 or later; OS/2 1.2 or later.
- ☐ A copy of BASDREL Program disk

- ❑ A dot matrix or laserjet printer (optional)

3.2. Backing Up Your Program Disk

We strongly suggest that you make a back-up copy of your BASDREL disk before you begin to use the program. That way, if something happens to your program disk, you will have a back-up copy. The BASDREL disk is not copy protected, so you can copy it using the DOS COPY command. For example, enter the command **COPY A:*. * B:** to copy from the A: drive to the B: drive. See your DOS manual for information on the COPY command.

3.3. Installing BASDREL on a Hard Disk System

BASDREL is best run from a hard disk. To install the program on your hard disk, follow these steps:

1. Turn on your computer system.
2. Put the BASDREL Back-Up disk in drive A (or drive B), and go to the A: (or B:) prompt
3. Type **SETUP** and press <Enter>.

The SETUP program is interactive and will install BASDREL on your hard drive in a directory of your choice. The program files installed are as follows:

| | |
|-------------|--|
| BASDREL.EXE | This is the BASDREL user interface and analysis program together in one code. You can run it directly from the DOS command line. If you also have the BABERDYN ball bearing dynamics analysis program, you can launch BASDREL from the BABRDYN2.EXE control program by selecting the BASDREL option in the dialog box. When you exit BASDREL it will exit to the BABRDYN2 control program if you have it, otherwise it will exit to the DOS prompt. |
| VISC.EXE | This is a viscosity/temperature calculator program. This program is run only from the DOS command line. See the Appendix of this manual for more information on this program. |

3.4. Starting The Program

To run BASDREL, do the following:

1. Turn on your computer system.
2. Go to the drive and directory where you wish to store your input and output files.
3. Start up BASDREL by entering the complete path name to where the BASDREL.EXE file is located. For example:

`\BEARING\BASDREL <Enter>`

If the directory containing BASDREL.EXE is in your PATH definition, then you do not need to type the whole directory name. See your DOS manual for more information on directories and PATH.

4. The opening screen allows you to choose between running BASDREL or BABERDYN. Select the BASDREL option with your mouse by simply clicking on the word BASDREL. Or, with a keyboard, press the <Tab> key until the word BASDREL is highlighted and press <Enter>.
5. When you are done running BASDREL, select the Exit option to exit back to the DOS prompt.

While you are executing the BASDREL program, it can be controlled in one of two ways:

- ☐ Manual operation via menus
- ☐ AutoRun

In manual operation you must indicate to the program what you want to do by making selections from the pull down menus. These menu items are described in the following sections. When performing an analysis for the first time, there is a certain logical progression to the menu choices. BASDREL's Auto Run feature takes you through this progression by making the menu selections for you. Every time you start BASDREL it starts out in Auto Run mode. Auto Run is also explained more fully in a later section. From this point, however, you can continue with Auto Run by simply making selections with your mouse or keyboard. Or you can abort Auto Run at any time by pressing the <escape> key on your keyboard.

3.5. Input Field Selection and Navigation

BASDREL comes with two types of input fields; text field and list field.

3.5.1. Text Field

You can select a specific text field for input by clicking the mouse on it or pressing the <Tab> key to highlight the text. The text field can handle both insertion or over typing. The carriage return is not needed for entering the data since pressing <Tab> or <Shift> <Tab> can take you to the next or previous input field.

3.5.2. List Field

You can highlight a specific list field for selection by clicking the mouse on it or pressing the <Tab> key to highlight the text. To select an item from the list, click the ↓ icon next to the list or press the <↓> or <↑> key.

3.6. Pull Down Menu System

The pull down menu bar provides easy access to all the functionality of the program. From the pull down menu you can open and save input data files, edit all design parameters, run an analysis, view various results, and print the results or save them to a file. This section describes the actions performed by each option in the menu system.

3.6.1. FILE Menu

This is a pull down menu that will allow you to 'save' and 'open' bearing data files from disk, and 'print' them on a printer. There are also 'create' and 'exit' functions available from this menu.

3.6.1.1. FILE/CREATE Menu Item

Selecting this menu item will reset the current bearing input model to the default set stored permanently in the program. The program also initiates the Auto Run sequence when you select this menu item. The same effect would result if you were to exit and re-enter the program.

3.6.1.2. FILE/OPEN Menu Item

Selecting this menu item will open a dialog box for retrieving a bearing input file from disk. When a valid file is retrieved from disk the bearing model inputs appearing in the file are read into memory and will replace the current set stored in computer memory. As you work, you're actually making changes to the copy in memory. To keep your work safely on disk, you should save your data after editing. If the Auto Run is turned on, your data will be saved automatically after editing.

3.6.1.3. FILE/SAVE Menu item

Selecting this menu item will save the currently stored set of model inputs to a disk file. If a file name has already been assigned, the file is overwritten.

3.6.1.4. FILE/SAVE AS Menu Item

Selecting this menu item will open a dialog box for saving the currently stored set of model inputs to a disk file. The user is expected to enter a file name, or select one from among those already on the disk. Always use a '.DAT' extension for your model input files, or you can type in the file name without the extension.

3.6.1.5. FILE/PRINT Menu Item

In BASDREL, after running the analysis calculation, you can print the analysis report to the printer or to a file in ASCII format. It is a good idea to save your work before you print. That way, if a printer error or other problem occurs, you won't lose any of the work you've done since you last saved.

To print a report

BASDREL supports LPT1, LPT2, and LPT3 for printer. Since it only generates a text output, you can print on virtually any matrix printers or laserjet printers.

1. From the File menu, choose Print (**ALT, F, P**).
2. If you want to print more than one copy, type or select the number of copies you want to print in the Copies box.
3. Click the OK button, or press **Enter**.

To print to a file

You can save a printed version of an analysis report in a file if you want to print it later or transfer it to another program.

1. From the File menu, choose Print (**ALT, F, P**).
2. Select the Print To File option box.
3. Type a name for the file to which you want to print. The report file will have a different extension from the data file.

4. Choose the OK button.

3.6.1.6. FILE/EXIT Menu Item

Selecting this menu item will exit the program. All data not saved to disk are lost when you exit.

3.6.2. EDIT Menu

This is a pull down menu that allows you to edit your bearing design data. The overall bearing model is divided into three sections. Each of these sections is accessed by a sub-item in this menu, which when selected displays a series of dialog boxes containing the inputs for that section.

When a dialog box is opened for one of the sections, it receives a copy of its values from the "current bearing input model."

3.6.2.1. EDIT/DESIGN DATA Menu Item

Selecting this menu item will open a series of dialog boxes for entering and modifying bearing design data. Section 4.2.1 explains these dialog boxes in detail.

3.6.2.2. EDIT/DESIGN PARAMETERS Menu Item

Selecting this menu item will open a series of dialog boxes for entering and modifying bearing design data. Section 4.2.2 explains these dialog boxes in detail.

3.6.2.3. EDIT/SHRINKAGE Menu Item

Selecting this menu item will open a dialog box for entering and modifying bearing design data. Section 4.2.3 explains this dialog box in detail.

3.6.3. VIEW Menu

This section describes the options available from the VIEW pull down menu.

3.6.3.1. VIEW/GRAPH Menu Item

Selecting this menu option will display a graphical representation of the bearing/shaft system on your screen. It will show the position and contact angle of each bearing row. This display shows whether the bearings have been arranged back-to-back, face-to-face, or in tandem.

3.6.3.2. VIEW/PRELOAD ANALYSIS Menu Item

Selecting this menu item will display, for each bearing, the following:

- normal approach
- axial deflection
- working contact angle
- preload
- maximum mean Hertzian contact stress

3.6.3.3. VIEW/REACTIONS & DEFLECTIONS Menu Item

Selecting this menu item will display, for each bearing row, the following:

- deflection in each axis
- reaction load in each axis

These are due to the combined influence of preload, axial load, radial load and moment load that you specify via the EDIT menu.

3.6.3.4. VIEW/LOAD TABLE Menu Item

Selecting this menu item will display for each loaded ball of each bearing row the following:

- ball to race contact loads and stresses
- actual running contact angle
- individual ball gyroscopic moments and centrifugal forces
- length of major axis of contact ellipse

These are due to the combined influence of preload, axial load, radial load and moment load that you specify via the EDIT menu.

3.6.3.5. VIEW/STIFFNESS & DEFLECTION Menu Item

Selecting this menu item will display for each ball of each bearing row the elastic constants and normal approaches.

These are due to the combined influence of preload, axial load, radial load and moment load that you specify via the EDIT menu.

3.6.3.6. VIEW/TORQUE & L_{10} LIFE Menu Item

Selecting this menu item will display for each bearing row the following:

- viscous shear torque
- friction torque (spinning torque)
- L_{10} Life

- Maximum raceway tensile stress

The system totals also will be displayed. The formulas used for these calculations are presented in Section 7.

These are due to the combined influence of preload, axial load, radial load, and moment load that you specify via the EDIT menu.

Also shown here is the maximum principle tensile stress in each bearing row. This value may be useful for life assessment of bearings having ceramic components, since such bearings do not always exhibit classical modes of fatigue failure. For more information on the calculation of these stress values, see Section 7.

3.6.3.7. VIEW/RELIABILITY VS LIFE Menu Item

Selecting this menu item will display a table of system survival percentages for different periods of life. These are computed directly from the L_{10} life which has a 90% survival rate. The table will start at a life in hours value just above the L_{10} life, and go down to 1 hour of life, and list the survival percentage for each.

These are due to the combined influence of preload, axial load, radial load and moment load that you specify via the EDIT menu.

3.6.3.8. VIEW/FILM THICKNESS Menu item

Selecting this menu item will display for each ball of each bearing row the following:

- EHD thickness at both races
- ball spin velocity
- ball spin/roll ratio

In BASDREL the ball spinning is due to mismatch in inner and outer race contact angles. Ball spinning caused by rubbing with the cage is not addressed by BASDREL but is addressed in the sister program BABERDYN.

These are due to the combined influence of preload, axial load, radial load and moment load that you specify via the EDIT menu.

3.6.3.9. VIEW/STIFFNESS TABLE Menu Item

Selecting this menu item will display tables of net system stiffness versus load in the radial, axial, and moment direction. The purpose of this output table is to provide an overall look at the load/deflection/stiffness characteristics of the bearing system in the axial, radial, and moment coordinates. Thus, detailed data such as individual ball loadings, etc are not printed out

as part of this output table. Detailed data are printed out only for the single combined loading case, as mentioned earlier in this section.

The axial stiffness table is computed by applying just an axial load component to the bearing system (in addition to the specified preload). The axial load will range start at one tenth your input value of axial load and go up to 10 times your input value in 10 equal increments. If your axial load input value is less than 10 lbf, however, the range will be set at 1 to 100 lbf. The data in the axial stiffness table is always written to an output file given the same name as your input data file name, but with a ".AXL" file extension.

The radial stiffness table is computed by applying only a radial load component in the x direction to the bearing system (in addition to the specified preload). The radial load will range start at one tenth your input value of radial load (the greater of your x and y input load components) and go up to 10 times your input value in 10 equal increments. If your radial load input value is less than 10 lbf, however, the range will be set at 1 to 100 lbf. The data in the radial stiffness table is always written to an output file given the same name as your input data file name, but with a ".RAD" file extension.

The moment stiffness table is computed by applying only a moment load component about the x axis to the bearing system (in addition to the specified preload). The radial load will range start at one tenth your input value of moment load (the greater of your about x and about y input load components), and go up to 10 times your input value in 10 equal increments. If your moment load input value is less than 10 in-lbf, however, the range will be set at 1 to 100 in-lbf. The data in the moment stiffness table is always written to an output file given the same name as your input data file name, but with a ".MT" file extension.

The creation of these three output tables requires that you respond "YES" when the program asks if "you want to calculate the stiffness table for three major directions." The program also advises you that the calculation may take a long time. This question is asked only after completion of an ANALYSIS (see the RUN pull down menu).

3.6.4. RUN Menu

This section describes the options available from the RUN pull down menu.

3.6.4.1. RUN/ANALYSIS Menu Item

Selecting this menu item will commence a two stage run process. This is where the program is performing the detailed simultaneous solution of each bearing row in the system. The first stage of calculation computes the system solution at the specific loading conditions you input. Upon completing that calculation the program will request permission to proceed to the second stage. The second stage takes much longer than the first stage since system solutions will be computed for several dozen different loadings. If you choose not to run the second stage

analysis at this time, you must re-run the first stage analysis should you decide later that you do want to run it.

Results of the first stage calculation make up the majority of program output and these are accessed via the VIEW pull down menu. All the VIEW menu items except the last one (VIEW/STIFFNESS TABLE) pertain to the results of the first stage calculation. The last menu item displays the results of the second stage calculation.

3.6.4.2. RUN/AUTO RUN Menu Item

Selecting this menu item will initiate the Auto Run mode of program operation. Normally, to input data, run an analysis, and view the results, the user needs to perform all appropriate actions in sequence by selecting from the pull down menus. Auto Run makes this easier by making the menu selections for you automatically. At the completion of each action, pressing <Enter> takes you to the next logical step. You can cancel out of Auto Run at any time by repeatedly pressing the <Escape> key or by repeatedly clicking on the cancel button with your mouse. The program automatically goes into Auto Run when the program first starts up, and it stays in that mode until you turn it off.

NOTE: The first step in Auto Run is to do either a FILE/CREATE or FILE/OPEN. This will erase all current data.

3.7. Parameter Input Dialog Boxes

All design parameters are entered via dialog boxes. All such dialog boxes are accessed via the EDIT pull down menu described earlier. These dialog boxes contain fields where you can type in your input values. The meaning of each input item is explained in this section.

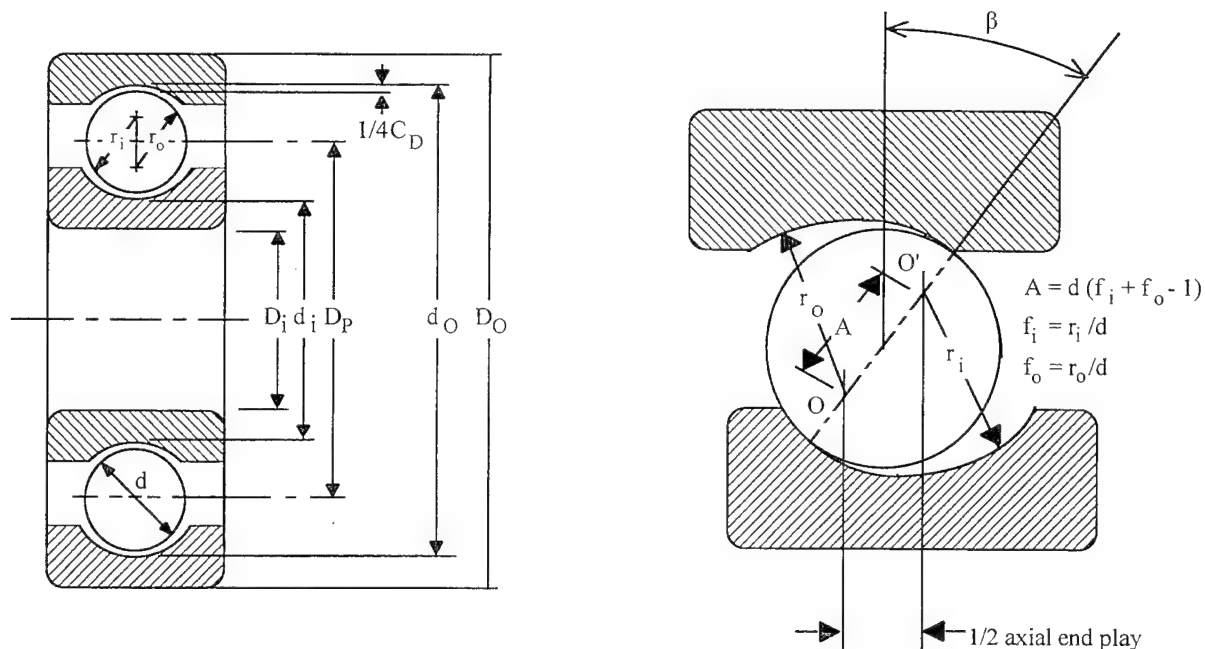


Figure 4. Illustration of Some Ball Bearing Geometry Parameters.

3.7.1. EDIT/DESIGN DATA Dialog Box

The following data items appear in the DESIGN DATA dialog boxes. This is a two stage dialog box. The first stage box contains input fields which apply to the entire bearing system being analyzed. The second stage box is repeated for each bearing row and it contains input fields which are specified independently for each bearing row in the system.

3.7.1.1. Run Identifier Field

This is a string of descriptive text to identify this analysis and can be up to 80 alpha numeric characters. This text will appear in analysis output files you save to disk, and in printouts created on your printer.

3.7.1.2. Number of Bearing Rows Field

This is the number of bearing rows appearing in the bearing system to be analyzed. N must be at least 2 and no greater than 10. When analyzing a single duplex pair, such as a DB or DF bearing, N would be 2.

3.7.1.3. Preload/Max Stress Check Box

BASDREL performs a separate preload analysis for each bearing row where it computes loads, stresses and deflections due to preload only. You can specify the preload force in pounds and the program will compute the resulting stresses and deflections. Or, you can specify the

stress in psi and the program will compute the forces and deflections. When you make your selection an 'X' will appear to indicate your choice. This selection is made one time only and applies to all bearing rows in the system.

3.7.1.4. More Button

Clicking on this button brings up the second stage dialog box which is repeated for each bearing row.

3.7.1.5. Cancel Button

Clicking on this button closes the DESIGN DATA dialog box and voids all input changes in that dialog box.

3.7.1.6. Distance Field

This is the axial distance, in inches, from the point of external load application to the bearing row mid-plane (i.e., at the ball centers). The value is specified independently for each bearing row in the system. Figure 5 illustrates the meaning of the distance value.

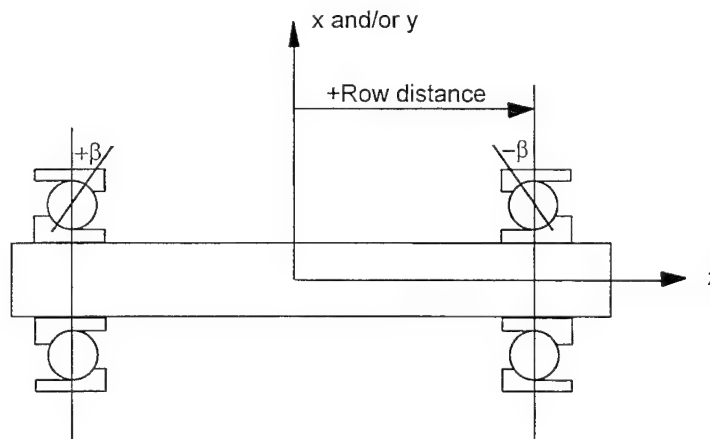


Figure 5. Illustration Of Row Distance Parameter.

3.7.1.7. Number of Balls Field

This is the number of rolling elements in the bearing row and must be greater than zero and not greater than 50. This value is specified independently for each bearing row in the system.

3.7.1.8. Ball Diameter Field

This is the diameter of the ball in inches just as it would be measured with a micrometer or caliper. This value must be greater than zero, and is specified independently for each bearing row in the system.

3.7.1.9. Pitch Diameter Field

The pitch diameter is the diameter of the bearing, in inches, measured at the centers of the balls. This value is specified independently for each bearing row in the system.

3.7.1.10. Unloaded Contact Angle Field

This is the free contact angle in degrees, also called the initial contact angle. This is contact angle when the bearing parts are snug but otherwise not loaded, and the races have not been pressed onto a shaft or into a housing. This value is usually given in manufacturer catalogs. This value is specified independently for each bearing row in the system. Adhere to the sign convention shown in Figure 1 for β , as β can be input as either positive or negative. The signs on your β values are the distinction between DB, DF and DT designs.

3.7.1.11. Inner Race Curvature Field

This is the inner race radius of curvature expressed as a fraction of the ball diameter. For most bearings this value will fall in the range of 0.52 to 0.57. This value is specified independently for each bearing row in the system.

3.7.1.12. Outer Race Curvature Field

This is the outer race radius of curvature expressed as a fraction of the ball diameter. For most bearings this value will fall in the range of 0.52 to 0.57. This value is specified independently for each bearing row in the system.

3.7.1.13. Raceway Material Properties Menu

This is a menu of material properties of a variety of commonly used bearing materials. Also in this menu are properties for more exotic materials such as ceramics. The library contains values for elastic modulus, Poisson's ratio, density and coefficient of thermal expansion. You can select a raceway material from the library or input your own properties as a User Defined material. The material you specify will be used for both inner and outer raceways, but you can specify different raceway materials for different bearing rows. The library is shown in Table 1.

Table 1. Raceway and Ball Material Property Library.

| MATERIAL NAME | YOUNG'S MODULUS psi | POISSON'S RATIO | CEX °R ⁻¹ | DENSITY lb/in ³ |
|-----------------------|------------------------|--------------------|-------------------------|-------------------------------|
| Brg.Stl.(AISI 52100) | 30E6 | .29 | 6.0E-6 | .288 |
| Steel Type 440-C | 29E6 | .3 | 5.6E-6 | .28 |
| Steel PH17-4-H-900 | 30E6 | .3 | 6.0E-6 | .286 |
| CRES Type 304 | 28E6 | .25 | 9.6E-6 | .290 |
| CRES Type 316 | 28E6 | .25 | 8.9E-6 | .29 |
| Titan. 6AL-4V | 17E6 | .33 | 5.7E-6 | .161 |
| Beryllium | 44E6 | .024 | 6.5E-6 | .066 |
| Magn. AZ80A-T5 | 6.5E6 | .33 | 16.0E-6 | .065 |
| Al. Type 6061-T6 | 10.1E6 | .34 | 12.4E-6 | .098 |
| Al. Type 2014-T6 | 10.6E6 | .33 | 12.8E-6 | .101 |
| M-50 steel | 28E6 | .28 | 6.83E-6 | .2746 |
| M-1 steel | 28E6 | .28 | 6.83E-6 | .2746 |
| Si3N4 | 45E6 | .26 | 1.61E-6 | .1156 |
| SiC | 59E6 | .25 | 2.78E-6 | .1156 |
| Al2O3 | 51E6 | .25 | 4.72E-6 | .1409 |
| TiC-Ni-Mo-NbC cermet | 57E6 | .23 | 5.94E-6 | .2276 |
| Cr-Co-Mo-V-W steel | 29E6 | .28 | 5.61E-6 | .2818 |
| User Defined Material | T.B.D. | T.B.D. | T.B.D. | T.B.D. |

CEX = Coefficient of Thermal Expansion

3.7.1.14. Ring Button

Clicking on this button brings up the User Defined Material Properties dialog box which will accept user defined material properties input for the Raceway.

3.7.1.15. Ball Material Properties Menu

This is the same menu of material properties used for selecting the raceway material, including the ceramic materials. You can select a ball material from the library, or input your own properties as a User Defined material. The ball material is specified independently for each bearing row in the system.

3.7.1.16. Ball Button

Clicking on this button brings up the User Defined Material properties dialog box which will accept user defined material properties input for the Ball.

3.7.1.17. Previous Button

Clicking on this button displays the input fields for the previous bearing row.

3.7.1.18. Next Button

Clicking on this button displays the input fields for the next bearing row.

3.7.1.19. Done Button

Clicking on this button validates the input fields for all bearing rows in DESIGN DATA dialog box and closes that dialog box.

3.7.1.20. Cancel Button

Clicking on this button closes the DESIGN DATA dialog box and voids all input changes in that dialog box.

3.7.2. EDIT/DESIGN PARAMETER Dialog Box

The following data items appear in the DESIGN PARAMETER dialog box. This box contains input fields for items which apply to the entire bearing system being analyzed.

3.7.2.1. Preload or Stress Field

This is the amount of thrust preload. It can be specified as either a force in pounds or stress in psi depending on the selection mode for Preload Type in the EDIT/DESIGN DATA dialog box. This value is specified one time and applies to every bearing in the system.

3.7.2.2. External Load Along X Field

This is the externally applied load, in pounds, acting in a radial direction. This load is applied to the shaft and the entire system of bearings will work together to react to the load.

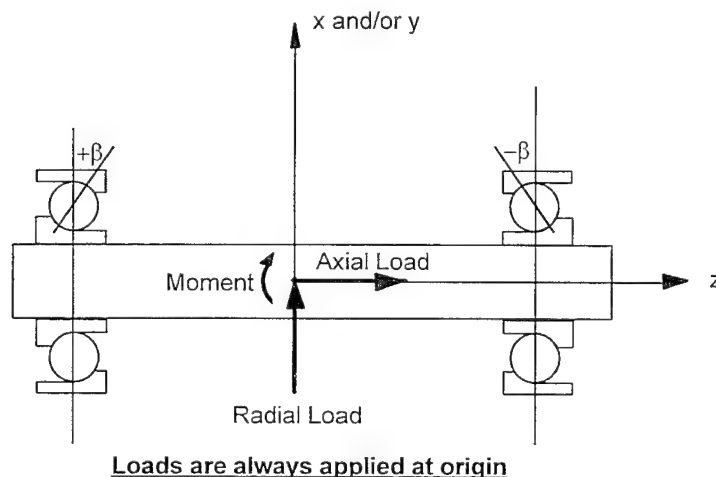


Figure 6. Illustration Of Applied Loads and Moments.

3.7.2.3. External Load Along Y Field

This is the externally applied load, in pounds, acting in a radial direction. This load is applied to the shaft and the entire system of bearings will work together to react to the load.

3.7.2.4. External Load Along Z Field

This is the externally applied load, in pounds, acting in the axial direction. This load is applied to the shaft and the entire system of bearings will work together to react to the load.

3.7.2.5. External Moment About X Field

This is the externally applied moment, in inch-pounds, acting about the X axis. This load is applied to the shaft and the entire system of bearings will work together to react to the load.

3.7.2.6. External Moment About Y Field

This is the externally applied moment, in inch-pounds, acting about the Y axis. This load is applied to the shaft and the entire system of bearings will work together to react to the load.

3.7.2.7. Outer Race Speed Field

This is the rotational speed of the outer race of each bearing row in revolutions per minute. This value is quite often zero.

3.7.2.8. Inner Race Speed Field

This is the rotational speed of the inner race of each bearing row in revolutions per minute.

3.7.2.9. Coefficient of Friction Field

This coefficient of friction is used in a post processing fashion to compute bearing torque contributions due ball spin components at each and every ball/raceway contact. This input value is used for each bearing row in the system.

3.7.2.10. Lubricant Viscosity Field

This is the kinematic viscosity, in centistokes, of the bearing lubricant for each bearing row in the system. This viscosity value is used only in a post processing fashion to compute elastohydrodynamic film thickness at each ball/race contact and to compute the viscous drag torque for each bearing row.

3.7.2.11. Lubricant Pressure Coefficient of Viscosity Field

This lubricant property, in units of in^2/lbf , is used only in a post processing fashion to compute elastohydrodynamic film thickness at each ball/race contact.

3.7.2.12. Lubricant Density Field

This is the density of the lubricant, in lbm/in^3 , for each bearing row in the system. This density value is used only in a post processing fashion to compute elastohydrodynamic film thickness at each ball/race contact and to compute the viscous drag torque for each bearing row.

3.7.2.13. Lubricant Quantity Menu

This is an empirically derived constant used in a formula for viscous drag torque for each bearing row in the system. For ball bearings, its value is determined by the method of lubrication employed, because this determines how much lubricant is present and being "churned" by the bearing. From the available menu choose the method that most closely resembles your application. The value of f is used only in a post processing fashion to compute the viscous drag torque for each bearing row.

3.7.2.14. Done Button

Clicking on this button validates the input fields in DESIGN PARAMETER dialog box and closes that dialog box.

3.7.2.15. Cancel Button

Clicking on this button closes the DESIGN PARAMETER dialog box and voids all input changes in that dialog box.

3.7.3. EDIT/SHRINKAGE Dialog Box

This is a multi-stage dialog box. Its purpose is to let the user either enter a value for shrinkage for each bearing row, or access additional dialog boxes to compute a value for shrinkage. The shrinkage value is specified independently for each bearing row in the system.

3.7.3.1. Shrinkage Field

The shrinkage value, in inches, is a change in bearing internal clearance from its *initial* unloaded and unmounted value, and is specified independently for each bearing row in the system. The *initial* internal clearance corresponds to the *unloaded* contact angle. Changes in internal clearance occur primarily because the inner and outer raceway groove diameters change when the races are pressed into a housing or onto a shaft. Another source is differences in thermal growth of the races and balls. The user can type a value in the input field or click on the shrinkage button to have the program perform a separate calculation (see below).

During the bearing system analysis, the inner and outer raceways of each individual bearing are effectively locked axially in position. A negative value for Shrinkage implies a decrease in the internal clearance for the bearing. Since the races cannot move, the balls will be squeezed an additional amount, and there will be a corresponding increase in the axial preload on the bearings. In the program output there is a section entitled Preload Analysis. This section does *not* include the effects of shrinkage. The shrinkage effects are applied at the same time as your specified external loads. If you want to see the effect of just the shrinkage, perform an analysis with all external load components set to zero. The individual bearing reactions will then show the axial preload with shrinkage included.

3.7.3.2. Shrinkage Button

Clicking on this button brings up a group of dialog boxes which will gather enough additional information from the user about the bearing row in question, so that the shrinkage value can be calculated. This additional information includes raceway interference fits, thermal differences between assembly and operation, and structural information to perform axial and radial stackup analyses.

If the user specifies the preload stress instead of preload force, the program cannot calculate the shrinkage (see 3.7.1.3 and 3.7.2.1), and the button is disabled. The inputs in these other boxes are described next.

3.7.3.2.1. Shrinkage/Adjacent Row Dialog Box

A shrinkage calculation is done in conjunction with another bearing row against which the current bearing row is preloaded. You must specify the other bearing row, and it must have the same geometry as the current row, and there must not be any other rows between these two rows.

3.7.3.2.2. Shrinkage/Geometry Dialog Box

This box comes up automatically after the Adjacent Row dialog box and contains input fields on bearing, shaft and housing geometry.

3.7.3.2.2.1. Bearing Outside Diameter Field

This is the outside diameter of the outer race, in inches.

3.7.3.2.2.2. Bearing Inside Diameter Field

This is the inside diameter of the inner race, in inches.

3.7.3.2.2.3. Outer Race Land Diameter Field

This is the diameter of the outer race land, in inches. Set it equal to zero if you don't know what it is.

3.7.3.2.2.4. Inner Race Land Diameter Field

This is the diameter of the inner race land, in inches. Set it equal to zero if you don't know what it is.

3.7.3.2.2.5. Bearing Raceway Width Field

This is the width of the bearing race, in inches.

3.7.3.2.2.6. Counterbore Check Box

Check this box on to make it display (X) if the bearing is counterbored (Figure 7).

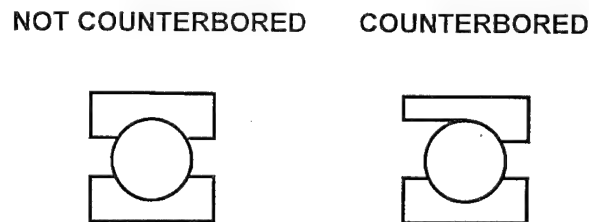


Figure 7. Illustration of a Counterbored Raceway.

3.7.3.2.2.7. Housing Material Properties Menu

This is the same menu of material properties used elsewhere to select race and ball material properties. You can choose a housing material from the library, or input your own properties as a User Defines material.

3.7.3.2.2.8. Housing Button

Clicking on this button brings up the User Defined Material Properties dialog box which will accept user defined material properties input for the Housing.

3.7.3.2.2.9. Shaft Material Properties Menu

This is the same menu of material properties used elsewhere to select race and ball material properties. You can choose a shaft material from the library, or input your own properties as a User Defines material.

3.7.3.2.2.10. Shaft Button

Clicking on this button brings up the User Defined Material Properties dialog box which will accept user defined material properties input for the Shaft.

3.7.3.2.2.11. Done Button

Clicking on this button validates the input fields in the SHRINKAGE/GEOMETRY dialog box and closes that dialog box.

3.7.3.2.2.12. Cancel Button

Clicking on this button closes the SHRINKAGE/GEOMETRY dialog box and voids all input changes in that dialog box.

3.7.3.2.3. Shrinkage/Parameters Dialog Box

This box comes up automatically after the Shrinkage/Geometry dialog box. It has input fields pertaining to the assembly and operating parameters of the bearing.

3.7.3.2.3.1. Inner Race Fit Field

This is the diametral fit between the inner race and the shaft (inches). Use a positive value for loose fit and negative for interference. The value should be the shaft outside diameter minus the inner race inside diameter, both taken prior to mounting on the shaft and at 70° F.

3.7.3.2.3.2. Outer Race Fit Field

This is the diametral fit between the outer race outside diameter and bearing housing inside diameter (inches). Use a positive value for looseness and negative for interference.

3.7.3.2.3.3. Uniform Force Field

This is the amount of force (lbf) applied radially and distributed evenly around the outer housing circumference. A positive value puts the outer housing in tension.

3.7.3.2.3.4. Inner Race Temperature Field

This is the operating temperature of the inner race. Enter its value in degrees F. Assembly temperature is assumed to be 70° F.

3.7.3.2.3.5. Outer Race Temperature Field

This is the operating temperature of the outer race. Enter its value in degrees F. Assembly temperature is assumed to be 70° F. The ball operating temperature is taken to be the average of the inner and outer race temperatures.

3.7.3.2.3.6. Elastic Hydrodynamic Film Thickness Estimate Field

This value, entered in inches, is needed when doing a Shrinkage calculation for a bearing row. This value is not to be confused with the elastohydrodynamic film thickness tables which are computed and printed by BASDREL. Typical values are in the range of 0 to .0001 inches, and are considered just an estimate to enable the Shrinkage calculations to account for EHD thickness.

3.7.3.2.3.7. Cancel Button

Clicking on this button closes the SHRINKAGE/PARAMETERS dialog box and voids all input changes in that dialog box.

3.7.3.2.3.8. Done Button

Clicking on this button validates the input fields in SHRINKAGE/PARAMETER dialog box and closes that dialog box.

3.7.3.2.4. Bearing Housing Dialog Boxes

This is a two stage dialog box used to enter inputs to model the diametral stiffness of the housing surrounding the bearing outer race. If the two bearing rows are pressed together (no spacer) you must model the housing surrounding both bearings. If the bearings are separated by spacers, you must model the housing surrounding one bearing. The housing and shaft are each analyzed using the principle of SUPERPOSITION. The housing, or shaft, is broken down into the minimum number possible of circular rings of constant outside and inside diameter as shown in Figure 8.

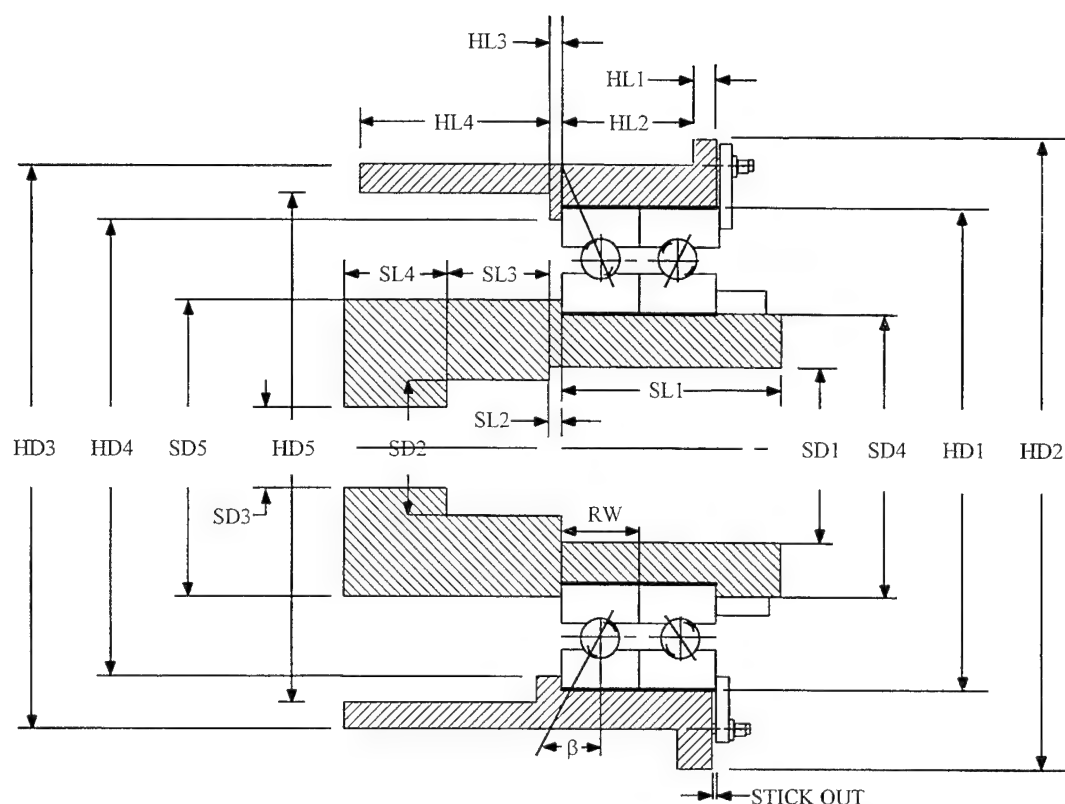


Figure 8. Shaft and Housing are Modeled as a Series of Solid Circular Cylinders.

After constructing a drawing of your housing and shaft, with the structures broken down into ring sections, count the number of individual ring sections and make two tables, one each for the housing and shaft, as illustrated in Table 2 for Figure 8:

Table 2. Housing/Shaft Cross Section Data Format.

| Ring Number | Outside Diameter (OD) | Inside Diameter (ID) | Width (W) |
|-------------|-----------------------|----------------------|-----------|
| N = 1 | HD3 | HD5 | HL4 |
| N = 2 | HD3 | HD4 | HL3 |
| N = 3 | HD3 | HD1 | HL2 |
| N = 4 | HD2 | HD1 | HL1 |

You will be entering the data from your tables in dialog boxes described in this section. When doing so, the program will perform a calculation to check your inputs. If the total housing or shaft width inputs add to a width greater than the theoretical "zone of influence" you will be prompted to reduce the number of sections (or reduce the width of the section farthest from the bearing) until the total width matches the "Elastic Curve Extent" value.

3.7.3.2.4.1. Number of Housing Ring Sections Field

Enter the number of ring sections you will use to model the housing. The value cannot be greater than 20.

3.7.3.2.4.2. Ring Section Outside Diameter Field

This is the outside diameter of the ring section (inches).

3.7.3.2.4.3. Ring Section Inside Diameter Field.

This is the inside diameter of the ring section (inches).

3.7.3.2.4.4. Ring Section Width Field

This is the axial width of the ring section (inches).

3.7.3.2.4.5. Done Button

Clicking on this button validates the input fields in SHRINKAGE/HOUSING dialog box and closes that dialog box.

3.7.3.2.4.6. Cancel Button

Clicking on this button closes the SHRINKAGE/HOUSING dialog box and voids all input changes in that dialog box.

3.7.3.2.4.7. Previous Button

Clicking on this button displays the input fields for the previous housing section.

3.7.3.2.4.8. Next Button

Clicking on this button displays the input fields for the next housing section.

3.7.3.2.5. Shaft Dialog Boxes

This is another two stage dialog box used to model the diametral stiffness of the shaft in a fashion analogous to that done for the bearing housing described above.

3.7.3.2.5.1. Number of Shaft Ring Sections Field

Enter the number of ring sections you will use to model the shaft. The value cannot be greater than 20.

3.7.3.2.5.2. Ring Section Outside Diameter Field

This is the outside diameter of the ring section (inches).

3.7.3.2.5.3. Ring Section Inside Diameter Field.

This is the inside diameter of the ring section (inches).

3.7.3.2.5.4. Ring Section Width Field

This is the axial width of the ring section (inches).

3.7.3.2.5.5. Done Button

Clicking on this button validates the input fields in SHRINKAGE/RING dialog box and closes that dialog box.

3.7.3.2.5.6. Cancel Button

Clicking on this button closes the SHRINKAGE/RING dialog box and voids all input changes in that dialog box.

3.7.3.2.5.7. Previous Button

Clicking on this button displays the input fields for the previous ring section.

3.7.3.2.5.8. Next Button

Clicking on this button displays the input fields for the next ring section.

3.7.3.2.6. Housing Between Outer Races Dialog Box

This dialog box appears automatically if the two bearing rows being analyzed are separated by more than 0.005 inches, since in this case an axial deformation analysis is required. This is a two stage dialog box for modeling the housing in a way analogous to that done previously for diametral stiffness. Now, however, the total axial width is predetermined to be the distance between the outer faces of the races. The first dialog box takes in the number of ring sections to be used to model the housing, and the second box takes in the section dimensions.

3.7.3.2.6.1. Number of Housing Ring Sections Field

Enter the number of ring sections to be used to model the axial stiffness of the housing between the two bearing outer races. The number of sections cannot exceed 20.

3.7.3.2.6.2. Ring Section Outside Diameter Field

This is the outside diameter of the ring section (inches).

3.7.3.2.6.3. Ring Section Inside Diameter Fields

This is the inside diameter of the ring section (inches).

3.7.3.2.6.4. Ring Section Width Field

This is the axial width of the ring section (inches). The total axial width of all sections must match the distance between the outside faces of the outer races.

3.7.3.2.6.5. Done Button

Clicking on this button validates the input fields in SHRINKAGE/HOUSING dialog box and closes that dialog box.

3.7.3.2.6.6. Cancel Button

Clicking on this button closes the SHRINKAGE/HOUSING dialog box and voids all input changes in that dialog box.

3.7.3.2.6.7. Next Button

Clicking on this button displays the input fields for the next housing section.

3.7.3.2.6.8. Previous Button

Clicking on this button displays the input fields for the previous housing section.

3.7.3.2.7. Shaft Between Inner Races Dialog Box

This dialog box appears automatically after the housing dialog boxes just described. This is also a two stage dialog box for modeling the axial stiffness, this time for the shaft.

3.7.3.2.7.1. Number of Shaft Ring Sections Field

Enter the number of ring sections to be used to model the axial stiffness of the shaft between the two bearing inner races. The number of sections cannot exceed 20.

3.7.3.2.7.2. Ring Section Outside Diameter Field

This is the outside diameter of the ring section (inches).

3.7.3.2.7.3. Ring Section Inside Diameter Field

This is the inside diameter of the ring section (inches).

3.7.3.2.7.4. Ring Section Width Field

This is the axial width of the ring section (inches). The total axial width of all sections must match the distance between the outside faces of the inner races.

3.7.3.2.7.5. Done Button

Clicking on this button validates the input fields in SHRINKAGE/RING dialog box and closes that dialog box.

3.7.3.2.7.6. Cancel Button

Clicking on this button closes the SHRINKAGE/RING dialog box and voids all input changes in that dialog box.

3.7.3.2.7.7. Next Button

Clicking on this button displays the input fields for the next ring section.

3.7.3.2.7.8. Previous Button

Clicking on this button displays the input fields for the previous ring section.

3.7.3.2.8. Inner and Outer Race Spacer Dialog Box

After modeling the axial stiffness of the housing and shaft, this dialog box automatically follows so as to model the axial stiffness of the inner and outer race spacers. Both spacers are assumed to have constant diameters (i.e., cylinders) and their axial width must be the space between the near faces of the races. Thus, only the inside and outside diameters for each will be entered.

3.7.3.2.8.1. Outer Race Spacer Inside Diameter Field

Enter the spacer inside diameter in inches. The spacer is assumed to have a constant inside diameter.

3.7.3.2.8.2. Outer Race Spacer Outside Diameter Field

Enter the spacer outside diameter in inches. The spacer is assumed to have a constant outside diameter.

3.7.3.2.8.3. Inner Race Spacer Inside Diameter Field.

Enter the spacer inside diameter in inches. The spacer is assumed to have a constant inside diameter.

3.7.3.2.8.4. Inner Race Spacer Outside Diameter Field

Enter the spacer outside diameter in inches. The spacer is assumed to have a constant outside diameter.

3.7.3.2.8.5. Inner Race Spacer Material Properties Menu

This is the same menu of material properties used for selecting the housing and shaft materials. You can select a material from the library, or input your own properties as a User Defined material. The material is specified independently for the inner and outer spacers.

3.7.3.2.8.6. Outer Race Spacer Material Properties Menu

This is the same menu of material properties used for selecting the housing and shaft materials. You can select a material from the library or input your own properties as a User Defined material. The material is specified independently for the inner and outer spacers.

3.7.3.2.9. Reset Nut Clamping Force Dialog Box

The program uses an algorithm based on structurally determinate systems in which the outer and inner races are clamped by a force of sufficient magnitude to prevent face-to-face or back-to-back races from separating under the influence of interference fits or thermal expansion of the shaft and housing. The program first performs the shrinkage calculation using an internally calculated value for clamping force on the ring pair. However, if the operator specified conditions result in race-to-clamping ring forces that exceed the computed value, a correct solution will not be obtained and this dialog box will be displayed. This dialog box will show the clamping forces used for the analysis, and show what their minimum required values are to prevent race separation. There are two input fields for the user to explicitly enter new clamping forces. After entering new clamping forces, the shrinkage calculation is redone. If the clamping forces are still not sufficient, this dialog box will reappear; otherwise the shrinkage calculation is complete.

3.7.3.2.9.1. Housing Nut Clamping Force Field

In this field, enter a value for the axial clamping force on the outer races (lbf). This value will be used to reperform the shrinkage calculation.

3.7.3.2.9.2. Shaft Nut Clamping Force Field

In this field enter a value for the axial clamping force on the inner races (lbf). This value will be used to reperform the shrinkage calculation.

3.7.3.2.9.3. Done Button

Clicking on this button validates the input fields in SHRINKAGE/SPACER dialog box and closes that dialog box.

3.7.3.2.9.4. Cancel Button

Clicking on this button closes the SHRINKAGE/SPACER dialog box and voids all input changes in that dialog box.

4. ANALYTICAL MODEL

BASDREL computer program is based on the theoretical work of A.B. Jones^[1], Tedrick Harris^[2], G. Lundberg, A. Palmgren^[3,4,5], and C.R. Meeks^[6]. The key equations and relationships are abstracted here to assist the user in understanding the computations. The user is referred to the individual works for a complete derivation of the analytical and empirical models.

NOMENCLATURE

| | | |
|---|---|---|
| a, b | = | semi axes of pressure area |
| B | = | total curvature = $(f_i + f_o - 1)$ |
| d | = | ball diameter |
| D_p | = | pitch circle diameter |
| E | = | moduli of elasticity |
| $f_{i,o}$ | = | race curvatures |
| H, V, M | = | horizontal and vertical components of normal ball load and moment about transverse axis through bearing center |
| $\left. \begin{matrix} h, k, \alpha \\ h', k', \alpha' \end{matrix} \right\}$ | = | relative displacements of outer and inner races ($h = h'(f_o + f_i - 1)d$, etc.) |
| $K(\epsilon), E(\epsilon)$ | = | elliptic integrals |
| n | = | number of balls |
| C_D | = | diametral clearance or tightness |
| P_o | = | normal load |
| $R_{a1}, R_{a2}, R_{b1}, R_{b2}$ | = | principal radii of curvature |
| β_o | = | contact angle, unloaded |
| β_1 | = | contact angle, working |
| δ_G | = | axial deflection |
| δ_N | = | normal approach (deflection) |
| ϵ | = | angle depending on conformity |
| J_a, J_b | = | elastic constants |
| m, n | = | Hertz factors |
| Σ | = | summation or total |
| ν | = | Poisson's ratio |
| ϕ | = | angular position of ball around pitch circle |

Note: The subscripts _o and _i applied to dimensions indicate, respectively, outer and inner races (does not apply to P_o).

4.1. Load vs Deflection Of Concentrated Contacts

The fundamental relationships for deflection versus load of two bodies of compound curvature were originally developed by Heinrich Hertz^[8].

Figure 9 illustrates the general case of two curved bodies pressed together under load P_o , creating an elliptical pressure area with semi axes a and b .

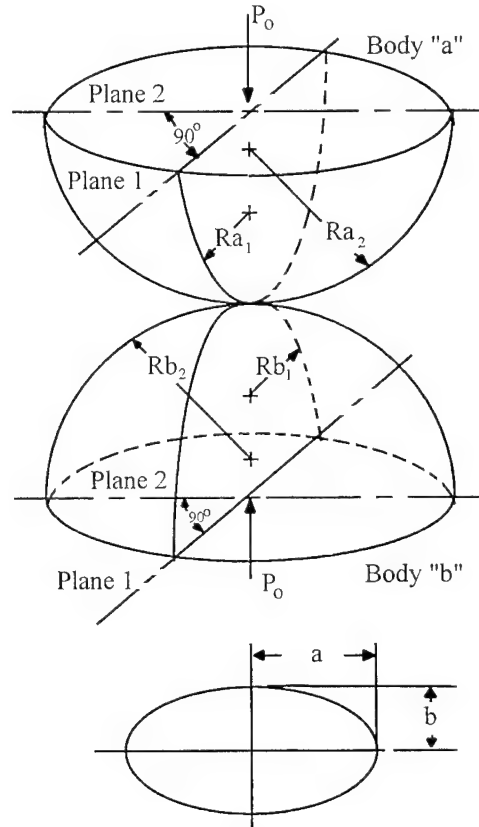


Figure 9. General Model of Two Bodies of Compound Curvature Pressed Together.

From Hertz, the dimensions of the pressure area in terms of the transcendental functions μ and n are:

$$a = \mu g \quad (7)$$

$$b = n g \quad (8)$$

where:

$$g = \sqrt[3]{\frac{3P_o (\vartheta_a + \vartheta_b)}{8 \left(\frac{1}{R_{a1}} + \frac{1}{R_{a2}} + \frac{1}{R_{b1}} + \frac{1}{R_{b2}} \right)}} \quad (9)$$

and J_a and J_b are elastic constants of the two bodies which depend in turn on the respective values of modulus of elasticity, E , and Poisson's ratio, ν

$$a = \frac{4(1 - \delta_a^2)}{E_a} \quad (10)$$

$$b = \frac{4(1 - \delta_b^2)}{E_b} \quad (11)$$

4.2. Normal Approach

The normal approach (δ_N) of two races and the ball complement (for one row of a duplex pair) is:

$$\delta_N = \frac{.1924 (J_a + J_b) K(\epsilon) \cos^{2/3} \epsilon}{\sqrt[3]{E(\epsilon)}} \quad (12)$$

where: $K(\epsilon)$ and $E(\epsilon)$ are elliptic integrals of the first and second order, having the modulus $\sin \epsilon$, i.e.:

$$K(\epsilon) = \int_0^{\pi/2} \frac{d\psi}{1 - \sin^2 \epsilon \sin^2 \psi} \quad (13)$$

$$E(\epsilon) = \int_0^{\pi/2} \sqrt{1 - \sin^2 \epsilon \sin^2 \psi} d\psi \quad (14)$$

4.3. Working Contact Angle

The actual working contact angle (β_1) is determined by solving two simultaneous equations:

$$\frac{T}{nd^2K} = \sin \beta_1 \left(\frac{1 - \frac{C_D}{2Bd}}{\cos \beta_1} - 1 \right)^{3/2} \quad (15)$$

and:

$$\delta_N = Bd \left(1 - \frac{C_D}{2Bd} \right) \tan \beta_1 \quad (16)$$

where T is the working thrust load.

4.4. Ball Load Distribution and Working Contact Angle Under Combined Loading Conditions

Determination of individual ball loading and working contact angles is achieved by simultaneous solution of three quasistatic equilibrium equations:

$$\sum H = Kd^2$$

$$\sum \frac{\left(\sqrt{(\sin \beta_0 + h' + \alpha' R_i \cos \phi)^2 + (\cos \beta_0 + k' \cos \phi)^2} - 1 \right)^{3/2} (\sin \beta_0 + h' + \alpha' R_i \cos \phi)}{\sqrt{(\sin \beta_0 + h' + \alpha' R_i \cos \phi)^2 + (\cos \beta_0 + k' \cos \phi)^2}} \quad (17)$$

$$\sum V = Kd^2$$

$$\sum \frac{\left(\sqrt{(\sin \beta_0 + h' + \alpha' R_i \cos \phi)^2 + (\cos \beta_0 + k' \cos \phi)^2} - 1 \right)^{3/2} (\cos \beta_0 + k' \cos \phi) \cos \phi}{\sqrt{(\sin \beta_0 + h' + \alpha' R_i \cos \phi)^2 + (\cos \beta_0 + k' \cos \phi)^2}} \quad (18)$$

$$\sum M = \frac{Kd^2}{2}$$

$$\sum \frac{\left(\sqrt{(\sin \beta_0 + h' + \alpha' R_i \cos \phi)^2 + (\cos \beta_0 + k' \cos \phi)^2} - 1 \right)^{3/2} (\sin \beta_0 + h' + \alpha' R_i \cos \phi) \cos \phi}{\sqrt{(\sin \beta_0 + h' + \alpha' R_i \cos \phi)^2 + (\cos \beta_0 + k' \cos \phi)^2}} \quad (19)$$

These nonlinear equations are solved simultaneously using a modified Newton-Raphson algorithm.

4.5. Fatigue Life/Reliability

Weibull determined that the ultimate strength of a material cannot be expressed as a single numerical value, but a statistical distribution is required for this purpose. Through application of calculus of probability, Weibull developed the basic theory:

$$\ln(1-\mathfrak{F}) = - \int_v n(\sigma) dv \quad (20)$$

Equation (20) describes the probability of failure \mathfrak{F} due to a given distribution of stress over volume n in which $n(\sigma)$ is a material characteristic.

Lundberg applied the Weibull theory to repeated cyclical loading of ball bearing raceway contacts and derived the form:

$$\ln \frac{1}{\mathfrak{F}} = f(\tau_0, N, z_0) \quad (21)$$

From endurance tests of ball bearings, it has been determined that the life of a bearing race (L) is the following function of the ratio of the dynamic load capacity (Q_c) (the load at which a contact will endure for one million revolutions of a bearing ring) to the actual applied load (Q):

$$L = \left(\frac{Q_c}{Q} \right)^3 \quad (22)$$

Further, applying the Weibull/Lundberg theory to a ball bearing with a number of balls, the basic dynamic capacity (Q_c) may be determine from:

$$Q_c = 7080 \left(\frac{2f}{2f-1} \right)^{0.41} \frac{(1 \pm \gamma)^{1.39}}{(1 \pm \gamma)^{1/3}} \left(\frac{\gamma}{\cos \beta_0} \right)^{0.3} d^{1.8} n^{-1/3} \quad (23)$$

where:

f = raceway curvature factor

$$\gamma = \frac{d}{D_p} \cos \beta_0$$

BASDREL computes the dynamic load capacity of every ball/race contact using equation 23. The dynamic capacity for any given race is taken as the minimum Q_c value computed for the race. BASDREL also computes the equivalent loads for the inner and outer races using the following formula:

$$Q = \frac{1}{n} \sqrt[3]{\sum P_o^3}$$

The L_{10} life for each race is then computed using equation 22. The resulting life for an individual bearing is then the combined life of the two races computed as:

$$L_{row} = \left(L_{i.r.}^{-1.11} + L_{o.r.}^{-1.11} \right)^{-0.9}$$

The L_{10} life for the system of bearings is then the combined life of all rows and is computed as follows:

$$L_{system} = \left(\sum L_{row}^{-1.11} \right)^{-.9}$$

The above equations yield fatigue life estimates in millions of revolutions. For program output this is converted to hours of operation by dividing by the differential speed between inner and outer races.

The L_{10} life is the life during which 10% of an identical bearing population will fail (or a 90% survival rate). BASDREL computes the survival percentages, S , for other periods of operation using the following formula:

$$S = e^{-.1044(L_s/L_{10})^{1.11}}$$

The life calculations performed by the program using these expressions take into account almost all significant affects on life including:

- diametral clearance
- preload
- speed and centrifugal loading
- mounting misalignment
- combined radial, axial and moment loads

The only two additional factors to consider are the influence of lubrication and material properties.

The AFBMA recently adopted a fatigue life formula as follows:

$$L'_{10} = A_2 A_3 L_{10}$$

where:

- | | | |
|-----------|---|--|
| L'_{10} | = | Corrected L_{10} fatigue life |
| A_2 | = | Life adjustment factor for material |
| A_3 | = | Life adjustment factor for lubrication |

These two life reduction factors are described in the following sections.

4.5.1. Material Factor, A_2

The reliability of a bearing depends strongly on what type of treatment is used in preparing the bearing material. The A_2 reliability factor for material vs treatment is summarized in Table 3.

Table 3. A_2 Factors.

| MATERIAL | TREATMENT | A_2 |
|----------------|---|-------|
| 52100 steel | Air melted | 1.0 |
| 52100 steel | Vacuum degassed | 3.0 |
| 52100 steel | Consumable electrode vacuum melted (CEVM) | 5.0 |
| 440c steel | Air melted | 0.5 |
| 440c steel | CEVM | 2.0 |
| M50 tool steel | CEVM | |

4.5.2. Lubrication Factor, A_3 , and EHD Film Thickness

Rolling element bearing manufacturers continually subject their products to fatigue testing to ascertain improvements in their bearing performances owing to alterations in metallurgy, manufacturing methods, and lubrication. To shorten fatigue test time requirements, efforts were made to run at increased spindle speeds. At these higher speeds, however, increased resistance to fatigue occurred, forcing manufacturers to test at slower speed to achieve meaningful results. Today, the reason for the anomalous behavior is clear. Increased rolling speed means increased lubricant film thickness, decreased metal-to-metal contact, decreased surface shear stresses, and, consequently, increased endurance^{[49,50]*}. Subsequently, Tallian^[51], based on test data obtained with 52100 rolling-element bearings, approximated fatigue life versus lubricant film thickness data in a single graph, which is shown in Figure 10.

* [] Brackets refer to reference numbers cited in Bamberger (Reference 7).

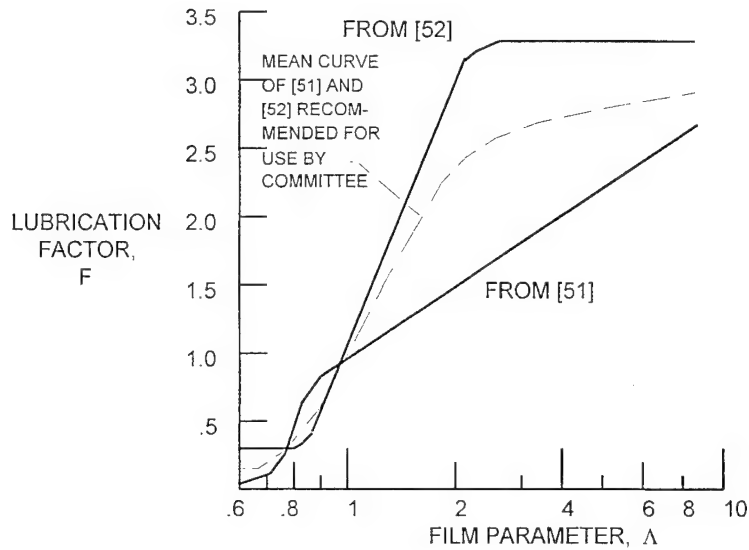


Figure 10. Lubrication Film Thickness Factor.

In Figure 10, the measure of the effectiveness of the lubricant film is the "lambda" (Λ) ratio; i.e., h/σ (film thickness divided by the composite surface roughness of the rolling-element surfaces). Usually the root mean square (rms) surface finishes of the contacting bodies, σ_1 and σ_2 , are used to determine the composite surface roughness as follows:

$$\sigma = (\sigma_1^2 + \sigma_2^2)^{1/2}$$

There are various means of defining the texture or roughness of a steel rolling surface. Although the curve of Figure 10 has been prepared using the rms estimate, an arithmetic average might be used.

Tallian [51], Skurka [52] and Danner [53] published data relating fatigue life of carburized steel roller bearings to lubricant film thickness. Reference [53] provides an interesting insight into tapered roller-bearing performance.

The L_{10} fatigue life calculation described earlier does not consider the effect of lubrication on fatigue life, and BASDREL does not presently accept surface finish as an input. In order to allow the user to utilize Figure 10 to account for lubrication effects on life, BASDREL computes elastohydrodynamic(EHD) film thickness using the following formula due to Hamrock and Dowson:

$$h = \frac{93.63 \bar{U}^{-0.68} \bar{G}^{0.49} (1 - e^{-0.68\kappa})}{\bar{Q}_Z^{0.073}}$$

where:

$$\Re = \frac{d}{2} \left(1 + \frac{d \cos \beta_1}{D_p} \right)$$

$$\bar{Q}_{Z=0} = \frac{P_o}{E' \mathcal{R}^2}$$

$$E' = \frac{2}{\frac{(1 - U_{\text{race}}^2)}{E_{\text{race}}} + \frac{(1 - U_{\text{ball}}^2)}{E_{\text{ball}}}}$$

$$\kappa = a / b$$

$$G = \lambda E'$$

λ = lubricant pressure coefficient of viscosity

$$\bar{U} = \frac{\mu_o U}{2E' \mathcal{R}}$$

μ_o = lubricant viscosity at atmospheric pressure

$$U = \text{entrainment velocity} = \frac{\Omega}{2} \left(\frac{D_p}{\cos \beta_1} + d \right)$$

$$\Omega = -W_{\text{race}} \cos \beta_1 + W_b \cos(\beta_1 - \alpha)$$

W_{race} = rotational speed of race in question (rad/s)

$$W_b = \frac{D_p}{d} (W_{\text{outer}} - W_{\text{inner}}) \frac{(1 - \gamma)}{\cos(\beta_{\text{outer}} - \alpha)}$$

$$\tan \alpha = \frac{\sin \beta_{\text{outer}} \cos \beta_{\text{outer}}}{\cos^2 \beta_{\text{outer}} + \gamma}$$

$$\gamma = \frac{d}{D_p} \cos \beta_{\text{outer}}$$

The above assumes outer race control.

By ratioing the computed film thickness to the rms surface finish, one can obtain the life correction factor due lubrication, F (same as A_3), directly from the curve of Figure 10 or Table 4. This factor is then multiplied by the L_{10} life to produce a corrected life estimate. When the speed of an oil lubricated bearing is low (<2000 rpm), a value of $F = 1$ should be used. For solid lubricated bearings, the author has found a value of $F = 0.1$ to give good results for predicting onset of heavy race micro spalling. For a more complete discussion of solid lubricated bearing life, see Reference 9.

In Figure 10, the curve of life versus "lambda" from reference [51] is terminated at $\Lambda = 0.6$ owing to the uncertainty of the validity of lambda values less than 0.6. The indicated range of data from reference [53] is $0.04 < \Lambda < 0.27$. Note that if lambda is less than 1.0, the bearing is operating in the boundary lubrication regime. In this regime, the failure mode is surface distress caused by metal-to-metal contact in which the AFBMA formula does not apply.

The data provided in reference [52] appear to be very useful. These data have been superimposed on the data of reference [51] in Figure 10. It can be seen that even though Tallian's data were developed for through-hardened point-contact bearings and Skurka's data pertain to carburized line contact bearings, the lubrication-life curves are somewhat similar in shape and not too different in magnitude. A mean curve of lubrication-life versus Λ is also shown in Figure 10.

Table 4. A_3 vs Lambda

| Lambda | A_3 |
|---------------|-------------------------|
| 1.0 | 0.25 |
| 1.25 | 0.6 |
| 1.5 | 1.00 |
| 3.5 | 1.5 |
| 5.75 | 2.0 |
| 10.0 | 3.0 |

4.6. Friction Torque

4.6.1. Background

One of the primary advantages of rolling element bearings is the low friction, or resistance to rolling, even when supporting moderate to heavy loads. Designers of heavy machinery, machine tools, and industrial products need to predict friction losses and heating for motor power requirement determination and cooling requirements. Instrument designers, gimbal designers, gyroscope designers and various optical, radar and target tracking gimbal designers are interested both in friction torque and frequencies and amplitudes of torques caused by rolling element bearings.

The methods for predicting torque and torque variation (i.e., "torque noise") are quite varied in adequacy and accuracy. Prior to the advent of the aerospace age, torque analysis methods for rolling element bearings were quite primitive, as designers were primarily interested in estimates of heating rates and temperature rises due to bearing torque. However, more sophisticated applications of rolling element bearings to inertial guidance gyroscopes, high precision pointing and tracking gimbals, and optical scanning and pointing systems have created a renewed interest in accurate prediction of bearing torque and particularly torque variation or noise. The designer of inertial guidance equipment and high precision pointing and tracking

gimbals is interested both in torque level and frequency content of torques. Consequently, in recent years, more rigorous analytical methods have been developed for rolling element bearing torque analysis. The following sections will cover both some approximate, simplified methods for calculating bearing torque and some of the newer, more accurate, more rigorous techniques.

BASDREL uses the best available algorithms for semi-empirical torque predictions as described in sections 3.6.2 through 3.6.2.2 below. For more rigorous torque prediction the reader is referred to the methods of BASDREL's companion program BABERDYN.

4.6.2. Friction Torque

Torque in rolling element bearings is due to a multitude of factors, some of which are accurately predictable and manageable by design and quality control and others which are not so consistent in real practice. The torque in a rolling element bearing is due to 1) hysteresis and rolling friction losses of the rolling element contact with the races, 2) friction between the cage and guiding race land(s), 3) friction between the cage and rolling elements, 4) lubricant viscous drag at the rolling element-to-cage contacts, (5) lubricant viscous drag at the rolling element-to-raceway contacts, and (6) lubricant viscous drag of the cage-to-guiding race land contacts. All of these losses are affected to varying degrees by the loads applied to the bearing.

4.6.2.1. Simplified, Approximate Torque Analysis

The torque of a rolling element bearing will be considered to consist of four major components. These are generally dealt with employing a combination of empirical and analytical techniques. The four components are as follows:

- a) zero load, low speed torque,
- b) load induced torque as a function of applied radial and axial loads,
- c) torque due to lubricant viscous effects which increases with rotating speed, and
- d) torque due to ball spinning motion present in high speed ball bearings.

These four torque components are discussed in this section. The total bearing friction torque is the simple sum of these four components. The BASDREL program computes the torques due only to c) and d) as they dominate the torque in high speed ball bearings. Torque components a) and b) are not addressed in the program, but can be calculated by the user, if desired, and added to the torque value computed by the program.

No Load Torque. The zero load bearing torque (M_0) has been determined empirically by various experiments^[10,11,12] and can be calculated using a simple coefficient of torque that is empirically determined.

The zero load torque (M_0) is:

$$M_o = f_o D_p \text{ (in-lb)} \quad (25)$$

where:

f_o = empirically determined torque coefficient

D_p = pitch diameter of bearing

Eschman^[19] performed an extensive survey of torque coefficients of various types of rolling element bearings. For lightly lubricated oil lubricated bearings, the values in Table 5 will give good approximate values of unloaded bearing friction torque.

Table 5. Torque Coefficient (f_o) For Various Bearing Designs With Zero Load.

| BEARING TYPE | TORQUE COEFFICIENT f_o |
|---|--------------------------|
| Deep groove ball bearings | 0.0015-0.003 |
| Self-aligning ball bearings | 0.001-0.003 |
| Angular contact ball bearings, single-row | 0.0015-0.002 |
| Angular contact ball bearings, double-row | 0.0024-0.003 |
| Cylindrical roller bearings | 0.001-0.003 |
| Needle roller bearings | 0.002 |
| Spherical roller bearings | 0.002-0.003 |
| Tapered roller bearings | 0.002-0.005 |
| Thrust ball bearings | 0.0012 |
| Spherical roller thrust bearings | 0.003 |
| Cylindrical roller thrust bearings | 0.004 |
| Needle roller thrust bearings | 0.004 |

The friction torque increases for larger rolling element bearings or i.e., larger cross section bearings. The smaller values in Table 5 apply to the light or extra-light series of bearing sizes and the larger values are for heavier cross section bearings such as medium and heavy series. Other effects such as overfilling with grease or torque buildup with contamination due to ingested dirt or wear debris will have to be determined experimentally.

Loaded Torque. As load is applied to rolling element bearings, the torque will increase because of added rolling losses and to increased rolling element-to-cage loads which increase the cage drag losses. The effect of load can be approximated by calculating the mean effective load (P_e) or square root of the sum of the squares. Thus:

$$P_e = \sqrt{P_r^2 + P_a^2} \quad (26)$$

where:

P_r = radial load

P_a = axial load

The bearing torque due to applied load effects can thus be calculated by:

$$M_l = f_l P_e D_p \quad (27)$$

where:

f_l = torque coefficient from Table 3-4

P_e = bearing mean effective load

D_p = pitch diameter of bearing

Table 6 also introduces the ratio of the applied bearing mean effective load (P_e) and the bearing static load rating (C_o)* for determining the torque coefficient.

Table 6. Torque Coefficients (f_l) for Loaded Rolling Element Bearings of Various Types.

| BEARING DESIGN | f_l |
|---|---|
| Deep groove ball bearings and angular contact ball bearings, single-row, with $b_o = 15^\circ$ | $0.002 (P_e/C_o)^{1/2*}$ |
| Self-aligning ball bearings | $0.001 (P_e/C_o)^{1/2}$ |
| Angular contact ball bearings, single-row $b_o = 20^\circ$ to 30° $b_o > 30^\circ$ | $0.002 (P_e/C_o)^{1/2}$ $0.0015 (P_e/C_o)^{1/3}$ |
| Angular contact ball bearings, double-row | $0.002 (P_e/C_o)^{1/3}$ |
| Thrust ball bearings | $0.0015 (P_e/C_o)^{1/3}$ |
| Cylindrical roller bearings Needle roller bearings | 0.0005 |
| Tapered roller bearings, single-row | 0.001 |
| Spherical roller bearings | 0.001 |
| Spherical roller thrust bearings | 0.0015 |
| Cylindrical roller thrust bearings Needle roller thrust bearings | 0.0035 |

Viscous Speed Dependent Torque. Oil lubricated bearings show increasing torques with rotating speed because of the increase in viscous shear losses in the oil films between the rolling elements and races, between the rolling elements and the cage, and between the cage and the guiding race lands. Experimental results and numerical analysis have yielded the relationship:

$$M_n = .0000142 f_o D_p^3 \left(\frac{P/.03611}{0.9} \right)^{\frac{2}{3}} (\Delta \omega v)^{\frac{2}{3}} (\text{in-lb}) \quad (28)$$

* C_o = Bearing static load rating

where:

f_o = torque coefficients from Table 7

n = viscosity of lubricant (lbf - sec/in²)

$\Delta\omega$ = differential speed between inner and outer races (rpm)

P = density of lubricant (lbf/in³)

The values in Table 7 corresponding to ball bearings are built into the program. The user selects which case fits his particular application by selecting from a 'Lubricant Quantity' menu.

Table 7. Torque Factors for Lubrication Effects.

| Bearing Type | Type of Lubrication | | | |
|--|---------------------|----------------------|--------------------|--|
| | Grease | Oil Mist | Oil Bath | Oil Bath (vertical shaft) or Oil Jet |
| Deep groove ball ^a | 0.7-2 ^b | 1 | 2 | 3-4 ^b |
| Self-aligning ball ^c | 1.5-2 ^b | 0.7-1 ^b | 1.5-2 ^b | 3-4 ^b |
| Thrust ball | 5.5 | 0.8 | 1.5 | 3 |
| Angular-contact ball ^a | 2 | 1.7 | 3.3 | 6.6 |
| Cylindrical roller with cage ^a | 0.6-1 ^b | 1.5-2.8 ^b | 2.2-4 ^b | 2.2-4 ^{b,d} |
| full complement | 5-10 ^b | ---- | 5 | ---- |
| Spherical roller ^c | 3.5-7 ^b | 1.7-3.5 ^b | 3.5-7 ^b | 7-14 ^b |
| Tapered roller ^a | 6 | 3 | 6 | 8-10 ^{b,d} |
| Needle roller | 12 | 6 | 12 | 24 |
| Thrust cylindrical roller | 9 | ---- | 3.5 | 8 |
| Thrust spherical roller | ---- | ---- | 2.5-5 ^b | 5-10 ^b |
| Thrust needle roller | 14 | ---- | 5 | 11 |

^a Use $2 \times f_o$ value for paired bearings or double row bearings.

^b Lower values are for light series bearings; higher values are for heavy series bearings.

^c Double row bearings only.

^d For oil bath lubrication and vertical shaft, use $2 \times f_o$.

Ball Spinning Torque. Additional torque losses in high speed ball bearings occur due to centrifugal loading on the balls. Centrifugal loading creates a mismatch between the inner and outer race contact angles. This mismatch means that the ball cannot be 'rolling' on each raceway. The result is that the ball must have a spinning component, which takes place most often at the inner race contact zone. The following analytical expression gives the friction torque about the

axis of spinning due to pure spin for one ball-to-race contact. The program computes the torque due to each rolling element and sums them to obtain the total spinning torque component.

$$M_{\text{spin}} = \frac{3}{8} \mu Q a \Sigma$$

where:

Q = ball to race contact load

μ = coefficient of friction for ball spin

a = semimajor axis length of contact ellipse

Σ = complete elliptic integral of the second kind with modulus $[1-(b/a)^2]^{1/2}$

4.6.2.2. Total Estimated Torque

The total bearing torque computed by BASDREL is the sum of the viscous speed dependent torque and the spinning torque. Consequently the total estimated running torque (M) is:

$$M = M_v + M_{\text{spin}} \text{ (in-lb)} \quad (29)$$

Static, or start-up torque is usually higher than the low speed running torque by 20% to 50%, i.e.:

$$M_{\text{static}} = (1.2 \text{ to } 1.5) M \quad (30)$$

The above equations will be useful for estimating torques of bearings for many machine design applications. However, many variables can cause torques that are significantly different than the simple estimates provided by these methods. Initial surface finish of races, cleanliness, raceway out of roundness, groove runout, race surface defects, lubricant quantity, and lubricant contamination can cause large variations in actual bearing torque. The above methods are useful for preliminary design, however, and used with experience and judgment can prove adequate. The author has found that torque measurement of bearings from the same manufacturer and the same design and manufacturing lot can vary by as much as 100% from the average torque of a population of bearings. Torque screening tests are suggested as a means for obtaining more accurate torque characteristics for critical applications.

4.6.2.3. More Rigorous Torque Analysis Methods.

Ball Bearings. Accurate prediction of torque and torque variation or "torque noise" in ball bearings involves both engineering science and practical art. Purely analytical methods for predicting torque and torque variations are often based on geometrically perfect or ideal bearing kinematics. Real bearings, however, exhibit torques and torque variations due to a multitude of factors that are the result of deviations from ideal or perfect geometry parts. As a matter of fact, the author has found *tests* of brand new bearings from the same lot and manufacturer reveal

torques that vary by a *factor of 2.0*. Examples of torque producing factors besides those that are the result of ideal bearing geometry and kinematics are:

- Flaws in race or ball surfaces such as inclusions, scratches, dents, and microscopic cracks. (These defects are often introduced during manufacturing processes or are the result of poor handling and quality control practices by the manufacturer, by receiving, inspection and the users of bearings).
- Out of roundness and waviness of raceway ball grooves.
- Variations in raceway groove curvature.
- Dirt and contamination (this can include particulate contamination, chemical corrosion of bearing surfaces and, in the case of solid lubricants, non-uniformities in the lubricant constituents).
- Bearing raceway distortions induced by installation (this includes out of roundness in housing bores and shaft journals, out of squareness in end face control flanges and imperfect seating of races into or onto mounting surfaces).
- Imperfections in ball cages (this includes variations in pocket clearances from pocket to pocket which critically affect bearing torque, warpage in thin section cages, and wear of ball pockets or land contact surfaces which change cage characteristics).

The following discussion will review the best available analytical and semi-empirical methods for estimating ball bearing friction torques.

4.6.2.3.1. Ideal Geometry Methods

Many different methods have been developed by bearing engineers for predicting static break-away torque and constant speed running torque. Some of these are purely analytical and some semi-empirical.

Ball/Raceway Rolling Friction Methods. Ball/race rolling friction is due to two factors. First, *internal hysteresis* in the semi-elastic deformation of the races and balls due to the imposed loads produces drag. This drag is a function of the elastic and hysteretic properties of the bearing materials and the degree of osculation of the balls and races. No purely analytical approach has been developed for predicting hysteresis rolling friction and again empirical techniques must be applied. Secondly, ball rolling friction is due to *sliding* which occurs at the ball race interfaces because of *area* contact rather than *point* contact. Under load, a ball will deform the race, forming an elliptical pressure area as shown in Figure 11.

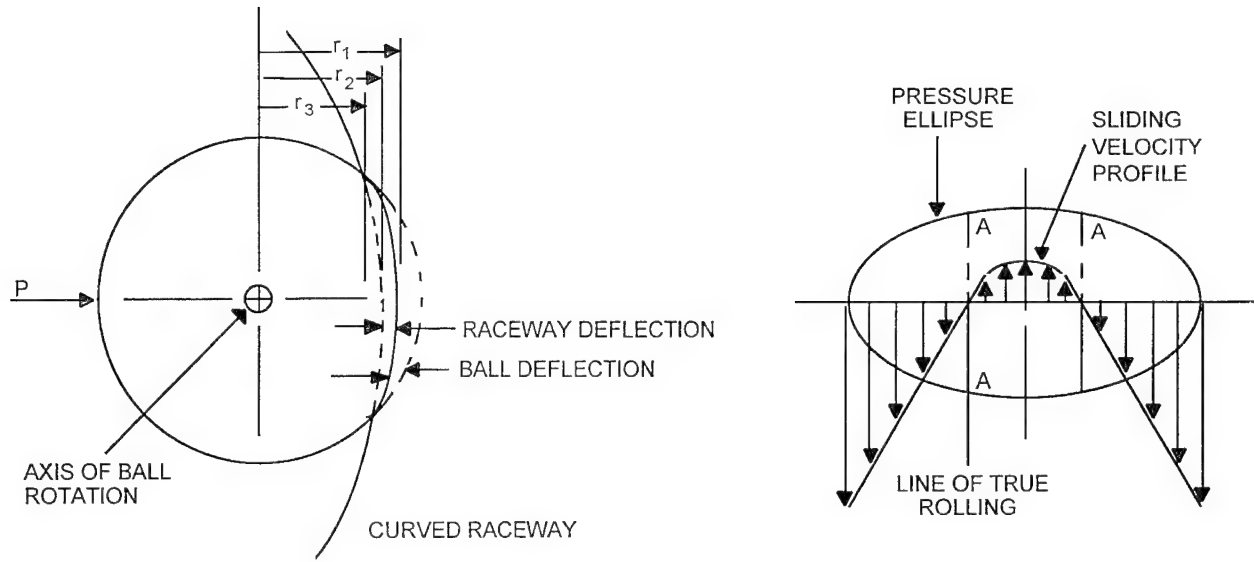


Figure 11. Ball/Race Contact Area Under Load.

Because the velocity of the ball surface is proportional to the distance from the ball axis of rotation (r_1 , r_2 , r_3 , etc.) slip must occur over the contact face. Only two lines of true rolling contact exist with slip occurring at all other contact points. Because this presents an interesting problem in applied mechanics, several investigators have analyzed the drag losses due this differential slip effect.

A.B. Jones^[13] derived a complex expression for analysis of ball slip friction drag:

$$M_r = \frac{3.392 \times 10^{-7} \mu E P^{1.662}}{n^{0.662} d^{1.324} \sin^{1.662} \beta} \left[\frac{(2f_o + 1)^{0.986} K_{R_o(1-\delta)}}{f_o^{0.324} (2f_o - 1)^{0.662}} + \frac{(2f_i + 1)^{0.986} (1 + \delta)}{f_i^{0.324} (2f_i - 1)^{0.662}} \right] \\ + \frac{1.482 \times 10^{-3} \mu d^{1/3} P^{4/3}}{n^{1/3} \sin^{1/3} \beta} \left[\left(\frac{f_o}{2f_o - 1} \right)^{1/3} D_{s_i} + \left(\frac{f_o}{2f_o - 1} \right)^{1/3} K_{s_i} \right] \quad (31)$$

where:

- M_r = rolling torque (in-lb)
- μ = Friction coefficient
- E = Modulus of elasticity of bearing races and balls (lb/in)
- P = Load resultant normal to race contact area center (lb)
- f_{o_i} = Curvature of outside and inside races, respectively

- K_{R_o, R_i} = Race curvature function, inside and outside, respectively (see Figure 12)
 d = $d \cos \beta / E$
 d = Ball diameter (in)
 b = Contact angle (deg)
 K_{s_o, s_i} = Race curvature function, inside and outside, respectively (see Figure 13)
 n = Number of balls

Poritsky, Hewlett & Coleman⁽¹⁴⁾ developed a somewhat simpler form:

$$M_r = Cma P^{4/3} \left(\frac{LD}{n} \cos (90^\circ - b) \right)^{1/3} \quad (32)$$

where:

$$C = 3/8 E \left(1 - \frac{b^2}{a^2} \right)$$

- b = Contact ellipse minor axis half length from hertzian analysis (in)
 a = Contact ellipse major axis half length from hertzian analysis (in)

$$a = \frac{a}{(PdL)^{1/3}}$$

$$D = \frac{4}{\frac{2}{r} + \frac{1}{R} + \frac{1}{R'}}$$

- r = Radius of ball (in)
 R, R' = Principal radii of curvature of races

$$L = \frac{3}{4} \left(\frac{1 - n^2}{E} \right)$$

- n = Poisson's ratio
 n = Number of balls
 b = Contact angle (deg)

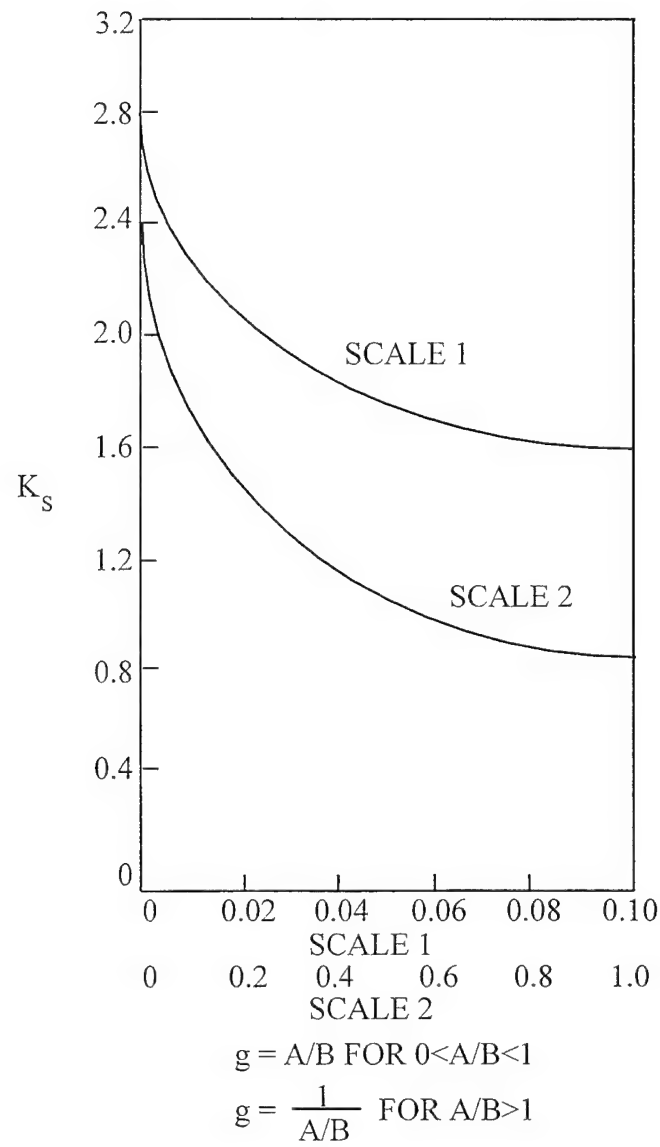


Figure 12. Values of K_R for Race Curvature. (Courtesy A.B. Jones).

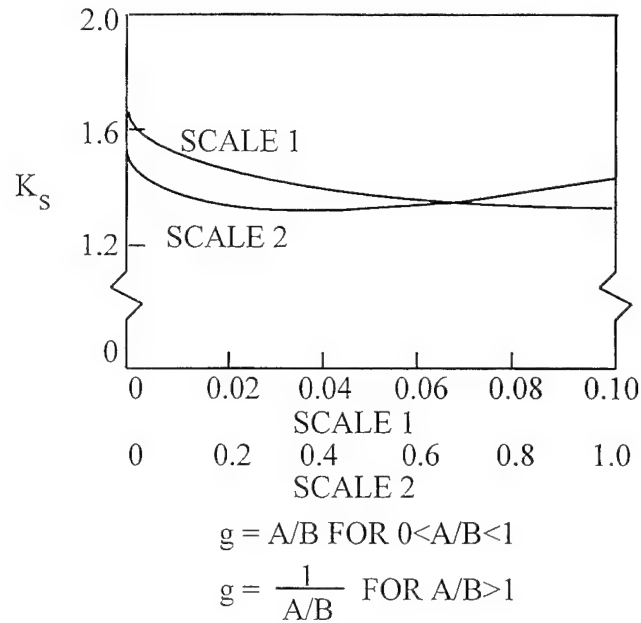


Figure 13. Values of K_s for Race Curvature. (Courtesy A.B. Jones).

A numerical solution of Equations 31 and 32 yield friction torque predictions that are usually an order of magnitude below *measured* friction torques. Although elaborate analyses of ball rolling friction are interesting, they are of very limited value in predicting *total* ball bearing friction torque because they only deal with one of the components of total bearing torque.

4.6.2.3.2. Imperfect Geometry Analysis Methods

Some useful methods exist presently for estimating analytically the torque effects due to raceway groove runout, out of roundness, and waviness^[12]. The author has used these tools with some limited success in estimating the magnitude of torques due to measurable raceway geometric imperfections. These methods are listed here for information and for the users own estimates of torque noise. BASDREL does not compute torque noise.

Mullin and Speece^[15] developed an analytical technique for predicting torque variations from race profilometry data. Applying certain assumptions regarding local conformity, material behavior and supporting conditions, the total energy absorbed in deforming race and balls for a small angle of displacement is equated to the external work done in rotation to arrive at an expression for the differential torque as:

$$\Delta M = C_n (y + \Delta)^{3/2} (\Delta y / \Delta x) \quad (33)$$

$$\begin{aligned}
 C_n &= K_n [D_p - d^2 \times \cos^2(\beta)] / 4 E \cos(\beta) \\
 K_n &= \text{load-deflection constant from Jones (Reference 15)} \\
 D_p &= \text{pitch diameter} \\
 \beta &= \text{contact angle}
 \end{aligned}$$

| | | |
|-----------------------|---|--|
| d | = | ball diameter |
| $y + \Delta$ | = | normal approach (y = imperfection height) |
| $\Delta y / \Delta x$ | = | slope of imperfection |

4.6.2.3.3. Torque Noise Approximate Methods

Kingsbury^[16] examined various sources of torque noise, including cage induced torques and those due to ball errors. Kingsbury developed a simple 2 degree-of-freedom model to characterize cage whirl and orbit frequencies for continuous rotation bearings with which he associated large torque variations. He also observed cage "squeal" (high frequency motion with large amplitude) which is sometimes random in nature. The basic frequency equations are given as:

$$\text{Max Whirl: } \alpha = 2\omega R_b / D_p \quad (34)$$

$$\text{Stable Mode: } \alpha = \dot{\theta} \quad (35)$$

$$\text{Ball Jump Mode: } \alpha = \theta \oslash (-\varepsilon) \quad (36)$$

where:

| | | |
|----------------|---|--------------------------------|
| α | = | whirl speed (rpm) |
| $\dot{\theta}$ | = | bearing rotational speed (rpm) |
| ε | = | small perturbation rate (rpm) |
| ω | = | ball angular velocity (rpm) |
| R_b | = | ball radius (in.) |
| D_p | = | bearing pitch diameter (in.) |

Greer and Mack^[17], in conjunction with experimental work, developed an analytical/empirical model of torque noise by curve fitting the power spectral density (PSD) plots. Here, a method was developed to separate the systematic and random sources of noise. The random portions were modeled as:

$$\text{PSD}(f) = a \oslash (f)^k \quad (37)$$

where:

| | | |
|--------|---|-----------------------|
| f | = | frequency of interest |
| a, k | = | empirical constants |

The systematic modes were segregated by measuring the energy at specific peaks in the PSD and superimposing these "spikes" with the analytical model of the random noise.

RMS values of torque were measured versus thrust load and compared favorably with analytical predictions using profilometry data on 1.3125 inch bore bearings.

Griep and Shibata^[18] developed careful measurements of Power Spectral Density for low speed, small bore (≈ 0.25 inch) gimbal-type bearings. The data were used to form a semi-empirical model for the torque noise in the 0-100 Hz frequency range. The PSD amplitude prediction equation is:

$$\text{PSD}(f) = (K/b)\dot{\theta} / [(f/b\dot{\theta})^2 + 1]^2 \text{ (in-oz)}^2/\text{Hz} \quad (38)$$

where:

| | | |
|---------------------|---|--|
| f | = | frequency (Hz) |
| $\dot{\theta}$ | = | angular velocity of bearing (deg/sec) |
| b | = | constant (Hz/deg/sec) |
| K | = | function of preload |
| $(K/b)\dot{\theta}$ | = | PSD amplitude (in-oz) ² /Hz |

4.6.2.3.4. Rigorous Analytical Prediction of Torque and Torque Noise in Ball Bearings

Torque, torque noise, and heating of high speed bearings can only be predicted accurately by the use of complete kinematic and dynamic models of the bearing races, rolling elements, and cage. A computer program was developed by the author that rigorously models all of the kinematic and dynamic relationships of ball bearings. This computer program BABERDYN is a complex program that 1) determines the time variant load, contact angle, and position of every ball in the bearing, 2) models the ball-to-race traction characteristics so as to predict ball-to-race slip and the associated forces, 3) models all collisions between the cage and all balls and the race land(s), and 4) then computes the cage and ball motions and energy exchanges through solution of differential equations using numerical integration. BABERDYN is described in another part of this manual.

4.7. Failure Modes of Ceramic Bearings

Primary raceway failure modes are: 1) classical fatigue due to repeated loading, 2) shear failure due to yielding (Von Mises), and 3) brittle fracture through cracking. The first mode of fatigue failure may be either surface or subsurface initiated and classical Weibul analysis algorithms are available for metal races. Shear failure may be related to the maximum difference in the orthogonal shear stress and the prediction method was formulated by Harris^[2]. Utilizing Harris's approach, Sibley^[22] correctly predicted the fatigue life of a steel/ceramic hybrid bearing. Therefore, those formulas have been incorporated into the BASDREL computer program (i.e., L_{10} life). In addition to that, it has been reported by several authors^[20], including Chiu^[21] at the Torrington company, that the failure of ceramic bearings sometimes initiates not beneath the surface, but along the edges of the ball/race elliptical contact zone, indicating tensile stress

failure, or brittle fracture, the third mode of failure. During conversations with Dr. Chiu, it was concluded that the third failure mode can be predicted by comparing the surface tensile stress at the edge of the Hertzian contact area and the tensile strength of the ceramic material. As the maximum predicted tensile stress approaches the ceramic material tensile strength, premature failure due to brittle cracking becomes more likely. An analytical approach to obtaining the maximum tensile stress in and around the contact zone has been provided by Dr. Chiu, and this has been used to arrive at the maximum tensile stress values which appear in the program output along with the classical L_{10} fatigue life.

5. SAMPLE PROBLEM

A sample problem, including the actual printer output of results, is presented in the following pages to aid the user in learning how to use the program. The sample problem is also useful for verifying the correctness of the operator's methods in executing the program.

Your program disk includes a data file called SAMPLE.DAT. When asked for the name of the existing file, if you want to run the sample problem, simply type in SAMPLE.DAT for the name of file. Tables 8 and 9 summarize the design inputs used for this sample case. The print out of the SAMPLE.DAT output file on the following pages shows the result of each phase of the analysis.

Table 8. System Specific Input Data for Sample Problem.

| Program Input | Value |
|--------------------------------|------------------------------|
| Number of Rows | 2 |
| Axial thrust Preload | 100 ksi |
| X Axis External Load | 10 lbf |
| Y Axis External Load | 15 lbf |
| Z Axis External Load | 0 lbf |
| Y Axis External Moment | 0 in-lbf |
| Z Axis External Moment | 0 in-lbf |
| Lubricant Viscosity | 85 cs |
| Lubricant Density | .0325 lbm/in ³ |
| Lubricant Pressure Coefficient | .000211 in ² /lbf |

Table 9. Row Specific Input Data for Sample Problem.

| Program Input | Row #1 Value | Row #2 Value |
|-----------------------|--------------|--------------|
| Number of Balls | 12 | 12 |
| Ball Diameter | 0.25 in | 0.25 in |
| Pitch Diameter | 5.0 in | 5.0 in |
| Location Distance | 0 in | 0.5 in |
| Initial Contact Angle | 20 degrees | -20 degrees |
| Inner Race Curvature | 0.53 | 0.53 |
| Outer Race Curvature | 0.53 | 0.53 |
| Shrinkage | 0 in | 0 in |
| Raceway Material | AISI 52100 | AISI 51200 |
| Ball Material | AISI 52100 | AISI 51200 |

5.1. OUTPUT FILE FOR SAMPLE PROBLEM

AVCON - Advanced Controls Technology, Inc.
Copyright 1993 - BASDREL 3.0

Design: SAMPLE.DAT Date: 06-24-1993 Time: 11:23:35
Title: New Design

SUMMARY OF INPUTS

* Bearing Geometry

- Row Number 1

| | |
|--|----------------------|
| Free Contact Angle (degree) | 20.00 |
| Number of Balls | 12 |
| Ball Diameter (inch) | 0.25000 |
| Pitch Diameter (inch) | 5.00000 |
| Inner Race Curvature | 0.53000 |
| Outer Race Curvature | 0.53000 |
| Ring Material Properties | Brg.Stl.(AISI 52100) |
| Young's Modulus (psi) | 3.0E+07 |
| Poisson's Ratio | 0.29 |
| Thermal Expansion Coefficient (in/in/degF) | 6.0E-06 |
| Density (lb/in^3) | .288 |
| Ball Material Properties | Brg.Stl.(AISI 52100) |
| Young's Modulus (psi) | 3.0E+07 |
| Poisson's Ratio | 0.29 |
| Thermal Expansion Coefficient (in/in/degF) | 6.0E-06 |
| Density (lb/in^3) | .288 |
| Load/Row Distance (inch) | 0.000 |

- Row Number 2

| | |
|-----------------------------|---------|
| Free Contact Angle (degree) | -20.00 |
| Number of Balls | 12 |
| Ball Diameter (inch) | 0.25000 |

| | |
|---|-----------------------|
| Pitch Diameter (inch) | 5.00000 |
| Inner Race Curvature | 0.53000 |
| Outer Race Curvature | 0.53000 |
| Ring Material Properties | Brg.Stl. (AISI 52100) |
| Young's Modulus (psi) | 3.0E+07 |
| Poisson's Ratio | 0.29 |
| Thermal Expansion Coefficient (in/in/degF) | 6.0E-06 |
| Density (lb/in^3) | .288 |
| Ball Material Properties | Brg.Stl. (AISI 52100) |
| Young's Modulus (psi) | 3.0E+07 |
| Poisson's Ratio | 0.29 |
| Thermal Expansion Coefficient (in/in/degF) | 6.0E-06 |
| Density (lb/in^3) | .288 |
| Load/Row Distance (inch) | -0.500 |
| | |
| * Other Parameters | |
| Stress due to preload (psi) | 100000.00 |
| Friction Coefficient | 0.110 |
| Lubricant Viscosity (centistokes) | 85.00 |
| Lubricant Quantity | oil bath or oil jet |
| Pressure Coefficient of Viscosity (in^2/lb) | 0.0002000 |
| Lubricant Density (lb/in^3) | 0.03000 |
| | |
| * Operating Condition | |
| Outer Ring Speed (rpm) | 0.0 |
| Inner Ring Speed (rpm) | 2000.0 |
| External Load | |
| Thrust <--- + (lbs) | 10.0 |
| Radial Along Y (lbs) | 15.0 |
| Radial Along Z (lbs) | 0.0 |
| Moment About Y (in-lb) | 0.0 |
| Moment About Z (in-lb) | 0.0 |
| | |
| SUMMARY OF OUTPUTS | |
| * Preload Analysis | |
| - Row Number 1 | |
| Preload (lbs) | 41.424 |
| Inner Race Maximum Mean Stress (psi) | 100000.0 |
| Outer Race Maximum Mean Stress (psi) | 95920.4 |
| Ball Load (lbs) | 9.489 |
| Normal Approach (inch) | 0.000128 |
| Axial Deflection (inch) | 0.0003731 |
| Contact Angle (degree) | 21.33 |
| Axial Stiffness (lb/in) | 1110150.0 |
| - Row Number 2 | |
| Preload (lbs) | 41.424 |
| Inner Race Maximum Mean Stress (psi) | 100000.0 |
| Outer Race Maximum Mean Stress (psi) | 95920.4 |
| Ball Load (lbs) | 9.489 |
| Normal Approach (inch) | 0.000128 |
| Axial Deflection (inch) | -.0003731 |
| Contact Angle (degree) | -21.33 |
| Axial Stiffness (lb/in) | 1110150.0 |

* Bearing Reaction Force (lbs)

| Row | Along X | Along Y | Along Z | About Y | About Z |
|-----|---------|---------|---------|---------|---------|
| 1 | 38.57 | -9.02 | -0.00 | -0.00 | -8.76 |
| 2 | -48.56 | -5.99 | 0.00 | -0.00 | 5.75 |

* Bearing Deflection

| Row | Along X | Along Y | Along Z | About Y | About Z |
|-----|-----------|-----------|----------|-----------|-----------|
| 1 | 0.000346 | -0.000014 | 0.000000 | -0.000000 | -0.000003 |
| 2 | -0.000400 | -0.000012 | 0.000000 | -0.000000 | -0.000003 |

* Outer Race

- Row Number 1

| Ball | Ball Load (lbs) | CA (deg) | MH Stress (psi) | MGYRO (in-lb) | CF (lbs) | ao (inch) |
|------|--------------------|-------------|--------------------|------------------|-------------|--------------|
| 1 | 8.882 | 20.95 | 93823.40 | -0.0027 | 0.1521 | 0.01371 |
| 2 | 8.089 | 20.91 | 90942.83 | -0.0027 | 0.1521 | 0.01329 |
| 3 | 7.525 | 20.88 | 88780.91 | -0.0027 | 0.1521 | 0.01298 |
| 4 | 7.323 | 20.87 | 87977.89 | -0.0027 | 0.1521 | 0.01286 |
| 5 | 7.525 | 20.88 | 88780.91 | -0.0027 | 0.1521 | 0.01298 |
| 6 | 8.089 | 20.91 | 90943.02 | -0.0027 | 0.1521 | 0.01329 |
| 7 | 8.882 | 20.95 | 93823.46 | -0.0027 | 0.1521 | 0.01371 |
| 8 | 9.701 | 20.98 | 96623.92 | -0.0027 | 0.1521 | 0.01412 |
| 9 | 10.316 | 21.00 | 98626.28 | -0.0027 | 0.1521 | 0.01441 |
| 10 | 10.545 | 21.01 | 99349.58 | -0.0027 | 0.1521 | 0.01452 |
| 11 | 10.316 | 21.00 | 98626.48 | -0.0027 | 0.1521 | 0.01441 |
| 12 | 9.701 | 20.98 | 96623.86 | -0.0027 | 0.1521 | 0.01412 |

- Row Number 2

| Ball | Ball Load (lbs) | CA (deg) | MH Stress (psi) | MGYRO (in-lb) | CF (lbs) | ao (inch) |
|------|--------------------|-------------|--------------------|------------------|-------------|--------------|
| 1 | 11.109 | -21.21 | 101092.45 | 0.0028 | 0.1521 | 0.01477 |
| 2 | 10.579 | -21.22 | 99459.84 | 0.0028 | 0.1521 | 0.01454 |
| 3 | 10.197 | -21.22 | 98248.94 | 0.0028 | 0.1521 | 0.01436 |
| 4 | 10.059 | -21.22 | 97801.98 | 0.0028 | 0.1521 | 0.01429 |
| 5 | 10.197 | -21.22 | 98248.94 | 0.0028 | 0.1521 | 0.01436 |
| 6 | 10.579 | -21.22 | 99459.78 | 0.0028 | 0.1521 | 0.01454 |
| 7 | 11.109 | -21.21 | 101092.38 | 0.0028 | 0.1521 | 0.01477 |
| 8 | 11.647 | -21.20 | 102700.61 | 0.0028 | 0.1521 | 0.01501 |
| 9 | 12.047 | -21.20 | 103862.98 | 0.0027 | 0.1521 | 0.01518 |
| 10 | 12.195 | -21.19 | 104285.34 | 0.0027 | 0.1521 | 0.01524 |
| 11 | 12.048 | -21.20 | 103863.40 | 0.0027 | 0.1521 | 0.01518 |
| 12 | 11.648 | -21.20 | 102701.15 | 0.0028 | 0.1521 | 0.01501 |

* Inner Race

- Row Number 1

| Ball | Ball Load (lbs) | CA (deg) | MH Stress (psi) | MGYRO (in-lb) | CF (lbs) | ao (inch) |
|------|--------------------|-------------|--------------------|------------------|-------------|--------------|
| 1 | 8.738 | 21.51 | 97295.21 | -0.0027 | 0.1521 | 0.01375 |
| 2 | 7.945 | 21.55 | 94257.89 | -0.0027 | 0.1521 | 0.01332 |
| 3 | 7.382 | 21.58 | 91975.73 | -0.0027 | 0.1521 | 0.01300 |
| 4 | 7.179 | 21.59 | 91127.16 | -0.0027 | 0.1521 | 0.01288 |
| 5 | 7.382 | 21.58 | 91975.14 | -0.0027 | 0.1521 | 0.01300 |
| 6 | 7.945 | 21.55 | 94257.82 | -0.0027 | 0.1521 | 0.01332 |
| 7 | 8.738 | 21.51 | 97295.27 | -0.0027 | 0.1521 | 0.01375 |
| 8 | 9.558 | 21.48 | 100245.69 | -0.0027 | 0.1521 | 0.01416 |

| | | | | | | |
|----|--------|-------|-----------|---------|--------|---------|
| 9 | 10.174 | 21.47 | 102353.98 | -0.0027 | 0.1521 | 0.01446 |
| 10 | 10.402 | 21.46 | 103114.73 | -0.0027 | 0.1521 | 0.01457 |
| 11 | 10.173 | 21.47 | 102353.64 | -0.0027 | 0.1521 | 0.01446 |
| 12 | 9.558 | 21.48 | 100245.62 | -0.0027 | 0.1521 | 0.01416 |

- Row Number 2

| Ball | Ball Load (lbs) | CA (deg) | MH Stress (psi) | MGYRO (in-lb) | CF (lbs) | ao (inch) |
|------|--------------------|-------------|--------------------|------------------|-------------|--------------|
| 1 | 10.966 | -21.64 | 104943.01 | 0.0028 | 0.1521 | 0.01483 |
| 2 | 10.437 | -21.67 | 103225.36 | 0.0028 | 0.1521 | 0.01459 |
| 3 | 10.055 | -21.70 | 101950.33 | 0.0028 | 0.1521 | 0.01441 |
| 4 | 9.916 | -21.71 | 101479.95 | 0.0028 | 0.1521 | 0.01434 |
| 5 | 10.055 | -21.70 | 101950.20 | 0.0028 | 0.1521 | 0.01441 |
| 6 | 10.437 | -21.67 | 103225.30 | 0.0028 | 0.1521 | 0.01459 |
| 7 | 10.966 | -21.64 | 104942.94 | 0.0028 | 0.1521 | 0.01483 |
| 8 | 11.505 | -21.61 | 106634.28 | 0.0028 | 0.1521 | 0.01507 |
| 9 | 11.905 | -21.58 | 107856.34 | 0.0027 | 0.1521 | 0.01524 |
| 10 | 12.053 | -21.58 | 108300.45 | 0.0027 | 0.1521 | 0.01530 |
| 11 | 11.905 | -21.58 | 107856.52 | 0.0027 | 0.1521 | 0.01524 |
| 12 | 11.505 | -21.61 | 106634.47 | 0.0028 | 0.1521 | 0.01507 |

* Minimum Shoulder Height (inch)

| | | |
|---------|-------------------|-------------------|
| Row # 1 | Outer Race: .0152 | Inner Race: .0157 |
| Row # 2 | Outer Race: .0157 | Inner Race: .0162 |

* Ball/Race Stiffness and Deflection

- Row Number 1

| Ball | KO (lb/in) | KI (lb/in) | DELO (in) | DELI (in) |
|------|------------|------------|------------|------------|
| 1 | 18631060.0 | 18371272.0 | 0.00006102 | 0.00006093 |
| 2 | 18631094.0 | 18371304.0 | 0.00005734 | 0.00005719 |
| 3 | 18631122.0 | 18371334.0 | 0.00005464 | 0.00005445 |
| 4 | 18631132.0 | 18371346.0 | 0.00005366 | 0.00005345 |
| 5 | 18631122.0 | 18371334.0 | 0.00005464 | 0.00005445 |
| 6 | 18631094.0 | 18371304.0 | 0.00005734 | 0.00005719 |
| 7 | 18631060.0 | 18371272.0 | 0.00006102 | 0.00006093 |
| 8 | 18631038.0 | 18371250.0 | 0.00006472 | 0.00006469 |
| 9 | 18631018.0 | 18371230.0 | 0.00006743 | 0.00006744 |
| 10 | 18631010.0 | 18371228.0 | 0.00006842 | 0.00006844 |
| 11 | 18631018.0 | 18371230.0 | 0.00006743 | 0.00006744 |
| 12 | 18631038.0 | 18371250.0 | 0.00006472 | 0.00006469 |

- Row Number 2

| Ball | KO (lb/in) | KI (lb/in) | DELO (in) | DELI (in) |
|------|------------|------------|------------|------------|
| 1 | 18630844.0 | 18371388.0 | 0.00007084 | 0.00007089 |
| 2 | 18630842.0 | 18371422.0 | 0.00006857 | 0.00006859 |
| 3 | 18630834.0 | 18371444.0 | 0.00006691 | 0.00006691 |
| 4 | 18630834.0 | 18371454.0 | 0.00006631 | 0.00006629 |
| 5 | 18630834.0 | 18371444.0 | 0.00006691 | 0.00006691 |
| 6 | 18630842.0 | 18371422.0 | 0.00006857 | 0.00006859 |
| 7 | 18630844.0 | 18371388.0 | 0.00007084 | 0.00007089 |
| 8 | 18630848.0 | 18371362.0 | 0.00007311 | 0.00007320 |
| 9 | 18630856.0 | 18371340.0 | 0.00007478 | 0.00007489 |
| 10 | 18630858.0 | 18371334.0 | 0.00007539 | 0.00007550 |
| 11 | 18630856.0 | 18371340.0 | 0.00007478 | 0.00007489 |
| 12 | 18630848.0 | 18371362.0 | 0.00007311 | 0.00007320 |

| | |
|--|---------|
| Viscous Shear Torque Bearing # 1 (in-oz) | 30.9849 |
| Spinning Torque Bearing # 1 (in-oz) | 0.0618 |
| Viscous Shear Torque Bearing # 2 (in-oz) | 30.9849 |
| Spinning Torque Bearing # 2 (in-oz) | 0.0832 |
| Total Viscous Shear Torque (in-oz) | 61.9698 |
| Total Spinning Torque (in-oz) | 0.1451 |

* L10 Bearing Life (Hours)

| | |
|------------------------------|----------|
| - Row Number 1 | 229182.9 |
| - Row Number 2 | 121321.7 |
| L10 Bearing Life for System: | 84570.9 |

* Maximum Contact Zone Tensile Stress (psi)

| | |
|----------------|--------|
| - Row Number 1 | 7938.6 |
| - Row Number 2 | 8332.8 |

* Reliability vs. Life

| Operation (hrs) | Row # 1 (%) | System (%) |
|-----------------|-------------|------------|
| 1000000 | 58.19 | 19.41 |
| 562341 | 75.15 | 42.12 |
| 316228 | 86.01 | 63.37 |
| 177828 | 92.36 | 78.61 |
| 100000 | 95.89 | 88.08 |
| 56234 | 97.81 | 93.52 |
| 31623 | 98.84 | 96.53 |
| 17783 | 99.39 | 98.15 |
| 10000 | 99.68 | 99.02 |
| 5623 | 99.83 | 99.48 |
| 3162 | 99.91 | 99.73 |
| 1778 | 99.95 | 99.86 |
| 1000 | 99.97 | 99.92 |
| 562 | 99.99 | 99.96 |
| 316 | 99.99 | 99.98 |
| 178 | 100.00 | 99.99 |
| 100 | 100.00 | 99.99 |
| 56 | 100.00 | 100.00 |
| 32 | 100.00 | 100.00 |
| 18 | 100.00 | 100.00 |
| 10 | 100.00 | 100.00 |

| Operation (hrs) | Row # 2 (%) | System (%) |
|-----------------|-------------|------------|
| 1000000 | 33.36 | 19.41 |
| 562341 | 56.04 | 42.12 |
| 316228 | 73.68 | 63.37 |
| 177828 | 85.12 | 78.61 |
| 100000 | 91.85 | 88.08 |
| 56234 | 95.62 | 93.52 |
| 31623 | 97.66 | 96.53 |
| 17783 | 98.76 | 98.15 |
| 10000 | 99.34 | 99.02 |
| 5623 | 99.65 | 99.48 |
| 3162 | 99.82 | 99.73 |
| 1778 | 99.90 | 99.86 |
| 1000 | 99.95 | 99.92 |
| 562 | 99.97 | 99.96 |

| | | |
|-----|--------|--------|
| 316 | 99.99 | 99.98 |
| 178 | 99.99 | 99.99 |
| 100 | 100.00 | 99.99 |
| 56 | 100.00 | 100.00 |
| 32 | 100.00 | 100.00 |
| 18 | 100.00 | 100.00 |
| 10 | 100.00 | 100.00 |

* Elasto-Hydrodynamic Isothermal Minimum Film Thickness

- Row Number 1

| Ball No. | O/R Film Thickness (micro-in) | I/R Film Thickness (micro-in) | Ball Spin Speed (rad/sec) | O/R S/R Ratio | I/R S/R Ratio |
|----------|----------------------------------|----------------------------------|------------------------------|---------------|---------------|
| 1 | 29.07 | 25.38 | -2090.58 | 0.38 | 0.39 |
| 2 | 29.27 | 25.56 | -2090.64 | 0.37 | 0.39 |
| 3 | 29.42 | 25.70 | -2090.69 | 0.37 | 0.39 |
| 4 | 29.48 | 25.75 | -2090.72 | 0.37 | 0.39 |
| 5 | 29.42 | 25.70 | -2090.69 | 0.37 | 0.39 |
| 6 | 29.27 | 25.56 | -2090.64 | 0.37 | 0.39 |
| 7 | 29.07 | 25.38 | -2090.58 | 0.38 | 0.39 |
| 8 | 28.89 | 25.21 | -2090.53 | 0.38 | 0.39 |
| 9 | 28.76 | 25.09 | -2090.50 | 0.38 | 0.39 |
| 10 | 28.72 | 25.05 | -2090.49 | 0.38 | 0.39 |
| 11 | 28.76 | 25.09 | -2090.50 | 0.38 | 0.39 |
| 12 | 28.89 | 25.21 | -2090.53 | 0.38 | 0.39 |

- Row Number 2

| Ball No. | O/R Film Thickness (micro-in) | I/R Film Thickness (micro-in) | Ball Spin Speed (rad/sec) | O/R S/R Ratio | I/R S/R Ratio |
|----------|----------------------------------|----------------------------------|------------------------------|---------------|---------------|
| 1 | 28.63 | 24.98 | -2090.49 | 0.38 | 0.39 |
| 2 | 28.73 | 25.07 | -2090.51 | 0.38 | 0.39 |
| 3 | 28.81 | 25.14 | -2090.53 | 0.38 | 0.39 |
| 4 | 28.84 | 25.17 | -2090.54 | 0.38 | 0.39 |
| 5 | 28.81 | 25.14 | -2090.53 | 0.38 | 0.39 |
| 6 | 28.73 | 25.07 | -2090.51 | 0.38 | 0.39 |
| 7 | 28.63 | 24.98 | -2090.49 | 0.38 | 0.39 |
| 8 | 28.53 | 24.89 | -2090.47 | 0.38 | 0.39 |
| 9 | 28.46 | 24.82 | -2090.46 | 0.38 | 0.39 |
| 10 | 28.43 | 24.80 | -2090.46 | 0.38 | 0.39 |
| 11 | 28.46 | 24.82 | -2090.46 | 0.38 | 0.39 |
| 12 | 28.53 | 24.89 | -2090.47 | 0.38 | 0.39 |

* Axial Stiffness Table

| Deflection (inch) | Load (lbs) | Stiffness (lb/in) | Max. Mean Stress (psi) |
|----------------------|---------------|----------------------|---------------------------|
| 0.000003 | 1.0 | 370251.3 | 101549.6 |
| 0.000029 | 10.9 | 370104.8 | 105235.0 |
| 0.000056 | 20.8 | 369695.6 | 108814.2 |
| 0.000083 | 30.7 | 368965.8 | 112300.9 |
| 0.000110 | 40.6 | 368460.1 | 115706.1 |
| 0.000137 | 50.5 | 367204.9 | 118977.9 |
| 0.000164 | 60.4 | 365353.5 | 122231.3 |
| 0.000191 | 70.3 | 362591.2 | 125431.8 |
| 0.000218 | 80.2 | 358329.9 | 128592.9 |

| | | | |
|----------|-------|----------|----------|
| 0.000246 | 90.1 | 351693.4 | 131734.5 |
| 0.000274 | 100.0 | 341945.1 | 134884.3 |

Radial Stiffness Table

| Deflection (inch) | Load (lbs) | Stiffness (lb/in) | Max. Mean Stress (psi) |
|----------------------|---------------|----------------------|---------------------------|
| 0.000001 | 1.0 | 1170349.0 | 101545.4 |
| 0.000010 | 10.9 | 1169738.0 | 105112.0 |
| 0.000019 | 20.8 | 1168076.0 | 108545.9 |
| 0.000027 | 30.7 | 1165263.6 | 111869.3 |
| 0.000036 | 40.6 | 1162104.1 | 115096.3 |
| 0.000045 | 50.5 | 1157379.0 | 118233.3 |
| 0.000054 | 60.4 | 1151375.0 | 121289.1 |
| 0.000063 | 70.3 | 1143088.3 | 124293.0 |
| 0.000072 | 80.2 | 1131633.4 | 127250.1 |
| 0.000081 | 90.1 | 1115692.3 | 130168.9 |
| 0.000091 | 100.0 | 1091636.6 | 133251.4 |

* Moment Stiffness Table

| Deflection (rad.) | Load (lb-in) | Stiffness (lb-in/rad) | Max. Mean Stress (psi) |
|----------------------|-----------------|--------------------------|---------------------------|
| 0.000001 | 1.0 | 1878763.5 | 101520.0 |
| 0.000006 | 10.9 | 1878481.0 | 103812.0 |
| 0.000012 | 20.8 | 1877382.9 | 106160.2 |
| 0.000017 | 30.7 | 1875577.5 | 108463.8 |
| 0.000023 | 40.6 | 1873012.3 | 110725.0 |
| 0.000028 | 50.5 | 1869591.3 | 112948.1 |
| 0.000034 | 60.4 | 1866382.0 | 115124.7 |
| 0.000039 | 70.3 | 1863226.8 | 117257.3 |
| 0.000045 | 80.2 | 1857715.3 | 119377.2 |
| 0.000050 | 90.1 | 1850970.6 | 121459.0 |
| 0.000056 | 100.0 | 1842835.4 | 123495.2 |

End of Report

6. REFERENCES

1. Jones, A.B., "Analysis of Stresses and Deflections," New Departure Division of General Motors Corp., Bristol, Connecticut, 1946.
2. Harris, T.A., "Rolling Bearing Analysis," John Wiley & Sons, Inc. 1966.
3. Lundberg, G. and Palmgren, A. "Dynamic Capacity of Rolling Element Bearings," Acta Polytechnica, Mechanical Engineering Series 1, R.R.A.E.E., No. 3, 7 (1947).
4. Lundberg, G. and Palmgren, A., "Dynamic Capacity of Rolling Element Bearings," Acta Polytechnica, Mechanical Engineering Series 2, R.S.A.E.E., No. 4, 96, 1952.
5. Palmgren, A., "Ball and Roller Bearing Engineering," 3rd Edition, Burbank 1959.
6. Meeks, C.R., "The Dynamics of Ball Separators in Ball Bearings - Part I: Analysis," ASLE Transactions, Vol. 28, 3, 277-287, July, 1985.
7. Bamberger, E.N. et al., "Life Adjustment Factors for Ball and Roller Bearings," The American Society of Mechanical Engineers, 345 East 47th Street, New York, N.Y.
8. Hertz, H., "Gesammelte Werke," Vol I, Leipzig, 1895.
9. Meeks, C.R., "Predicting Life of Solid Lubricated Ball Bearings," ASLE Transactions Vol. 29, 2, 203-213 May 1986.
10. Delfosse, M., "Sur le couple de roulements a billes," (Dissertation Lille (1936)).
11. Muzzoli, M., "L'attrito nei cuscinetti a rotolamento-Reibung in den Walzlagern," (Ricerca di Ingegneria 2 (1934), 5, 205-238, Deutsche Ubersetzung: (1937), 6, 1-14).
12. Palmgren, A., "Neuere Untersuchungen uber Energieverluste in Walzlagern," (VDI-Bericht (1957), 20, 117-121, Konstruktion 8 (1956), 11, 467-468).
13. Jones, A.B. and Rothbart, H.A. (editor), "Mechanical Design & Systems Handbook," McGraw Hill, c. 1964.
14. Poritsky, H., Hewlett Jr., C.W. and Coleman, R.E. Jr., "Sliding Friction of Ball Bearings of the Pivot Type," Journal of Applied Mechanics, December 1947.
15. Mullin, J.V. and Speece, A.C., "Prediction of Bearing Torque Variation Based on Profilometry Data," 69-WA/Lub-4.

16. Kingsbury, E.P., "Torque Variations in Instrument Ball Bearings," ASLE Transactions 8, 435-441 (1965).
17. Greer, H. and Mack, R.A., "Experimental Investigation of Torque Noise in Satellite Bearings," American Institute of Aeronautics and Astronautics, Guidance and Control Conference, August 20-22, 1975.
18. Griep, D.J. and Shibata, H., "Torque Noise Model for Large Diameter Ball Bearings at Low Velocity," Aerospace Corp., June 10, 1968.
19. Eschman, P., "Betriebssicherheit und Gebrauchsdauer von Walzlagern," (Walzlagertechnik 13 (1974), 1, 3-8).
20. SKF, NSK, Torrington internal technical reports.
21. Chiu, Y.P., "DARPA Briefing," 1992.
22. Sibley, L., "Silicon Nitride Bearing in High Speed Application," Journal of STLE, 1981.

7. INTRODUCTION - BABERDYN COMPUTER PROGRAM

7.1. BACKGROUND

Ball bearing life, torque level and torque noise, wear life, internal heating, audio noise and general performance are very dependent on bearing dynamics. Oscillation of the ball cage can cause vibration, excessive ball-to-race skidding, high race wear, excessive ball cage wear and even structural damage of the ball cage. Ball-to-raceway skidding due to cage dynamics can cause high wear and premature bearing failure. Adverse bearing dynamics can cause vibration of gyroscope bearings and other critically balanced machines, as well as cause premature failure of the ball cage or raceways. The purpose of this bearing design and analysis software package is to serve as a tool to allow scientific optimization of bearing design and bearing dynamics and to aid in rational design of bearings in ways that avoid poor performance. Earlier versions of BABERDYN were utilized in a variety of problem solving efforts^[1,2,3,4], and has proven its efficiency in providing concrete guidelines for the bearing and machinery designer.

BABERDYN is a rigorous simulation of the dynamics of a six degree of freedom model of the bearing and cage and a holonomic model of the ball motions. The program computes the vector sum of all interactions of all balls and cage-raceway contacts. The ball/cage interactions are modeled as a spring with damping for normal forces and coulomb or viscous friction for forces tangential to the contact surface. Raceway/cage interactions are handled similarly. Ball slip forces on the raceways are modeled as a viscous drag proportional to ball slip speed and proportional to ball-to-raceways normal loads. Ball-to-race contact loads are computed, including the effects of preload, axial load, radial load, moment loads and the effects of centrifugal ball-to-raceway loading. Any combination of ball-guided or race-guided cage and any variation of single or double shoulder raceway contact can be simulated.

Empirical data on ball-to-race traction forces vs slip rate must be available from tests conducted on a "ball bearing simulator", or traction test machine. Ball-to-race slip forces vs slip rate are entered as part of the bearing input and are used in a look-up table.

The program is in the FORTRAN 77 computer language for high calculational efficiency and adaptability to most computer systems. All equations of motion are in polar coordinates. The simultaneous six degree of freedom vector matrix equations are solved in a rotating cage coordinate system to simplify numerical integration of the equations of motion and to minimize computing time and maximize accuracy. The results are transformed to a fixed inertial reference frame for visualization of the motions and for easy comparison with experimental data on cage motions.

Maximum bearing operating time in a computer run is made possible by varying the integration step size. The program automatically selects a larger integration time step size when no collision is occurring between the cage and balls or cage and raceways, and small time steps during collisions. The numerical integration algorithm employed was developed

by the Computing and Mathematics Research Division of the Lawrence Livermore Laboratory. The selected algorithm solves the problem with a full or banded Jacobian matrix when the problem is stiff, but it automatically selects between non-stiff (Adams) and stiff (Backward Differentiation) methods. It uses the nonstiff method initially, and dynamically monitors data (eigenvalues of the Jacobian matrix) in order to decide which method to use, and adjusts the integration step size accordingly. The method has been tested for very stiff situations and performs successfully and effectively.

The results of cage motion predictions can be plotted in conventional time domain plots for identification of characteristic cage frequencies and amplitudes of motions. The program also computes all ball-to-cage collision forces; position, velocity, and acceleration of spinning for each ball; friction torque and torque noise due to all collisions; and all friction and heating losses. All of these parameters can be plotted in time domain plots. Torque and torque noise can be plotted in the frequency domain using a built-in Fourier analysis routine.

7.2. GENERAL INFORMATION

BABERDYN-II is a state of the art analysis software system for the design of moderate to high speed ball bearings (see Figure 14). The program is used for dynamic analysis and takes into account deflections of the loaded balls due to preload, external forces and moments and also motions of the ball cage in the bearing. The program is run in several phases:

- bearing model preparation
- quasi-static bearing analysis
- bearing dynamic analysis
- output display reporting

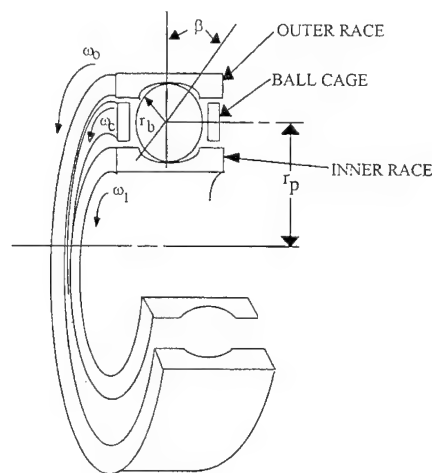


Figure 14. Ball Bearing Analyzed by BABERDYN.

Figure 15 pictorially illustrates the bearing analysis procedure where the BASDREL code is used as a preprocessor to compute the quasi-static loads and deflections of the bearing, to be passed to BABERDYN. Bearing model preparation is performed with a user friendly Graphical User Interface (GUI). Using the mouse and/or keyboard one enters the bearing design data and sets all pertinent analysis parameters. The GUI makes this easy by providing on-line help and when needed will guide the user through every step.

The quasi-static analysis of a bearing is explained in-depth in the BASDREL program documentation. BASDREL can be used to analyze duplex bearings as well as multi-bearing systems mounted on a common shaft. BASDREL also can perform bearing fit-up calculations to compute mounted contact angles at assembly and/or operating conditions. BABERDYN performs its calculations on one bearing row. Thus, the quasi-static results of just one selected bearing are passed from BASDREL to BABERDYN.

The numerical analysis phase of BABERDYN is a calculation intensive process. Due to the complexity of the calculations being carried out, this step can take from ten minutes to more than one hour, on a 486 class desktop computer. There is no user interaction during the analysis, but the program does display messages to keep the user informed as to the progress of the simulation.

The output phase includes viewing and/or printing of written tables of various simulation parameters. Also, an interactive graphical post processing capability makes it easy to get attractive, report quality plots.

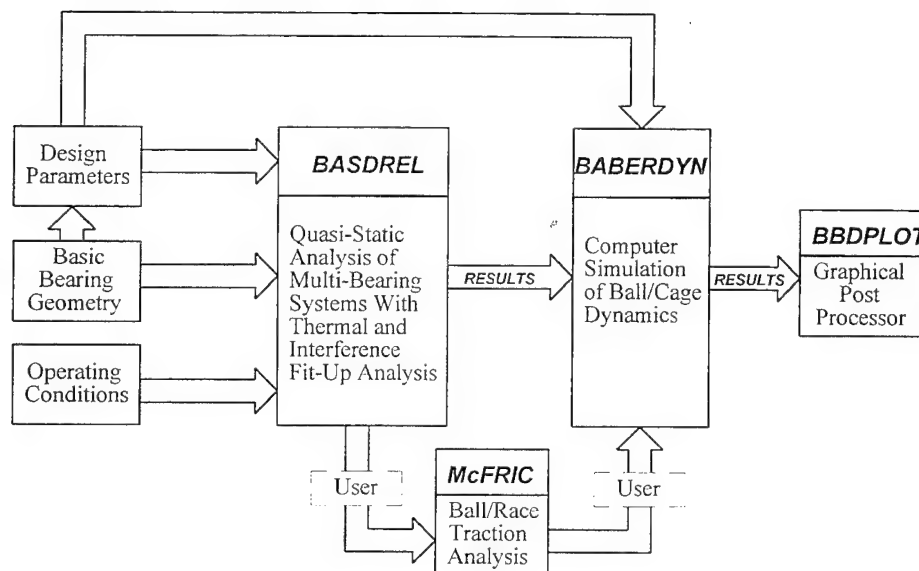
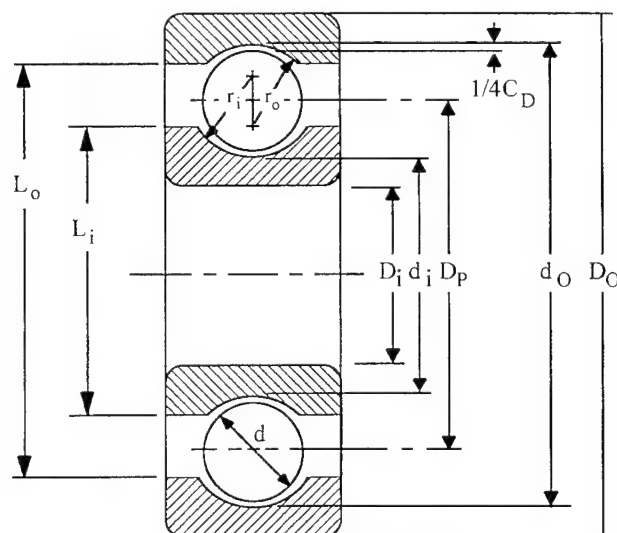


Figure 15. Quasi-Static and Dynamic Bearing Analysis Software System.

7.3. REASONS FOR DEVELOPMENT OF BABERDYN

As discussed above, ball cage life, ball cage structural integrity, bearing vibration, raceway and ball wear life, torque and internal heating are radically affected by ball bearing design parameters. One of the primary causes of poor bearing performance and premature failure are ball and cage dynamic interactions. Some of the symptoms characteristic of bearing dynamic problems are:

- machine vibration
- broken ball cages
- heavy wear scars on ball cage lands or in ball pockets
- heavy raceway wear caused by excessive ball skidding
- high levels of audio noise (sometimes referred to as "squeal")
- rapid increases in friction torque level or torque variation (torque noise)



| | | |
|------------|---|--------------------------|
| D_O | = | Outside diameter |
| D_i | = | Inside diameter |
| d | = | Ball diameter |
| d_i, d_o | = | Raceway groove diameters |
| L_O, L_i | = | Land diameters |
| r_o, r_i | = | Raceway curvature radii |
| D_p | = | Pitch diameter |
| C_d | = | Diametral play |

Figure 16. Some Bearing Design Geometry Parameters.

Careful choice of bearing design parameters such as preload, ball diameter, contact angle, ball cage design including working clearances, and ball cage mass properties can minimize bearing degradation due to undesirable dynamic effects. However, to make intelligent choices of design parameters, theoretical modeling is essential. Without a

theoretical basis, the engineer is left to "cut-and-try" methods which are both costly and often times totally ineffective. At best they leave the engineer not knowing how much margin a design might have or, i.e., how soon a problem may recur because of minor tolerance variations or operating condition changes.

A.B. Jones^[5] developed analytical methods for quasi-static ball bearing design analysis. Jones' methods consider externally applied loads, bearing internal geometry, and centrifugal ball-to-raceway loading. The Jones methods are very effective at determining ball-to-race loads and stresses, working contact angles, and fatigue life. However, they do not treat ball and ball-cage dynamics, including ball-to-cage collisions, cage-to-race collisions, and ball-raceway skidding effects. Only an analytical model that addresses ball-to-race skidding and cage motions in all six degrees-of-freedom can offer insight into dynamic behaviors.

Walters^[6] developed an analytical model for analyzing ball bearing dynamic effects. This model was later modified by Gupta^[7]. However, experience by users of the computer program associated with this model has shown that the computer run times are prohibitively long and do not allow cost-effective optimization of designs. The Gupta/Walters analytical equations were written in an inertially fixed coordinate frame which results in multi-term expressions with numerous sine and cosine terms, as well as Coriolis, centrifugal, and transport terms in the dynamic equations. Integration of these complex equations, as well as integration of traction forces over the Hertzian ball-to-race contact areas for every ball, results in extremely long computer run times. Often over a half hour of processing time is required for a single shaft revolution, and experience has shown that a minimum of three to four revolutions are required to produce a meaningful equilibrium solution^[2]. In addition, inaccuracies result from integration of such complex equations due to computer truncation errors.

Kannel and Bupara^[8] developed a "Simplified Model of Cage Motion in Angular Contact Bearings..." by treating cage motion as planar or, i.e., modeling cage motions with only *three-degrees-of-freedom*. In this model the cage is assumed to move only in the plane of its major diameter. Experimental work by the Air Force Wright Aeronautical Laboratory^[9] and analytical/experimental correlation studies by C.R. Meeks^[3,4] have shown that the ball cage motions are far too complex to be correctly represented by the overly simplified model of Kannel and Bupara.

The BABERDYN-II analytical model and computer program was developed in such a way as to overcome some of the difficulties associated with the Gupta/Walters work. The equations of motion for the ball cage and balls are written in a rotating coordinate frame which greatly simplifies the expressions which must be numerically integrated. The results are transformed back to a fixed coordinate frame with a small angle transformation matrix so the results show actual ball and cage motions with respect to a fixed observer. In addition, the ball-to-race traction characteristics are measured experimentally rather than calculated by integrating complex pressure and velocity functions over the Hertzian contact zone. These

two differences result in significant improvements in accuracy and cost effectiveness of ball bearing dynamic analysis.

Many of the modern, high performance applications of ball bearings today require more rigorous and sophisticated analysis tools than the quasi-static methods of A.B. Jones. Previous efforts by Gupta, Walters and Kannel have pioneered the path to a rigorous methodology for addressing ball bearing dynamic design.

Magnetic storage drives, gyroscopes, spacecraft gimbals and antenna drives, spacecraft reaction and momentum wheels, aircraft turbine engines, and space shuttle turbopumps are just a few of the many systems in dire need of analytical methods for optimizing the *dynamic* design of ball bearings.

8. PROGRAM OPERATION

BABERDYN-II has a friendly intuitive Graphical User Interface (GUI). The GUI makes full use of the mouse and keyboard to make it easy to enter your bearing design data and control all actions of the program. The GUI also has on-line help which explains the inputs and calculation options. BABERDYN-II can save your input data to a disk file for later recall, permitting easy design iteration studies. You run BABERDYN-II from the GUI after entering your design data. Upon completion of the calculation, however, you will be returned to the DOS command prompt since the GUI cannot be restarted from that point. BABERDYN output is always written to a disk file as a set of output tables. After running your analysis, you can view the output file with any text file viewing or editing program. You can also obtain a printout of the output file by simply copying it to the printer device with a DOS command like:

```
COPY OUTPUT.FIL PRN <ENTER>
```

You can also first load the file into your favorite word processing program, apply some formatting if you wish, and then print it from within the word processing program. The file form of output permits easy plotting of results using your own choice of plotting software or spreadsheet program. Report quality plots can also be obtained using the separate plotting software supplied along with BABERDYN. BABERDYN also has a handy Auto Run feature which takes you through the natural series of steps involved in entering input, performing calculations, and viewing or saving results.

8.1. Computer Hardware/Operating System

To run BABERDYN (PC) you need:

- An IBM PC/286/386/486 or PS/2, with at least 512K of memory available.
- At least one high density floppy drive.
- An EGA or VGA monitor.
- A mouse is required to run the BBDPLOT program.
- An MS-DOS 3.30 or later; OS/2 1.2 or later.
- A copy of BABERDYN Program disk
- A dot matrix or laserjet printer (optional)

8.2. Backing Up Your Program Disk

We strongly suggest that you make a back-up copy of your BABERDYN-II disk before you begin to use the program. That way, if something happens to your program disk, you will have a back-up copy. The BABERDYN-II disk is not copy protected, so you can copy it using the DOS `COPY` command. For example, enter the command `COPY A:*. * B:` to copy from the A: drive to the B: drive. See your DOS manual for information on the `COPY` command.

8.3. Installing BABERDYN on Your Hard Disk

BABERDYN is best run from a hard disk. To install the program on your hard disk, follow these steps:

1. Turn on your computer system.
2. Put the BABERDYN-II Back-Up disk in drive A: (or drive B:), and go to the A: (or B:) prompt
3. Type `SETUP` and press `<Enter>`.

The `SETUP` program is interactive and will install BABERDYN-II on your hard drive in a directory of your choice. The program files installed are as follows:

| | |
|--------------|---|
| BABRDYN2.EXE | This is a central control program. Running this program will display a dialog box from which you can launch either the BASDREL or BABERDYN user interface programs, or QUIT back to the DOS prompt. |
| BBD.EXE | This is the BABERDYN user interface program. You can run it directly from the DOS command line, or you can launch it from the BABRDYN2.EXE control program by selecting the BABERDYN option in the dialog box. When you exit this program it is not to the DOS command line, but rather to the BABRDYN2 control program. |
| BABERDYN.EXE | This is the ball bearing dynamics numerical analysis program. You normally would not run this program directly from the DOS command line. This program is launched when you select the RUN ANALYSIS option from within the BBD.EXE user interface program. When this program completes the numerical analysis, it automatically starts the BBDPLOT.EXE program. |
| BBDPLOT.EXE | This is the interactive BABERDYN plotting program. It is run automatically by the BABERDYN.EXE program upon successful completion of a numerical analysis. You can also run it directly from the DOS command line, in which case it will prompt you for the base file name of your plot data file set (sequentially numbered fname.F01 thru fname.F11). When you exit this program you will always be returned to the DOS prompt. |
| MCFRIC.EXE | This is a ball bearing traction analysis program. It is run from the DOS command line. See the Appendix of this manual for more information on this program. |

8.4. Starting The Program

Before running BABERDYN-II, you must run BASDREL to generate certain important parameters that are a function of the bearing design and external load conditions. Data generated by BASDREL can be automatically passed into BABERDYN-II when the user specifies the quasi-static data file to use.

To run BABERDYN, do the following:

1. Turn on your computer system.
2. Go to the drive and directory where you wish to store your input and output files.

3. Start up BABERDYN2 by entering the complete path name to where the BABRDYN2.EXE file is located. For example:

`\BEARING\BABRDYN2 <Enter>`

If the directory containing BABRDYN2.EXE is in your PATH definition, then you do not need to type the whole directory name. See your DOS manual for more information on directories and PATH.

4. The opening screen allows you to choose between running BASDREL or BABERDYN. Select the BABERDYN option with your mouse by simply clicking on the word BABERDYN. Or, with a keyboard, press the `<Tab>` key until the word BABERDYN is highlighted and press `<Enter>`.
5. When you are finished running BABERDYN, select the Exit option to exit back to the DOS prompt.

While you are executing the BABERDYN program, it can be controlled in one of two ways:

- ☐ Manual operation via menus
- ☐ AutoRun

In manual operation you must indicate to the program what you want to do by making selections from the pull-down menus. These menu items are described in the following sections. When performing an analysis for the first time, there is a certain logical progression to the menu choices. BABERDYN's Auto Run feature takes you through this progression by making the menu selections for you. Every time you start BABERDYN it starts out in Auto Run mode. Auto Run is also explained more fully in a later section. From this point, however, you can continue with Auto Run by simply making selections with your mouse or keyboard. You also can abort Auto Run at any time by turning off Auto Run from the RUN menu.

8.5. Input Field Selection and Navigation

BABERDYN comes with two types of input fields; text field and list field.

8.5.1. Text Field

You can select a specific text field for input by clicking the mouse on it or pressing the `<Tab>` key until the text gets highlighted. The text field can handle both insertion or

over-typing. The carriage return is not needed for entering the data since pressing <Tab> or <Shift> <Tab> can take you to the next or previous input field.

8.5.2. List Field

You can highlight a specific list field for selection by clicking the mouse on it or pressing the <Tab> key until the text gets highlighted. To select an item from the list, click the ↓ icon next to the list or press the (↓) or (↑) key.

8.6. Pull Down Menu System

The pull-down menu bar provides easy access to all the functionality of the program. From the pull-down menu you can open and save input data files, edit all design parameters, and run an analysis. This section describes the actions performed by each option in the menu system.

8.6.1. FILE MENU

This is a pull down menu that will allow you to 'save' and 'open' bearing data files from disk. There are also 'create' and 'exit' functions available from this menu.

8.6.1.1. FILE/CREATE Menu Item

Selecting this menu item will reset the current bearing input model to the default set stored permanently in the program. The same effect would result if you were to exit and re-enter the program.

8.6.1.2. FILE/OPEN Menu Item

Selecting this menu item will open a dialog box for retrieving a bearing input file from disk. When a valid file is retrieved from disk, the bearing model inputs appearing in the file are read into memory and will replace the current set stored in computer memory. As you work, you're actually making changes to the copy in memory. To keep your work safely on disk, you should save your data after editing.

8.6.1.3. FILE/SAVE Menu item

Selecting this menu item will save the currently stored set of model inputs to a disk file. If a file name has already been assigned, the file is overwritten.

8.6.1.4. FILE/SAVE AS Menu Item

Selecting this menu item will open a dialog box for saving the currently stored set of model inputs to a disk file. The user is expected to enter a file name, or select one from among those already on the disk. Always use a '.BBD' extension for your model input files.

8.6.1.5. FILE/EXIT Menu Item

Selecting this menu item will exit the program. All data not saved to disk is lost when you exit.

8.6.2. EDIT MENU

This is a pull down menu that allows you to edit your bearing design data. The overall bearing model is divided into nine sections. Each of these sections is accessed by a sub-item in this menu, which when selected displays a series of dialog boxes containing the inputs for that section.

When any dialog box is opened for one of the sections, it receives a copy of its values from the current bearing input model held in memory.

8.6.2.1. EDIT/CAGE INPUTS Menu Item

Selecting this menu item will open a dialog box for entering and modifying data associated with the bearing cage.

8.6.2.2. EDIT/BEARING INPUTS Menu Item

Selecting this menu item will open a dialog box for entering and modifying your bearing design data.

8.6.2.3. EDIT/FRICTION & LUBRICANT Menu Item

Selecting this menu item will open a dialog box for entering and modifying the parameters associated with the frictional forces at work in the bearing. Also in this box are the cage to ball contact stiffness coefficients.

8.6.2.4. EDIT/TRACTION DATA Menu Item

Selecting this menu item will open a series of dialog boxes for entering and modifying traction data associated with ball skidding.

8.6.2.5. EDIT/CAGE POCKET GEOMETRY Menu Item

Selecting this menu item will open a series of dialog boxes for entering and modifying the dimensions of each cage pocket. In addition to the requisite size and azimuth location of each pocket, in this box you also can enter pocket parameters specific to ball guided cage designs.

8.6.2.6. EDIT/BALL CONTACT PARAMETERS Menu Item

Selecting this menu item will open a series of dialog boxes for entering parameters related to the quasi-static loading condition of the bearing. Normally, all these inputs will be computed by BASDREL, and at the user's option can be imported automatically from a BASDREL output file.

8.6.2.7. EDIT/OPERATING CONDITIONS Menu Item

Selecting this menu item will open a dialog box for entering and modifying the operating conditions of the bearing. These include things like raceway speed, raceway and/or ball imperfections, and rotating unbalance forces and/or moments to be applied to the cage.

8.6.2.8. EDIT/INTEGRATION PARAMETERS Menu Item

Selecting this menu item will open a dialog box for entering and modifying the parameters which control the numerical integration. This includes things like simulation length, numerical error tolerance, and also initial conditions of position and velocity for the cage.

8.6.2.9. EDIT/BALL SLIP & SPIN Menu Item

Selecting this menu item will open a series of dialog boxes in which to enter the initial conditions of position and velocity for each ball.

8.6.3. RUN MENU

This section describes the options available from the RUN pull down menu.

8.6.3.1. RUN/ANALYSIS Menu Item

Selecting this menu item will start the execution of the numerical analysis. It is important to realize that the numerical program is a separate program from the GUI interface program. The numerical program will pass the file name of the input file you are currently working on within the GUI program. Therefore, if you have made any editing changes to the bearing model inputs, you will need to re-Save your input file prior to invoking the Run command.

While BABERDYN is running, it will write all output to data files which are described in the File Formats chapter of this manual. All the output files will have the same base file name as your input file name, but with different extensions. You can review the results of the analysis by inspecting the contents of these files with a file viewing or editing utility, or by running the plotting program BBDPLOT. Upon completion of the numerical analysis, the program will request permission to proceed automatically to the plotting program.

8.6.3.2. RUN/AUTO RUN Menu Item

Selecting this menu item will toggle on or off the Auto Run mode of program operation. Normally, to input data, run an analysis, and view results, the user needs to perform all appropriate actions in sequence by selecting from the pull down menus. Auto Run makes this easier by making the menu selections for you automatically. At the completion of each action, pressing <Enter> takes you to the next logical step. The program automatically goes into Auto Run when the program first starts up, and it stays in that mode until you turn it off (by selecting this menu item).

8.7. Parameter Input Dialog Boxes

All input parameters are entered via dialog boxes. All such dialog boxes are accessed via the EDIT pull down menu described earlier. These dialog boxes contain fields where you can type in your input values. The meaning of each input item is explained in this section.

8.7.1. EDIT/CAGE INPUTS Dialog Box

This dialog box accepts values for cage inputs which apply to the entire cage. A subsequent box described later is used for entering cage pocket dimensions which can be unique for each ball pocket. Figure 17 defines the cage dimension inputs.

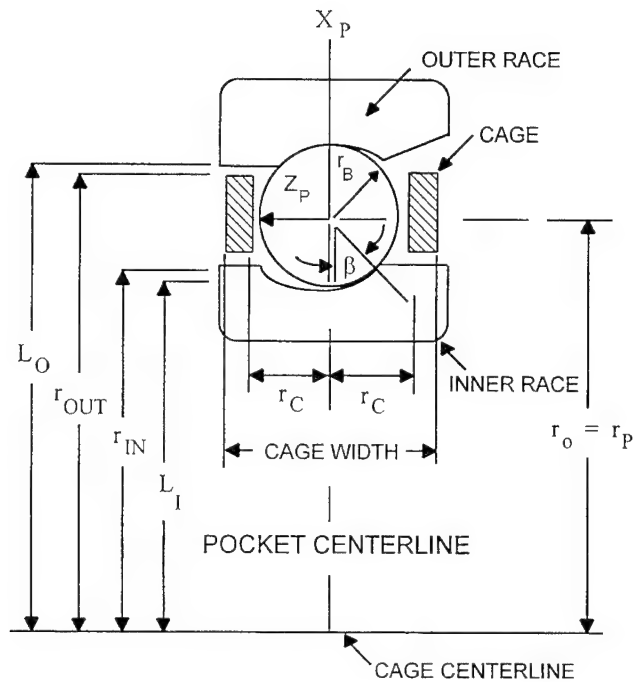


Figure 17. Cage Dimensional Inputs.

8.7.1.1. CAGE OUTER DIAMETER Field

This is the outside diameter of the cage (inches). In outer race guided cage designs this is the diameter at which the cage will contact the outer race land. For outer race guided cages, this value is used in the computation of a viscous drag torque due to the presence of lubricant within the close clearance between the cage and land.

8.7.1.2. CAGE INNER DIAMETER Field

This is the inner diameter of the cage (inches). For inner race guided cage designs this is the diameter at which the cage will contact the inner race land. For inner race guided cages, this value is used in the computation of a viscous drag torque due to the presence of lubricant within the close clearance between the cage and land.

8.7.1.3. CAGE WIDTH Field

This is the width of the cage (inches). This value is used to compute the stiffness of the cage and viscous drag torque due to the presence of lubricant.

8.7.1.4. CAGE HARDNESS Field

This is the hardness of the cage to be used for wear calculations.

8.7.1.5. CAGE WEAR COEFFICIENT Field

This is the dimensionless coefficient of abrasive wear which occurs at the contacts between the balls and cage pockets.

8.7.1.6. CAGE MASS Field

This is the translational mass of the cage (slugs). If you don't know the mass of the cage, enter zero and the program will estimate it from the cage dimensions and density assuming uniform thickness and cylindrical pockets.

8.7.1.7. CAGE ROTATIONAL INERTIA Fields

These are three fields for entering the principal mass moments of inertia for the cage (slugs-in²). If you don't know these values, entering zero for any one of them will cause the program to estimate all three from the cage dimensions and density assuming uniform thickness, cylindrical pockets and symmetry ($I_{xx}=I_{yy}$).

8.7.1.8. CAGE MATERIAL PROPERTIES Menu

Three common types of ball bearing cages are metal ribbon, crown and machine cages. The metal ribbon cage is usually made of soft stainless steel and has a large area of contact with the balls and race lands. It has a high wear rate especially when the lubricant is not thick enough (i.e., low viscosity) to separate the two mating contact surfaces. The crown cage is made of hardened stainless steel and generally outperforms a ribbon type cage in terms of wear resistance. However, the most common type of cage used for spacecraft applications and gyro instrumentations is the porous nonmetallic cage. The typical material used for nonmetallic cages are:

- laminated phenolic
- sintered nylon
- sintered polyimide

If properly vacuum-impregnated with oil, the nonmetallic cage provides several major advantages over the previously mentioned cage types, such as:

- acts as a lubricant resupply reservoir which prolongs life,
- has low friction coefficient and density, and
- has good dynamic characteristics (low stiffness, high damping).

The material properties for metal ribbon and crown cages are available in many textbooks and technical literature. Therefore, in this section only a table of nonmetallic material properties is presented (see Table 10).

Table 10. Synthetic Cage Material Properties.

| Material | Coefficient of Friction | Cage/Ball Stiffness (lb/in^{1.5}) | Elastic Modulus (psi) | Coefficient of Restitution |
|----------------------------------|--------------------------------|--|------------------------------|-----------------------------------|
| Synthane | .19 | 1400 | 162000 | .09 |
| Nitrile Acrylic Copolymer | .20 | 650 | 51000 | .24 |
| HS Dixon | .12 | 1200 | 127000 | .12 |
| L60 Dixon | .12 .48 (dry) | 900 | 84000 | .17 |
| DuPont Vespel | .17 .56 (dry) | 750 | 69000 | .20 |

8.7.1.9. DONE Button

Click on this button when you have completed entering your input values into the dialog box.

8.7.1.10. CANCEL Button

Clicking on this button will close this dialog box and remove it from the screen, canceling any changes made to any of its input fields.

8.7.2. EDIT/BEARING INPUTS Dialog Boxes

All inputs which specify the basic design of the bearing are entered in this dialog box. These inputs are described below. You can instruct the program to read many of these inputs from a BABERDYN input file by clicking on the IMPORT button. This is also described below. You will find that this is actually a two stage dialog box. The first stage box takes as input a descriptive run identifier for the analysis along with the acceleration of gravity constant. The second stage box contains various numeric input fields for entering the bearing design parameters.

8.7.2.1. BEARING DESIGN Dialog Box #1

8.7.2.1.1. RUN IDENTIFIER Field

This a string of descriptive text to identify this analysis and can be up to 80 alphanumeric characters. This text will appear in analysis output files you save to disk, and in printouts created on your printer.

8.7.2.1.2. GRAVITATIONAL ACCELERATION Field

The gravitational constant (ft/s^2) is used for two things: 1) the calculation of ball and cage inertia from your input values of weight density, and 2) to compute the weight of the cage so that the gravitational load on the cage can be applied in the minus z direction

(negative axial direction). You cannot run an analysis without the presence of the gravitational force.

8.7.2.1.3. DONE Button

Clicking on this button will close this dialog box and open the second stage box of bearing design inputs.

8.7.2.1.4. CANCEL Button

Clicking on this button will close this dialog box and remove it from the screen, and cancel any changes made to any of its input fields.

8.7.2.2. BEARING DESIGN Dialog Box #2

8.7.2.2.1. BALL DIAMETER Field

This is the diameter of the ball in inches just as it would be measured with a micrometer or caliper. This value must be greater than zero.

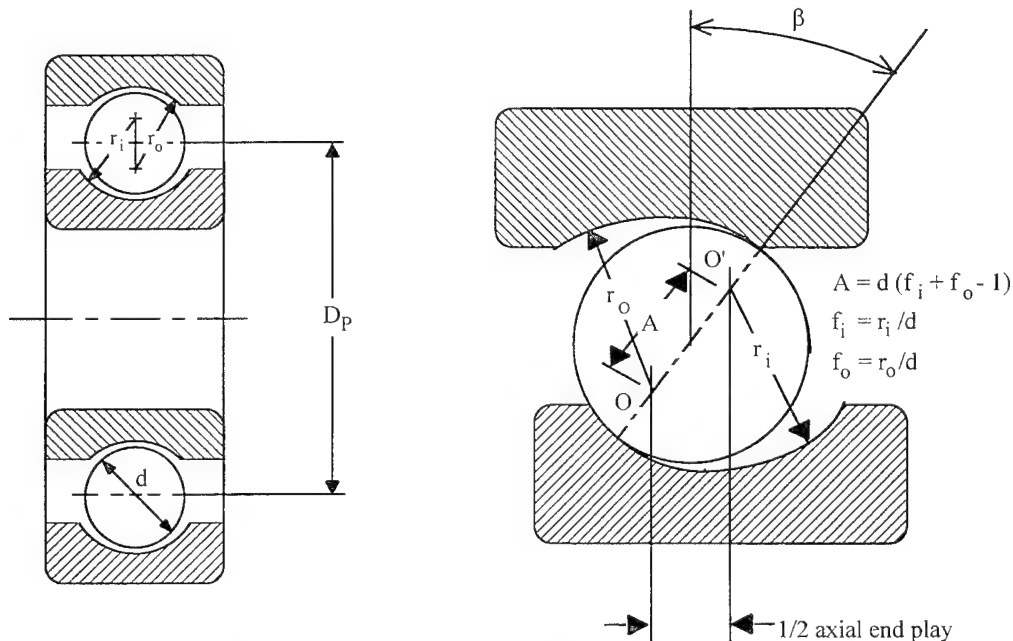


Figure 18. Illustration of Some Ball Bearing Geometry Parameters.

8.7.2.2.2. NUMBER OF BALLS Field

This is the number of rolling elements in the bearing row and must be greater than zero and not greater than 100.

8.7.2.2.3. PITCH DIAMETER Field

The pitch diameter is the diameter of the bearing, in inches, measured at the centers of the balls.

8.7.2.2.4. WORKING CONTACT ANGLE Field

This is the working, loaded contact angle, in degrees. This is the contact angle when the bearing parts are mounted on the shaft and under load. For high speed bearings with different inner and outer race contact angles, enter the average value. The contact angle can also vary around the circumference for bearings subjected to heavy radial loads. In this case, again enter an average value. The input value must not be negative.

When you select the IMPORT button, all the inner and outer race contact angles for all balls will be read from the selected BASDREL output file. The numerical average of all these values is then computed and inserted in this field.

8.7.2.2.5. INNER RACE CURVATURE Field

This is the inner race radius of curvature expressed as a fraction of the ball diameter.

8.7.2.2.6. OUTER RACE CURVATURE Field

This is the outer race radius of curvature expressed as a fraction of the ball diameter.

8.7.2.2.7. INNER RACE LAND DIAMETER Field

This is the land outside diameter of the inner race, in inches. For inner race guided cage designs, this is the diameter of the surface at which the cage contacts the inner race.

8.7.2.2.8. OUTER RACE LAND DIAMETER Field

This is the land inside diameter of the outer race, in inches. For outer race guided cage designs, this is the diameter of the surface at which the cage contacts the outer race.

8.7.2.2.9. BALL MATERIAL PROPERTIES Menu

This is a menu of material properties of a variety of commonly used bearing materials. Also in this menu are properties for more exotic materials such as ceramics. The library contains values for elastic modulus, Poisson's ratio, density and coefficient of thermal expansion. You can select a ball material from the library or input your own properties as a User Defined material. The material you specify will be used for each ball in the bearing.

8.7.2.2.10. RACEWAY MATERIAL PROPERTIES Menu

This is a menu of material properties of a variety of commonly used bearing materials. Also in this menu are properties for more exotic materials such as ceramics. The library contains values for elastic modulus, Poisson's ratio, density and coefficient of thermal expansion. You can select a raceway material from the library or input your own properties as a User Defined material. The material you specify will be used for both inner and outer raceways.

8.7.2.2.11. IMPORT Button

Clicking on the import button will open a dialog box allowing you to select a BASDREL output file. Most of the inputs described in this section will be read from the file. The only ones which are not read are the Run Identifier and Land Diameters.

8.7.2.2.12. DONE Button

Click on this button when you are finished entering your inputs in this dialog box.

8.7.2.2.13. CANCEL Button

Clicking on this button will close this dialog box and remove it from the screen, canceling any changes made to any of its input fields.

8.7.3. EDIT/FRICTION & LUBRICANT Dialog Box

In this dialog box (and the next dialog box) the user enters parameters used for modeling the friction and damping mechanisms in the bearing. In this dialog box the user specifies parameters regarding viscous and coulomb damping forces between the cage and races, and cage and balls. Likewise, contact stiffness coefficients are also specified along with the lubricant viscosity.

8.7.3.1. CAGE/RACE DAMPING COEFFICIENT Field

This is the viscous damping coefficient acting at the cage to race point of contact (lbf-s/in). This coefficient will be used for both the inner and outer raceways.

8.7.3.2. CAGE/BALL DAMPING COEFFICIENT Field

This is the viscous damping coefficient acting at the cage to ball point of contact (lbf-s/in). This coefficient will be used for each ball in the bearing.

8.7.3.3. CAGE/RACE STIFFNESS COEFFICIENT Field

This is the contact stiffness coefficient acting at the cage to race point of contact (lbf/in^{1.5}). This coefficient will be used for both the inner and outer raceways. You can enter zero for this stiffness, in which case the program will compute the value based on the closed form solution given in Chapter 5.

8.7.3.4. CAGE/BALL STIFFNESS COEFFICIENT Field

This is the stiffness coefficient acting at the cage to ball point of contact (lbf/in^{1.5}). This coefficient will be used for each ball in the bearing. You can enter zero for this stiffness, in which case the program will compute the value based on the closed form solution given in Chapter 6.

8.7.3.5. CAGE/RACE COULOMB FRICTION COEFFICIENT Field

This is the coulomb damping coefficient acting at the cage to race point of contact (dimensionless). This coefficient will be used for both the inner and outer raceways. For normal operation, the cage/race coulomb coefficient is about twice the cage/ball coefficient.

8.7.3.6. CAGE/BALL COULOMB FRICTION COEFFICIENT Field

This is the coulomb damping coefficient acting at the cage to ball point of contact (dimensionless). This coefficient will be used for each ball in the bearing. Typical values are from 0.06 to 0.1 for good lubrication, and 0.1 to 0.3 for poor lubrication such as lubricant starvation.

8.7.3.7. LUBRICANT VISCOSITY COEFFICIENT Field

This is the absolute (or dynamic) viscosity of the bearing lubricant at the operating temperature (lbf-s/in²). This parameter is used only to compute the viscous drag component of torque to be applied to the cage, and is due to the cage's close clearance with the inner (or outer) raceway for race guided cage designs.

8.7.3.8. DONE Button

Clicking on this button will close this dialog box and open the second stage dialog box which allows the user to input the ball/race traction table.

8.7.3.9. CANCEL Button

Clicking on this button will close this dialog box and remove it from the screen, canceling any changes made to any of its input fields.

8.7.4. EDIT/TRACTION DATA Dialog Box

This is a two stage dialog box in which to enter a table of traction coefficients for modeling forces occurring when the ball is skidding against the inner and/or outer raceways.

The ball-to-race traction characteristics describe the relationship between the ball-to-race slip rate and the force required to produce ball slip. This parameter can be determined experimentally in the same fashion as friction coefficients are empirically determined. The recommended method for determining the traction characteristics is by testing the balls, races and lubricant system of the bearing of interest using a ball bearing simulator as described in reference 2. Some representative traction curves are included in the Appendix, and the user may find a bearing similar to his in the included traction curves. The traction curve can also be derived from basic disk-on-disk machine test data using the methods described in reference 15. References 16 through 20 are sources for additional traction data. The traction curve can also be determined by using a program called McFric which calculates traction characteristics from lubricant properties and ball-to-raceway parameters (see Figure below).

The user has the choice of

- entering the traction data manually
- importing the traction table from a BABERDYN output file

If you wish to enter the data manually, first specify the number of points in the traction table. Then input the traction curve X-Y coordinates. The data curve is in terms of pounds of drag force per pound of normal force as a function of drag velocity. The more points input, the more accurate the analytical result. The author has found that 10 points usually give acceptable accuracy. You can obtain traction data points from references, from test results, or calculate them with the McFRIC traction analysis program available from the Air Force and described in the Appendix of this manual.

Figure 19 illustrates what a typical traction curve may look like, including the limiting lubricant shear stress phenomena.

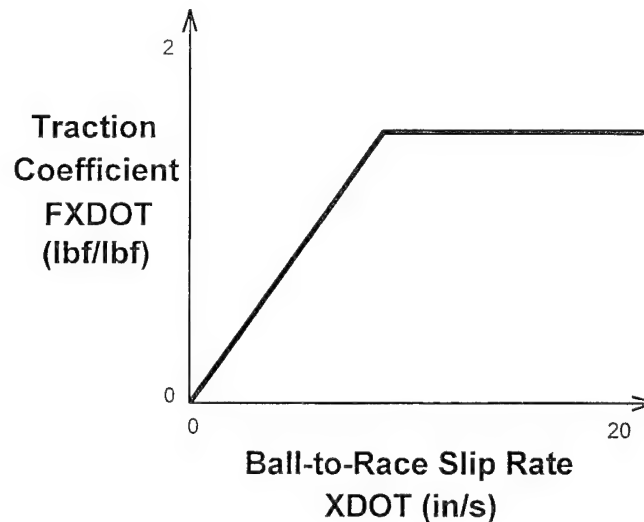


Figure 19. Representative Traction Curve, for Illustration Only.

If you wish to import the traction table, select the IMPORT button and choose a BABERDYN output file from the file selection dialog box.

8.7.4.1. Traction Data Dialog Box #1

8.7.4.1.1. Number of Points Field

Enter in this field the number of data points you wish to enter for the traction curve.

8.7.4.1.2. OK Button

Select this button, or press Enter, when you are ready to proceed to the traction data point entry dialog box.

8.7.4.1.3. CANCEL Button

Clicking on this button will close this dialog box and remove it from the screen, canceling any changes made to any of its input fields.

8.7.4.1.4. IMPORT Button

Selecting this button will open a file selection dialog box allowing you to select a BABERDYN output file from which to import a traction data table. When you perform this action the imported table will effectively replace the current table.

8.7.4.2. Traction Data Dialog Box #2

8.7.4.2.1. SLIP RATE Field

This is the slip rate velocity (in/s).

8.7.4.2.2. SLIP DRAG FORCE COEFFICIENT Field

This is the coefficient of drag force per pound of normal force (lbf/lbf).

8.7.4.2.3. NEXT Button

The dialog box displays the values for one point at a time. Clicking on this button will advance the dialog box to the next point. The number of the currently displayed point is always indicated in the box.

8.7.4.2.4. PREVIOUS Button

In a way analogous to the NEXT button, clicking on this button will back up the dialog box to the preceding point. The number of the currently displayed point is always indicated in the box.

8.7.4.2.5. DONE Button

Clicking on this button will close this dialog box.

8.7.4.2.6. CANCEL Button

Clicking on this button will close this dialog box and remove it from the screen, canceling any changes made to any of its input fields.

8.7.4.2.7. IMPORT Button

Selecting this button will open a file selection dialog box allowing you to select a BABERDYN output file from which to import a traction data table. When you perform this action the imported table will effectively replace the current table.

8.7.5. EDIT/CAGE POCKET GEOMETRY Dialog Box

The program can analyze two cage pocket configurations: ball guided and race guided (see Figure 20). The ball guided configuration requires the input of a cone angle and cylindrical pocket radius. If the cone angle is 90 degrees, the cage pocket configuration is race guided. For ball guided designs the program will also need to know the cage center-to-ball distance (see below). In addition, the program allows users to specify the angular location independently for each pocket.

BALL GUIDED CAGE

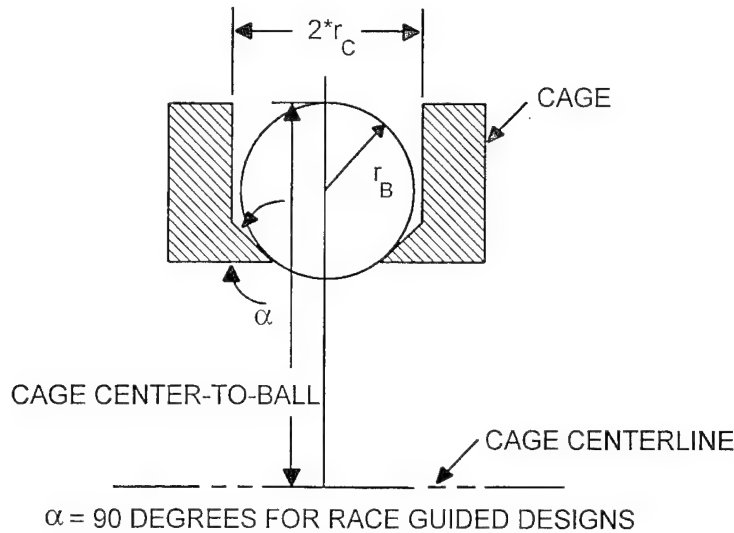


Figure 20. Illustration of Ball Cage-to-Center Parameter Necessary for Ball Guided Cage Designs.

8.7.5.1. CAGE POCKET CONE AZIMUTH ANGLE Field

This is the circumferential location of the center of the ball pocket (degrees). This value must be entered independently for each cage pocket. This allows the pockets to be located unevenly about the cage circumference.

8.7.5.2. CAGE POCKET RADIUS Field

This is the radius of the cage pocket cylinder (inches). This value can be different for each cage pocket.

8.7.5.3. CAGE POCKET CONE ANGLE Field

This is the angle of the cage pocket in ball guided cage designs and shown in Figure 2-4 (degrees). This value can be different for each cage pocket.

8.7.5.4. CAGE CENTER-TO-BALL Field

This parameter applies to ball guided cage designs. When a ball is moved radially inward until it is touching both sides of the cage pocket, this is the distance from the center of the cage to the outermost point on the ball (inches). For race guided cage designs, enter zero for this parameter.

8.7.5.5. NEXT Button

The dialog box displays the values for one ball at a time. Clicking on this button will advance the dialog box to the next ball. The number of the currently displayed ball is always indicated in the box.

8.7.5.6. PREVIOUS Button

In a way analogous to the Next button, clicking on this button will back up the dialog box to the previous ball. The number of the currently displayed ball is always indicated in the box.

8.7.5.7. DONE Button

Click on this button when you are finished entering your input values into the dialog box.

8.7.5.8. CANCEL Button

Clicking on this button will close this dialog box and remove it from the screen, canceling any changes made to any of its input fields.

8.7.6. EDIT/BALL CONTACT PARAMETERS Dialog Box

These quasi-static data are computed by the quasi-static bearing analysis program module, BASDREL. These data consist of individual ball load, ball/race stiffness, and ball/race deformation constants. The ball load is required in order to calculate the traction force at the ball/race interface during cage/race contact. The ball/race contact stiffness and deformation are required only if bearing imperfections are being included in this analysis.

8.7.6.1. BALL LOAD AT INNER RACE Field

This is the ball to inner race contact load (lbf). This value must be entered separately for each ball in the bearing.

8.7.6.2. BALL LOAD AT OUTER RACE Field

This is the ball to outer race contact load (lbf). This value must be entered separately for each ball in the bearing.

8.7.6.3. BALL/INNER RACE CONTACT STIFFNESS Field

This the ball to inner race contact stiffness (lbf/in). This value must be entered separately for each ball in the bearing.

8.7.6.4. BALL/OUTER RACE CONTACT STIFFNESS Field

This is the ball to outer race contact stiffness (lbf/in). This value must be entered separately for each ball in the bearing.

8.7.6.5. BALL/INNER RACE CONTACT DEFORMATION Field

This is the ball to inner race contact deformation (in). This value must be entered separately for each ball in the bearing.

8.7.6.6. BALL/OUTER RACE CONTACT DEFORMATION Field

This is the ball to outer race contact deformation (in). This value must be entered separately for each ball in the bearing.

8.7.6.7. NEXT Button

The dialog box displays the values for one ball at a time. Clicking on this button will advance the dialog box to the next ball. The number of the currently displayed ball is always indicated in the box.

8.7.6.8. PREVIOUS Button

In a way analogous to the NEXT button, clicking on this button will back up the dialog box to the preceding ball. The number of the currently displayed ball is always indicated in the box.

8.7.6.9. CANCEL Button

Clicking on this button will close this dialog box and remove it from the screen, canceling any changes made to any of its input fields.

8.7.6.10. IMPORT Button

The import button provides an easy way to enter the preceding group of ball loading parameters. Selecting this button will display a file selection dialog box from which you can select a BASDREL output file. The program will then attempt to read the ball loading parameters for all balls from the BASDREL output file and insert them into the fields described above.

8.7.7. EDIT/OPERATING CONDITIONS Dialog Box

In this dialog box, the user enters parameters which specify the operating conditions of the bearing. These include ball and race imperfections, rotating bias forces (and moments) to be applied to the cage, and the rotational speeds of the inner and outer races.

Race imperfection for either the inner, outer, or both races is modeled using a raceway waviness profile shown in Figure 21. The profiles are based on a wave amplitude, and the number of waves that are present around the race. These are input separately for each race. The relative phase of the waves is really like an initial condition, since usually the inner race is turning while the outer race is stationary.

Ball imperfections are modeled as a random distribution of ball size. The user specifies the minimum and maximum allowable ball size, and the program uses a uniform variate random number generator to select a diameter between these limits for each ball.

In some advanced cage design applications, a centrifugally induced bias force or moment is used to enhance cage stability. By introducing induced biased forces or moments on the cage, the cage can be virtually locked sideways onto the balls, which in turn reduces the possibility of cage instability. The program allows input of completely general force and moment vectors which will act at the cage center, and rotate with it. In practice controlled amounts of these forces can be produced by introducing careful amounts of mass center unbalance to the cage.

Example of 4 lobe imperfection from profilometry data

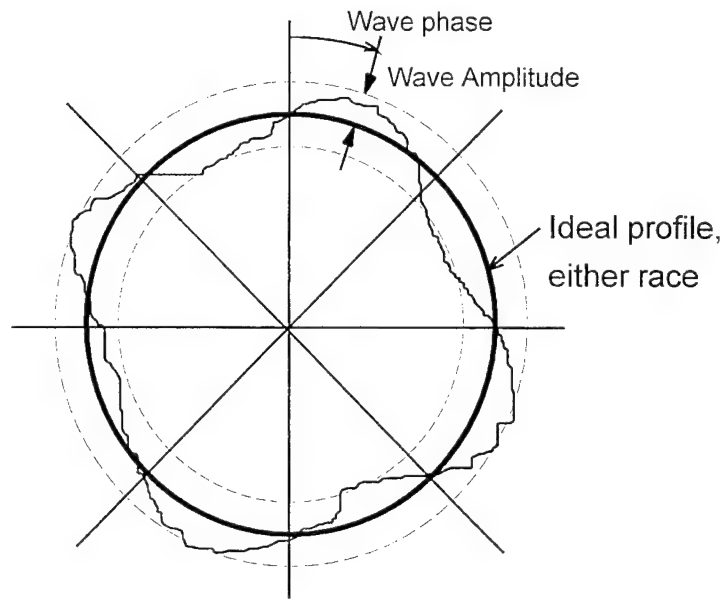


Figure 21. Race Profile Imperfection Representation

8.7.7.1. OUTER RACE WAVE AMPLITUDE Field

In this field enter the zero to peak amplitude of the sine wave for the outer race surface imperfection (inches). See the above figure.

8.7.7.2. INNER RACE WAVE AMPLITUDE Field

In this field enter the zero to peak amplitude of the sine wave for the inner race surface imperfection (inches). See the above figure.

8.7.7.3. OUTER RACE LOBE NUMBER Field

In this field enter the number of lobes, or waves, present on the outer race surface (dimensionless). See the above figure.

8.7.7.4. INNER RACE LOBE NUMBER Field

In this field enter the number of lobes, or waves, present on the inner race surface (dimensionless). See the above figure.

8.7.7.5. RACE PROFILE PHASE SHIFT Field

In this field enter the phase shift between the inner and outer race imperfection profiles (degrees). If you enter exactly zero for this value, the program will select one in a random fashion. This input is much like an initial condition since usually the inner race is turning while the outer race is stationary.

8.7.7.6. MINIMUM BALL SIZE Field

This value will be the lower limit on ball diameter (inches). The program uses a uniform random number generator to generate ball diameters to be used for the simulation.

8.7.7.7. MAXIMUM BALL SIZE Field

This value will be the upper limit on ball diameter (inches). The program uses a uniform random number generator to generate ball diameters to be used for the simulation.

8.7.7.8. INNER RACE SPEED Field

This is the rotational speed of the inner race given in revolutions per minute.

8.7.7.9. OUTER RACE SPEED Field

This is the rotational speed of the outer race given in revolutions per minute.

8.7.7.10. X, Y, AND Z COMPONENTS OF CAGE BIAS FORCE Fields

These three fields accept the xyz components of a constant force applied at the cage centroid, which rotates with the cage. The x and y axes are radial coordinates, and the z axis is axial.

Note that applying a force in the z axis to offset the gravitational weight of the cage will not work completely as intended. This is because the weight force is always along the inertial z axis, and the bias force is along the cage fixed z axis. These two axes will not be parallel due to the pitch and yaw rotations of the cage about the x and y axes.

8.7.7.11. X, Y AND Z COMPONENTS OF CAGE BIAS MOMENT Fields

These three fields accept the xyz components of a constant moment applied at the cage centroid, which rotates with the cage. The z component of bias force would generally be zero.

8.7.7.12. DONE Button

Click on this button when you are finished entering your input values into the dialog box.

8.7.7.13. CANCEL Button

Clicking on this button will close this dialog box and remove it from the screen, canceling any changes made to any of its input fields.

8.7.8. EDIT/INTEGRATION PARAMETERS Dialog Box

In this dialog box the user specifies parameters controlling the numerical simulation. This includes start and stop times for the integration, the allowable truncation error, and initial conditions of position and velocity for the cage and balls with respect to the cage. When desired, the program can be instructed to read the initial conditions from a BABERDYN output file and insert them into the appropriate dialog box.

8.7.8.1. SIMULATION START TIME Field

In this field enter the start time for the numerical integration in seconds. Most often the start time will be zero seconds.

8.7.8.2. SIMULATION FINAL TIME Field

In this field enter the final time for the numerical integration in seconds. Selecting this value to allow for 3 or 4 complete revolutions of the shaft will usually give good steady state results by the end of the simulation.

8.7.8.3. GLOBAL TRUNCATION ERROR Field

The integration time step size is variable; the user is to specify a global truncation error parameter. A typical value is $1.e-5$. Specifying a smaller value will increase the accuracy of the numerical integration but will require more computer time. The user may experiment with this value to test the effect on the simulation results. Some generic tests have suggested that entering this value as less than $1.e-7$ will increase the computer time drastically without significantly improving the accuracy.

8.7.8.4. CAGE XYZ INITIAL POSITION Fields

In these three fields enter the inertial XYZ components of the initial position of the cage (inches). This value can be read from a file; see below.

8.7.8.5. CAGE XYZ INITIAL ROTATION Fields

In these three fields enter the inertial XYZ components of the initial rotation of the cage (radians). This value can be read from a file; see below.

8.7.8.6. CAGE XYZ INITIAL VELOCITY Fields

In these three fields enter the inertial XYZ components of the initial velocity of the cage (inches/s). This value can be read from a file; see below.

8.7.8.7. CAGE XYZ INITIAL ANGULAR VELOCITY Fields

In these three fields enter the inertial XYZ components of the initial angular velocity of the cage (radians/s). This value can be read from a file; see below.

8.7.8.8. IMPORT Button

The import button provides an easy way to enter the preceding group of cage initial conditions. Selecting this button will display a file selection dialog box from which you can select a BABERDYN output file. The program will then attempt to read the final conditions from the output file and insert them into the fields described above.

8.7.8.9. DONE Button

Click on this button when you are finished entering your input values into the dialog box.

8.7.8.10. CANCEL Button

Clicking on this button will close this dialog box and remove it from the screen, canceling any changes made to any of its input fields.

8.7.9. EDIT/BALL SLIP & SPIN Dialog Box

This is a series of dialog boxes which allow the user to specify the initial conditions for ball spinning and slipping. The numerical simulation will attain a steady state solution more quickly if given a good set of initial conditions. When desired, the program can be instructed to read the final conditions from a BABERDYN output file and insert them into the dialog boxes as initial conditions for this analysis.

In the analytical bearing model, the state of each ball is described by two degrees of freedom. First is a pure circumferential slip displacement relative to where the ball would be if it were purely rolling and not slipping (i.e., the center of the pocket). Second is a spin rotation angle that is necessary because the balls pick up spin components from rubbing against the sides of the pockets.

The ball spin position initial value is actually not significant since the balls are perfect spheres. Changing just the spin initial position will never change the results of a simulation. The ball spin initial velocity, of course, is important because of the viscous and coulomb damping forces generated at the points of cage/ball contact.

8.7.9.1. BALL SLIP INITIAL POSITION Field

In this field enter the initial slip position (inches).

8.7.9.2. BALL SLIP INITIAL VELOCITY Field

In this field enter the initial slip velocity (in/s).

8.7.9.3. BALL SPIN INITIAL POSITION Field

In this field enter the initial spin position (radians).

8.7.9.4. BALL SPIN INITIAL VELOCITY Field

In this field enter the initial spin velocity (rad/s).

8.7.9.5. NEXT Button

The dialog box displays the values for one ball at a time. Clicking on this button will advance the dialog box to the next ball. The number of the currently displayed ball is always indicated in the box.

8.7.9.6. PREVIOUS Button

In a way analogous to the NEXT button, clicking on this button will back up the dialog box to the preceding ball. The number of the currently displayed ball is always indicated in the box.

8.7.9.7. IMPORT Button

The import button provides an easy way to enter the preceding group of ball initial conditions. Selecting this button will display a file selection dialog box from which you can select a BABERDYN output file. The program will then attempt to read the final conditions for all balls from the output file and insert them into the fields described above.

8.7.9.8. DONE Button

Click on this button when you are finished entering your input values into the dialog box.

8.7.9.9. CANCEL Button

Clicking on this button will close this dialog box and remove it from the screen, canceling any changes made to any of its input fields.

9. DATA FILE FORMATS

The BABERDYN program reads its input from a disk file and writes its outputs to a number of different disk files. Technically, one could create an input file with almost any text editor, and run BABERDYN from the DOS command line. However, it is much easier to use the GUI program to create and edit your input files, and run the analysis program. The next chapter describes the GUI front end and explains all the program input variables and options. This chapter explains the format of the input file created by the 'SAVE' option in the GUI, which is needed to perform an analysis. This chapter also explains the basic formats of the various output files which are written while the program executes.

9.1. INPUT DATA FILE NOMENCLATURE

The following nomenclature is defined for easy cross reference in the next section which defines the input data file format. Full detail on each of these input variables can be found in the chapter on how to use the GUI.

| | | |
|---------|---|---|
| TITLE 1 | = | Alphanumeric string to appear in program output, up to 80 characters long. |
| TITLE 2 | = | Alphanumeric string to appear in program output, up to 80 characters long. |
| PITDIA | = | Ball orbit pitch diameter (in) |
| BALLDIA | = | Ball diameter (in) |
| LIND | = | Land inner diameter (in) |
| LOUTD | = | Land outer diameter (in) |
| FI, FO | = | Ratio of transverse radius of inner and outer ball races to ball diameter respectively (Dimensionless) |
| NBALL | = | Number of balls in the bearing (dimensionless). |
| ANGLE | = | Nominal angular location of the i-th ball (degree) |
| ROUTD | = | Retainer outer diameter (in) |
| RIND | = | Retainer inner diameter (in) |
| RETW | = | Retainer width (in) |
| CYLDIA | = | Diameter of the i-th retainer pocket (in) |
| ALPHA | = | Cone angle of the i-th retainer pocket (degree) |
| CTB | = | Distance from cage center to outermost point on a ball when the ball is pushed inwards to contact all sides of its cage pocket (in) |

| | | |
|--|---|---|
| RETPOIS, RETYLD, RETD RETTITL | = | Poisson's ratio, modulus of elasticity, density , and descriptive title of cage material, respectively (dimensionless), (lbf/in ²), lbf/in ³) |
| RHRDNS | = | Cage hardness |
| RWCOEFF | = | Cage abrasive wear coefficient |
| BALLPOIS, BALLYLD, BALLD BALLTITL | = | Poisson's ratio, modulus of elasticity, density , and descriptive title of ball material, respectively (dimensionless), (lbf/in ²), lbf/in ³) |
| LANDPOIS, LANDD LANDTITL | = | Poisson's ratio, density , and descriptive title of land material, respectively (dimensionless), lbf/in ³) |
| RETMS | = | Cage mass (lbf) |
| RINER(1,2,3) | = | Cage principle second moments of inertia |
| G | = | Gravity (ft/sec ²) |
| CL | = | Viscous damping coefficient between cage and race (lbf-sec/in) |
| CB | = | Viscous damping coefficient between cage and ball (lbf-sec/in) |
| KBALL | = | Contact stiffness between cage and ball (lbf/in ^{1.5}) |
| KRACE | = | Contact stiffness between cage and race (lbf/in ^{1.5}) |
| MURC | = | Coulomb friction coefficient between cage and race (dimensionless) |
| MUBC | = | Coulomb friction coefficient between cage and ball (dimensionless) |
| YLUB | = | Lubricant viscosity (lbf-s/in ²) |
| LUBNAME | = | Lubricant name, up to 40 characters |
| LUBNOTE | = | Lubricant note, up to 60 characters |
| NPT | = | Number of points in the traction coefficient table to be entered next |
| XDOT | = | Slip velocity of ball on race (in/sec) |
| FXDOT | = | Traction coefficient (lbf/lbf) enter XDOT and FXDOT NPT times. |
| CA | = | Average loaded contact angle (degrees) |
| NORMI, NORMO | = | Contact loads at inner and outer races of i-th ball position (lbf) |
| KI, KO | = | Elastic stiffness constant at inner and outer races of i-th ball position (lbf/in ^{1.5}) |

| | | |
|---------------|---|---|
| DELI, DELO | = | Elastic normal approach at inner and outer races of i-th ball position (in) |
| BRI,BRO | = | Inner and outer race imperfection, waviness zero to peak amplitudes (in) |
| AI,AO | = | Inner and outer race imperfection, number of waves around circumference |
| PHI | = | Phase angle shift between inner and outer race imperfection profiles (degrees) |
| BMIN,BMAX | = | Min and max diameters for random ball diameter generation. |
| OMEGA0 | = | angular velocity of outer land (rpm) |
| OMEGA1 | = | Angular velocity of inner land (rpm) |
| BIFORC(1..3) | = | Rotating bias force acting at the cage center, x-axis, y-axis, and z-axis (lbf) |
| BIMOM(1..3) | = | Rotating bias moment acting at the cage center, x-axis, y-axis, and z-axis (in-lbf) |
| TFINAL | = | End of integration time period (sec) |
| TINIT | = | Start of integration time period (sec) |
| EPSILON | = | Specified global integration error tolerance |
| VAR(4..6) | = | Initial cage displacement in the x, y, and z direction respectively (in) |
| VAR(10..12) | = | Initial cage rotation in the x, y, and z direction respectively (radians) |
| DERIV(4..6) | = | Initial cage velocity the x, y, and z direction respectively (in/s) |
| DERIV(10..12) | = | Initial cage angular velocity in the x, y, and z direction respectively (rad/s) |
| SLIP | = | Initial slip position of the i-th ball from the nominal position (in) |
| SLIPDOT | = | Initial slip velocity of the i-th ball (in/s) |
| SPIN | = | Initial spin position of the i-th ball from the nominal position (radians) |
| SPINDOT | = | Initial spin velocity of the i-th ball (rad/s) |

9.2. SAMPLE INPUT DATA FILE

The format of a BABERDYN input file is best illustrated by example. The following sample input file shows that the file is a simple ASCII text file which can be created and edited with a simple text editor like the Microsoft DOS 5.0 EDIT.EXE program or the Windows NOTEPAD.EXE program. All data items are read in free format by the program. This means that character string inputs do not need quote symbols, and floating point numeric inputs can optionally use 'E' format. The line structure of the file is important. Data items grouped together on a line must always appear on that line in the order shown. Blanks serve as separators (do not use commas), so any input that is zero must be explicitly entered as such.

If you choose to use the direct file editing approach to performing your work, it becomes extra important to double check the input section of the resulting output files to be sure that the program correctly interpreted your inputs.

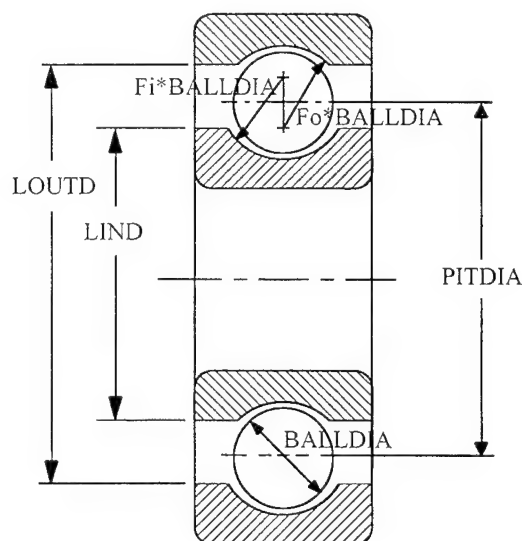


Figure 2 2. Illustration of Some Ball Bearing Geometry Parameters.

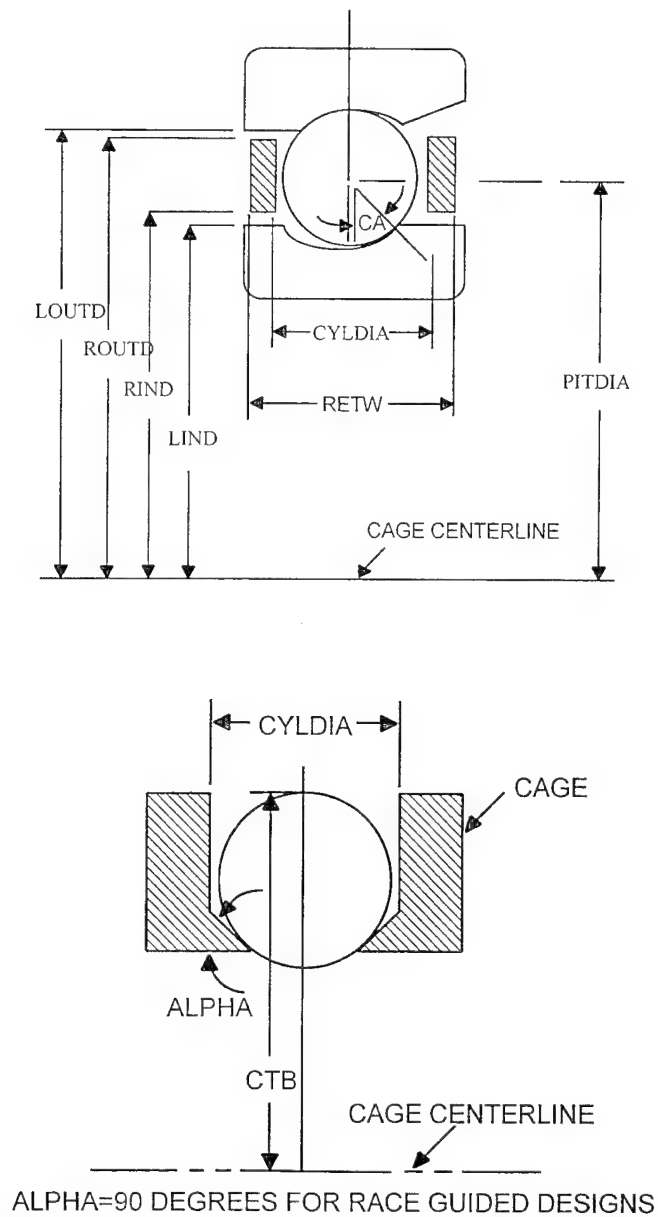


Figure 23. Illustration of Additional Bearing Geometry Parameters.

SAMPLE INPUT DATA FILE

| | | | | | | | | | | |
|---------------------|----------|---------|--------|--------|-----|-------|---|--|--|--|
| Test Sample | | | | | | | | | | TITLE1 |
| 07-21-1993 | 14:24:48 | | | | | | | | | TITLE2 |
| 1.868 | 1.576 | .635 | .4688 | 1.565 | 2.6 | 1 | | | | ROUTD,RIND,RETWIDTH,BALLDIA,LIND,LOUTD,1 |
| .53 | | .52 | | | 10 | 1.743 | | | | FI,FO,NBALL,PITDIA |
| 0 | | .48 | | | 90 | .8715 | | | | ANGLE(i),CYLDIA(i),ALPHA(i),CTB(i) |
| 36 | | .48 | | | 90 | .8715 | | | | " |
| 72 | | .48 | | | 90 | .8715 | | | | " |
| 108 | | .48 | | | 90 | .8715 | | | | " |
| 144 | | .48 | | | 90 | .8715 | | | | " |
| 180 | | .48 | | | 90 | .8715 | | | | " |
| 216 | | .48 | | | 90 | .8715 | | | | " |
| 252 | | .48 | | | 90 | .8715 | | | | " |
| 288 | | .48 | | | 90 | .8715 | | | | " |
| 324 | | .48 | | | 90 | .8715 | | | | " |
| 700000 | .3 | .046 | 10000 | .00075 | 17 | | | | | RETYLD,RETPOIS,RETD,RHRDNS,RWCOEFF |
| 2.9E+07 | .3 | | | .28 | 1 | | | | | BALLYLD,BALLPOIS,BALLD |
| 2.9E+07 | .3 | | | 1 | | | | | | LANDYLD,LANDPOIS |
| 0 | 0 | 0 | 0 | 0 | 0 | | | | | RETMS,RINER(1..3) |
| 32.2 | .025 | .025 | 2500 | 1300 | .2 | .1 | 0 | | | G,CL,CB,KBALL,KRACE,MUBC,MURC,YLUB |
| Test Lubricant | | | | | | | | | | LUBNAME |
| Lubricant Note Test | | | | | | | | | | LUBENOTE |
| 3 | | | | | | | | | | NPT |
| 0 | 0 | | | | | | | | | XDOT(i),FXDOT(i) |
| 3.3 | .036 | | | | | | | | | " |
| 90 | .036 | | | | | | | | | " |
| 12.6 | | | | | | | | | | CA |
| 25 27 | 1000000 | 1000000 | .00001 | .00001 | | | | | | NORMI,NORMO,KI,KO,DELI,DELO |
| 24 26 | 1000000 | 1000000 | .00001 | .00001 | | | | | | " |
| 20 22 | 1000000 | 1000000 | .00001 | .00001 | | | | | | " |
| 16 18 | 1000000 | 1000000 | .00001 | .00001 | | | | | | " |
| 13 15 | 1000000 | 1000000 | .00001 | .00001 | | | | | | " |
| 12 14 | 1000000 | 1000000 | .00001 | .00001 | | | | | | " |
| 13 15 | 1000000 | 1000000 | .00001 | .00001 | | | | | | " |
| 16 18 | 1000000 | 1000000 | .00001 | .00001 | | | | | | " |
| 20 22 | 1000000 | 1000000 | .00001 | .00001 | | | | | | " |
| 24 26 | 1000000 | 1000000 | .00001 | .00001 | | | | | | " |
| .000005 | .000005 | 4 | 4 | 0 | | | | | | BRO,BRI,AO,AI,PHI |
| .4688 | .4688 | | | | | | | | | BMIN,BMAX |
| 0 | 6000 | | | | | | | | | OMAGAO,OMEGAI |
| 0 | 0 | 0 | 0 | 0 | 0 | 0 | | | | BIFORC(1..3),BIMOM(1..3) |
| .10 | 0 | .0001 | | | | | | | | TFINAL,TINIT,EPSILON |
| .0002 | 0 | 0 | | | 0 | 0 | 0 | | | VAR(4..6, 10..12) |
| 0 | 1 | 0 | | | 0 | 0 | 0 | | | DERIV(4..6, 10..12) |
| 0 | 0 | 0 | | | 0 | | | | | SLIP(i),SLIPDOT(i),SPIN(i),SPINDOT(i) |
| 0 | 0 | 0 | | | 0 | | | | | " |
| 0 | 0 | 0 | | | 0 | | | | | " |
| 0 | 0 | 0 | | | 0 | | | | | " |
| 0 | 0 | 0 | | | 0 | | | | | " |
| 0 | 0 | 0 | | | 0 | | | | | " |
| 0 | 0 | 0 | | | 0 | | | | | " |
| 0 | 0 | 0 | | | 0 | | | | | " |
| 0 | 0 | 0 | | | 0 | | | | | " |
| 0 | 0 | 0 | | | 0 | | | | | " |
| 0 | 0 | 0 | | | 0 | | | | | " |
| 0 | 0 | 0 | | | 0 | | | | | " |
| Steel Type 440-C | | | | | | | | | | BALL MATERIAL TITLE |
| User Defined Mat'l | | | | | | | | | | CAGE MATERIAL TITLE |
| Steel Type 440-C | | | | | | | | | | LAND MATERIAL TITLE |

9.3. OUTPUT DATA FILE FORMATS

When the program BABERDYN executes, it writes data to 13 different files. These files are described as follows:

- Primary printed output file using a name and extension you specify. The contents of this file are described in detail in the next section.
- A plot data file always named `fname.CAG`, where `fname` is a file name specified by the user at the time the analysis is run. This file contains 8 columns of values. The first 6 columns are the inertial displacement and rotation of the cage not including the gross rotation, the 7th column is the gross rotation of the cage (i.e., $\omega_c t$), and the 8th column is the gross rotation of the shaft (i.e., $\omega_s t$). One line of data is written to this file approximately 25 times per cage revolution. This file is useful for performing 3D animations of computed cage motion.

The next 11 plot data files are read by the BABERDYN plotting program, BBDPLOT, to produce 11 different plot frames.

- A plot data file named `fname.F01`, where `fname` is a file name specified by the user at the time the analysis is run. This file contains 4 columns of values. The 1st column is the instantaneous integration time, the remaining columns are the lateral displacements of the cage in cage fixed coordinates. This file is read by the separate BABERDYN plotting program to produce plot frame number 1.
- A plot data file named `fname.F02`, where `fname` is a file name specified by the user at the time the analysis is run. This file contains 4 columns of values. The 1st column is the instantaneous integration time, the remaining columns are the rotational displacements of the cage in cage fixed coordinates, in degrees. This file is read by the separate BABERDYN plotting program to produce plot frame number 2.
- A plot data file named `fname.F03`, where `fname` is a file name specified by the user at the time the analysis is run. This file contains 5 columns of values. The 1st column is the instantaneous integration time, the remaining columns are: PXX, PYY, PZZ, and VSLIDE. PXX would be the output of a displacement transducer measuring the displacement of the cage's midplane in the inertial X axis. PYY is the same but for the inertial Y axis. PZZ would be the output of a transducer measuring the axial motion of the cage at a point near the cage OD, and situated along the inertial X axis. VSLIDE is the relative sliding velocity between the cage and race. It is used to compute the viscous drag torque on the cage due to the lubricant, and is present in the file for information only. This file is read by the separate BABERDYN plotting program to produce plot frame number 3.
- A plot data file named `fname.F04`, where `fname` is a file name specified by the user at the time the analysis is run. This file contains 4 columns of values. The 1st column is the instantaneous integration time, the remaining columns are: AVG, TNOISE, and RWORK(11). AVG is the cage power dissipation due to cage impact and viscous drag (milliwatt). TNOISE is

the bearing's running torque induced by cage impact and viscous drag (in-lb). RWORK(11) is the current integration step size. This file is read by the separate BABERDYN plotting program to produce plot frame number 4.

- A plot data file named fname.F05, where fname is a file name specified by the user at the time the analysis is run. This file contains 4 columns of values. The 1st column is the instantaneous integration time, the remaining columns are the BFORCE(1..3) for ball number NBALL. BFORCE are the components of ball/cage impact force for ball number 1 resolved in the cage pocket coordinate system (lbf). This file is read by the separate BABERDYN plotting program to produce plot frame number 5.
- A plot data file named fname.F06, where fname is a file name specified by the user at the time the analysis is run. This file contains 4 columns of values. The 1st column is the instantaneous integration time, the remaining columns are the BFORCE90(1..3) for ball number N2BALL. BFORCE90 are analogous to BFORCE but for a ball approximately 90 degrees from ball number one. This file is read by the separate BABERDYN plotting program to produce plot frame number 6.
- A plot data file named fname.F07, where fname is a file name specified by the user at the time the analysis is run. This file contains 4 columns of values. The 1st column is the instantaneous integration time, the remaining columns are the PWEAR(1) the wear volume for cage pocket #1, PWEAR(N2BALL) the wear volume for cage pocket 90 degrees from #1, and CRWEAR(2) the cage circumferential wear volume. This file is read by the separate BABERDYN plotting program to produce plot frame number 7.
- A plot data file named fname.F08, where fname is a file name specified by the user at the time the analysis is run. This file contains 4 columns of values. The 1st column is the instantaneous integration time, the remaining columns are the VAR(ISL1), VAR(ISL2), and DERIV(ISL2). These are the slip coordinate position, velocity and acceleration for ball number one. This file is read by the separate BABERDYN plotting program to produce plot frame number 8.
- A plot data file named fname.F09, where fname is a file name specified by the user at the time the analysis is run. This file contains 4 columns of values. The 1st column is the instantaneous integration time, the remaining columns are the TCBFORCE(1..3). TCBFORCE is the net of all ball/cage impact forces resolved in the rotating coordinate system rotating at the nominal cage speed. This file is read by the separate BABERDYN plotting program to produce plot frame number 9.
- A plot data file named fname.F10, where fname is a file name specified by the user at the time the analysis is run. This file contains 4 columns of values. The 1st column is the instantaneous integration time, the remaining columns are the FORCE(1..3). FORCE is the same as TCBFORCE with the addition of cage/race contact forces and viscous drag, if any. This file is read by the separate BABERDYN plotting program to produce plot frame number 10.
- A plot data file named fname.F11, where fname is a file name specified by the user at the time the analysis is run. This file contains 4 columns of values. The 1st column is the

instantaneous integration time, the remaining columns are the DELMIT, DELMOT, and DELM. DELMIT is the perturbation in torque due to the balls running over the imperfections on the inner race. DELMOT is for the outer race imperfections. DELM is the sum of these two. This file is read by the separate BABERDYN plotting program to produce plot frame number 11.

9.4. DESCRIPTION OF PRIMARY OUTPUT DATA FILE

A sample BABERDYN primary output file is shown at the end of this section. The file consist of two parts: 1) your input values including default input values computed for you, and 2) results of the bearing dynamics simulation. Be aware that the primary output file contains only summary-like information pertaining to the numerical simulation. For detailed information on bearing behavior during the simulation, please use the post processor plotting program.

Header: This is a display of the program version number and other similar information.

Inputs: This is a summary of your input values. It should exactly reflect the values you entered into the input file by using either the GUI or a file editor.

Calculated Constants: This section of the output file shows values calculated for various constants. These include:

- ball mass - this is always calculated from the ball diameter and density
- cage mass - this is calculated only if your input is zero
- cage moments of inertia - all 3 are computed if any one is input as zero
- cage speed - computed from your input value of average contact angle
- ball spin speed - computed from your input value of average contact angle
- ball number $\approx 90^\circ$ from ball 1 - results for these two balls are used by the plotting program
- cage/inner land relative velocity - used for damping force calculations (inner race speed - WBR)
- cage/outer land relative velocity - used for damping force calculations (WBR - outer race speed)
- cage/inner land radial clearance - used for damping force calculations
- cage/outer land radial clearance - used for damping force calculations
- raceway guide flag - indicates which race will guide the cage for race guided designs: +1 if cage/inner race clearance is larger than cage/outer race clearance; -1 if cage/inner race clearance is smaller than cage/outer race clearance; and 0 if clearances are equal
- omega for race - equals the land relative velocity for the land with the smaller clearance
- cage radius used - either inner or outer cage radius, used with the above omega value
- race radius used - either inner or outer land radius, used with the above omega value
- viscous moment term - coefficient of a constant drag torque on the cage due to lubricant in the close clearance between the cage and raceway land for race guided

cages; the actual drag torque is the product of this value and the sliding velocity in in/s.

Simulation Output: This section of the output file summarizes some of the results of the numerical simulation. These include:

- integration statistics
- damping summary table - this gives an indication of what segments of the traction force curve were utilized the most during the simulation
- cage/race collisions summary - for race guided designs this is the number of time steps in which the cage/race contact force was nonzero
- final cage state vector - this is useful as an initial state vector for a subsequent simulation
- final ball state vector - this is useful as an initial state vector for a subsequent simulation
- cage wear summary - this summarizes the wear of the *cage* within each pocket (linear wear model of Archad) and against each race land. NOTE: ball and race wear are not part of this output

SAMPLE OUTPUT FILE

AVCON-ADVANCED CONTROLS TECHNOLOGY, INC
COPYRIGHT 1993

BABERDYN : BEARING CAGE DYNAMIC PROGRAM

THE FOLLOWING ARE INCLUDED IN THE MODEL:

- * RETAINER-RACEWAY INTERACTION, BALL SLIPPING & SPINNING EFFECTS
- * COMPUTATION OF TORQUE NOISE, IMPERFECTION OF RACE EFFECTS
- * VISCOUS DAMPING EFFECTS, AND HERTIZIAN CONTACT STIFFNESS
- * BALL AND RACE IMPERFECTION MODEL

DATE : 07/22/93

TIME 11:14:05

*** BEARING CONSTANTS ***

| | |
|------------------------------|--------------|
| PITCH DIAMETER= | 1.00000 INCH |
| AVERAGE CONTACT ANGLE= | 12.6 DEGREE |
| OUTER RACE ANGULAR VELOCITY= | 0.000 RPM |
| INNER RACE ANGULAR VELOCITY= | 6000.000 RPM |

*** BEARING CAGE DATA ***

| | |
|------------------------|---------------------------------|
| CAGE OUTER DIAMETER= | 1.86800 INCH |
| CAGE INNER DIAMETER= | 1.57600 INCH |
| CAGE WIDTH= | 0.63500 INCH |
| CAGE YOUNGS MODULUS= | 700000.00000 LB/IN ³ |
| CAGE POISSON RATIO= | 0.30000 |
| CAGE DENSITY= | 0.04600 LB/IN ³ |
| CAGE HARDNESS= | 10000.00000 LB/IN ² |
| CAGE WEAR COEFFICIENT= | 0.00075 |

*** CAGE POCKET DATA ***

| POCKET | ANGLE | CYL DIA | ALPHA | CTR |
|--------|-------|---------|-------|--------|
| 1 | 0.0 | 0.4800 | 90.00 | 0.8715 |

| | | | | |
|----|-------|--------|-------|--------|
| 2 | 36.0 | 0.4800 | 90.00 | 0.8715 |
| 3 | 72.0 | 0.4800 | 90.00 | 0.8715 |
| 4 | 108.0 | 0.4800 | 90.00 | 0.8715 |
| 5 | 144.0 | 0.4800 | 90.00 | 0.8715 |
| 6 | 180.0 | 0.4800 | 90.00 | 0.8715 |
| 7 | 216.0 | 0.4800 | 90.00 | 0.8715 |
| 8 | 252.0 | 0.4800 | 90.00 | 0.8715 |
| 9 | 288.0 | 0.4800 | 90.00 | 0.8715 |
| 10 | 324.0 | 0.4800 | 90.00 | 0.8715 |

*** BEARING RACE DATA ***

LAND INNER DIAMETER= 1.56500 INCH
 LAND OUTER DIAMETER= 2.60000 INCH
 OUTER RACE CURVATURE= 0.520 IN⁻¹
 INNER RACE CURVATURE= 0.530 IN⁻¹
 LAND YOUNGS MODULUS= 0.29000E+08 LB/IN³
 LAND POISSON RATIO= 0.30000
 RETAINER - INNER RACE FLAG= 0
 RETAINER - OUTER RACE FLAG= 0

*** BALL CONSTANTS ***

BALL DIAMETER= 0.46880 INCH
 NUMBER OF BALL= 10
 BALL YOUNGS MODULUS= 29000000.00000 LB/IN³
 BALL POISSON RATIO= 0.30000
 BALL DENSITY= 0.28000 LB/IN³

| BALL NO | IR LOAD LB | OR LOAD LB | KO LB/IN ^{1.5} | KI LB/IN ^{1.5} | DELO IN | DELI IN |
|---------|---------------|---------------|----------------------------|----------------------------|------------|------------|
| 1 | 25.00 | 27.00 | 0.1E+07 | 0.1E+07 | 0.1E-04 | 0.1E-04 |
| 2 | 24.00 | 26.00 | 0.1E+07 | 0.1E+07 | 0.1E-04 | 0.1E-04 |
| 3 | 20.00 | 22.00 | 0.1E+07 | 0.1E+07 | 0.1E-04 | 0.1E-04 |
| 4 | 16.00 | 18.00 | 0.1E+07 | 0.1E+07 | 0.1E-04 | 0.1E-04 |
| 5 | 13.00 | 15.00 | 0.1E+07 | 0.1E+07 | 0.1E-04 | 0.1E-04 |
| 6 | 12.00 | 14.00 | 0.1E+07 | 0.1E+07 | 0.1E-04 | 0.1E-04 |
| 7 | 13.00 | 15.00 | 0.1E+07 | 0.1E+07 | 0.1E-04 | 0.1E-04 |
| 8 | 16.00 | 18.00 | 0.1E+07 | 0.1E+07 | 0.1E-04 | 0.1E-04 |
| 9 | 20.00 | 22.00 | 0.1E+07 | 0.1E+07 | 0.1E-04 | 0.1E-04 |
| 10 | 24.00 | 26.00 | 0.1E+07 | 0.1E+07 | 0.1E-04 | 0.1E-04 |

*** FORCE MODEL CONSTANTS ***

GRAVITY= 32.20000 FT/SEC²
 DAMPING COEFFICIENT AT CAGE/RACE= 0.02500 LB-SEC/IN
 DAMPING COEFFICIENT AT CAGE/BALL= 0.02500 LB-SEC/IN
 COMBINED STIFFNESS AT CAGE/RACE= 1300.0 LB/IN^{1.50}
 COMBINED STIFFNESS AT CAGE/BALL= 2500.0 LB/IN^{1.11}
 FRICTION COEFFICIENT AT CAGE/RACE= 0.10000 LB/LB
 FRICTION COEFFICIENT AT CAGE/BALL= 0.20000 LB/LB

| | X DIR | Y DIR | Z DIR |
|----------------|---------|---------|---------|
| BIASED FORCE : | 0.00000 | 0.00000 | 0.00000 |
| BIASED MOMENT: | 0.00000 | 0.00000 | 0.00000 |

*** INTEGRATION CONSTANTS ***

INTEGRATION METHOD: ADVANCED GEAR WITH LOCAL ERROR CONTROL
 FINAL INTEGRATION TIME= 0.10000 SEC
 INITIAL INTEGRATION TIME= 0.00000 SEC
 LOCAL INTERGRATION TOLERANCE= 0.1E-03

*** RETAINER INITIAL STATE VECTOR ***

| | RX | RY | RZ | THETAX | THETAY | THETAZ |
|----------|-----------|-----------|-----------|-----------|-----------|-----------|
| POSITION | 0.200E-03 | 0.000E+00 | 0.000E+00 | 0.000E+00 | 0.000E+00 | 0.000E+00 |

VELOCITY 0.000E+00 0.100E+01 0.000E+00 0.000E+00 0.000E+00 0.000E+00

*** BALL & RACE IMPERFECTION DATA ***

MAXIMUM O/R PEAK-TO-PEAK VALUE 0.0000050 INCH
MAXIMUM I/R PEAK-TO-PEAK VALUE 0.0000050 INCH
NUMBER OF LOBES ON O/R 4
NUMBER OF LOBES ON I/R 4
PHASE SHIFT BETWEEN I/R AND O/R 0.00 DEGREE
MINIMUM BALL DIAMETER 0.4688000 INCH
MAXIMUM BALL DIAMETER 0.4688000 INCH

*** TRACTION DATA ***

LUBRICANT NAME : Test Lubricant

NOTE :Lubricant Note Test

LUBRICANT VISCOSITY= 0.00000 LB-SEC/IN^2

| J | XDOT (IN/SEC) | F(XDOT) (LB/LB) |
|---|------------------|--------------------|
| 1 | 0.00E+00 | 0.00E+00 |
| 2 | 0.33E+01 | 0.36E-01 |
| 3 | 0.90E+02 | 0.36E-01 |

BALL SLIP & SPIN INIT STATE VECTOR

| BALL | DTHETA | DTHETA DOT | SPIN | SPIN DOT |
|------|-----------|------------|-----------|-----------|
| 1 | 0.000E+00 | 0.000E+00 | 0.000E+00 | 0.000E+00 |
| 2 | 0.000E+00 | 0.000E+00 | 0.000E+00 | 0.000E+00 |
| 3 | 0.000E+00 | 0.000E+00 | 0.000E+00 | 0.000E+00 |
| 4 | 0.000E+00 | 0.000E+00 | 0.000E+00 | 0.000E+00 |
| 5 | 0.000E+00 | 0.000E+00 | 0.000E+00 | 0.000E+00 |
| 6 | 0.000E+00 | 0.000E+00 | 0.000E+00 | 0.000E+00 |
| 7 | 0.000E+00 | 0.000E+00 | 0.000E+00 | 0.000E+00 |
| 8 | 0.000E+00 | 0.000E+00 | 0.000E+00 | 0.000E+00 |
| 9 | 0.000E+00 | 0.000E+00 | 0.000E+00 | 0.000E+00 |
| 10 | 0.000E+00 | 0.000E+00 | 0.000E+00 | 0.000E+00 |

CALCULATED CONSTANTS

BALL MASS= 0.46910E-03 SLUG
CAGE MASS= 0.33907E-03 SLUG
CAGE MOMENT OF INERTIA
Ixx= 0.13798E-03
Iyy= 0.13798E-03
Izz= 0.25317E-03
WBR= 170.42841 RAD/SEC
WBMAG= -529.86576 RAD/SEC
N2BALL= 3
DELTA OMEGA FOR INNER RACE= 457.89041 RAD/SEC
DELTA OMEGA FOR OUTER RACE= -170.42841 RAD/SEC
CAGE/INNER RACE RAD. CLEARANCE= 0.00550 IN
CAGE/OUTER RACE RAD. CLEARANCE= 0.36600 IN
RACE FLAG= -1 -1 INNER RACE GUIDED
1 OUTER RACE GUIDED

*** FOR OIL LUBRICANT: ***

OMEGA FOR RACE= 457.89041 RAD/SEC
RETAINER RADIUS USED= 0.78800 IN
RACE RADIUS USED= 0.78250 IN
VISCOS MOMENT TERM= 0.00000 LB-SEC

 *** MAX TIME REACHED, SIMULATION IS COMPLETED ***

TOTAL SIMULATION TIME = 0.100013 SEC
 TOTAL COMPUTER REAL TIME = -40445 SEC
 TOTAL NUMBER OF INTEGRATION STEPS = 57227
 TOTAL NUMBER OF DERIV EVALUATIONS = 152403
 TOTAL NUMBER OF JACOBIAN EVALS = 31432

*** DAMPING SUMMARY TABLE ***

| SEGMENT | NO. OF POINTS |
|---------|---------------|
| 1 | 3086099. |
| 2 | 1. |
| 3 | 0. |

NO. OF COLLISIONS BETWN CAGE AND RACES = 59757

*** CAGE FINAL STATE VECTOR ***

(UNITS IN INCH, IN/SEC, RAD, RAD/SEC)

| | RX | RY | RZ | THETAX | THETAY | THETAZ |
|-----|-----------|-----------|-----------|-----------|-----------|-----------|
| POS | 0.55E-02 | -0.10E-02 | 0.55E-04 | -0.22E-02 | -0.11E-01 | -0.42E-04 |
| VEL | -0.34E+00 | 0.13E+01 | -0.14E-01 | 0.24E+01 | -0.67E+00 | 0.45E+00 |

*** BALL SLIP & SPIN FINAL STATE VECTOR ***

| BALL | DTHETA | DTHETA DOT | SPIN | SPIN DOT |
|------|-----------|------------|----------|----------|
| 1 | -0.14E-03 | -0.45E-02 | 0.25E-03 | 0.22E-02 |
| 2 | -0.16E-03 | 0.98E-02 | 0.27E-03 | 0.27E-03 |
| 3 | -0.44E-04 | 0.61E-01 | 0.30E-03 | 0.18E-01 |
| 4 | -0.22E-04 | 0.48E-01 | 0.40E-03 | 0.23E-01 |
| 5 | -0.60E-04 | -0.23E-02 | 0.48E-03 | 0.82E-03 |
| 6 | -0.65E-04 | 0.11E-01 | 0.42E-03 | 0.43E-02 |
| 7 | -0.25E-04 | -0.36E-02 | 0.41E-03 | 0.34E-02 |
| 8 | 0.10E-04 | -0.90E-02 | 0.31E-03 | 0.35E-02 |
| 9 | -0.99E-04 | -0.11E-01 | 0.33E-03 | 0.84E-02 |
| 10 | 0.18E-06 | 0.51E-02 | 0.22E-03 | 0.15E-02 |

*** BEARING CAGE WEAR RESULT ****

POCKET NO. WEAR VOLUME (IN^3)

| | |
|----|----------|
| 1 | 0.32E-12 |
| 2 | 0.38E-12 |
| 3 | 0.46E-12 |
| 4 | 0.73E-12 |
| 5 | 0.59E-12 |
| 6 | 0.44E-12 |
| 7 | 0.34E-12 |
| 8 | 0.47E-12 |
| 9 | 0.77E-12 |
| 10 | 0.45E-12 |

BEARING CAGE OUTER RACE WEAR VOLUME = 0.00E+00 IN^3
 BEARING CAGE INNER RACE WEAR VOLUME = 0.00E+00 IN^3

10. RUNNING THE BBDPLOT PROGRAM

The software system consist of 3 modules: BBD, BABERDYN, and BBDPLOT.

- BBD is the user interface program used to create the input file read by the BABERDYN numerical analysis program.
- BABERDYN is the numerical analysis program which reads all inputs from an input file, and writes all outputs to one primary output file and a set of plot data files.
- BBDPLOT is a post-processing plot program used to produce x-y graphs of the simulation results written to the set of plot data files by BABERDYN while it is running.

Instructions for running the BBD and BABERDYN programs are given in another chapter. This chapter explains how to run the plotting program. The plotting program creates 11 frames of graphs, with 3 graphs in each frame. The data for each complete frame is read from one of the 11 sequentially numbered plot data files written by BABERDYN. The content of these 11 frames is listed in the table below. See the chapter on data file formats for additional information on the meanings of these quantities.

When BABERDYN executes, 11 plot data files of the results are created. These files will have the same base file name as your BABERDYN input file but will have sequentially numbered file extensions '.F01' through '.F11'.

When BABERDYN finishes execution it automatically starts the BBDPLOT program for you, and will pass it the name of your plot files. Alternatively, you can run the BBDPLOT program directly from the DOS command line by typing the following command:

BBDPLOT [PlotFileName] <Enter>.

If you don't provide the plot data file name on the command line, you will be prompted for it. The name you provide should be the same as your BABERDYN input file, but with no extension. Upon doing this, the program will proceed to display frame number 1, and your screen should look something like that shown in Figure 24.

Table 11. BBDPLOT Frames.

| DESCRIPTION | PLOT | PLOT FRAME NUMBER |
|---|--------------------------------|--------------------------|
| Cage Lateral Motion in Cage Fixed Coordinates | X, Y, Z | 1 |
| Cage Angular Motion in Cage Fixed Coordinates | Theta(X,Y,Z) | 2 |
| Ball Cage Radial Motion in Inertial Coordinates | PXX, PYY, PZZ | 3 |
| Cage Power Dissipation, Torque Noise, and Time Step Size | AVG, TNOISE, DELT | 4 |
| Cage Pocket Impact Force at Ball Number 1 | BFORCE(X,Y,Z) | 5 |
| Cage Pocket Impact Force at Ball 90° from Ball Number 1 | BFORCE90(X,Y,Z) | 6 |
| Pocket and Circumferential Cage Wear Volumes | PWEAR(1),PWEAR(90), and CRWEAR | 7 |
| Ball Number 1 Slip Position, Velocity and Acceleration | SLIP,SLIPDOT,SLIPDDOT | 8 |
| Net Cage Pocket Impact Force | TCBFORCE(X,Y,Z) | 9 |
| Net Impact Force For Entire Cage | FORCE(X,Y,Z) | 10 |
| Bearing Component Imperfection Torque Noise, Both Balls and Races | DELMIT,DELMOT,DELM | 11 |

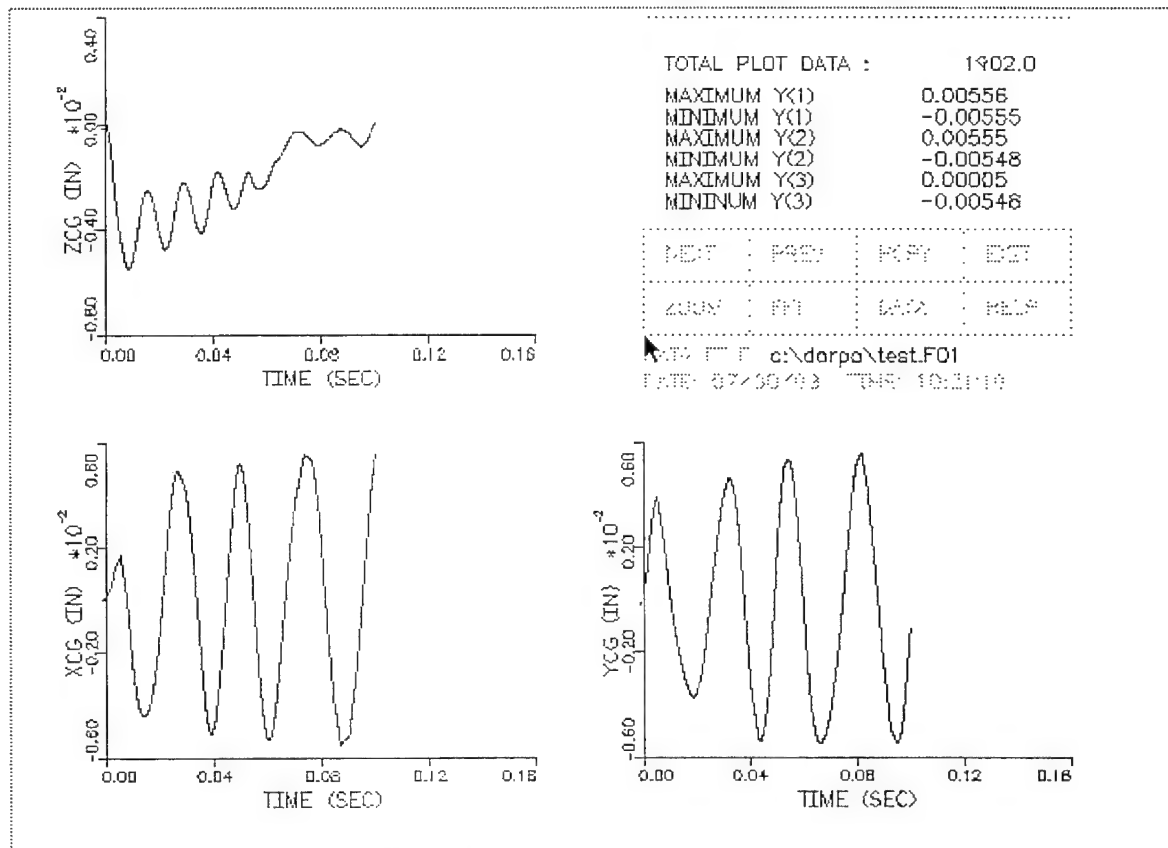


Figure 24. Sample BBDPLOT Frame.

10.1. FRAME SELECTION

Figure 24 shows the interactive menu used to control the actions of the plotting program. A mouse is required to select from the options shown. The program cannot be controlled from the keyboard. The options available for selection are as follows:

10.2. NEXT

Clicking on this option will advance the display to next sequentially numbered frame. Advancing from frame 11 wraps back around to frame number 1.

10.3. PREVIOUS

Clicking on this option will back up the display to previously numbered frame. Selecting Previous when frame 1 is displayed will bring up frame 11.

10.4. ZOOM

By default, all graphs show time history style plots for the entire simulation. The ZOOM option allows you to specify a subinterval of time, and the currently displayed frame will be redisplayed for the interval you specify. When you click on ZOOM a prompt will appear in the upper left corner of the screen asking you to enter new start and end times for the plot. Type these in, separated by a comma or a space, and press Enter.

If either the start or stop times lie outside the interval contained in the plot data files, a message to that effect is displayed. Just press Enter to clear the message. You should know that entering a value outside the range will effectively reset that value to its default. Thus, to reset the start and stop times, click on ZOOM and enter values like 0,99, then press Enter in response to the out of range error message(s).

Also, note that the start and stop times are always reset when you select either NEXT or PREVIOUS.

The ZOOM option also works with an FFT display. Instead of entering time values in seconds, enter frequency values in Hz.

10.5. FFT

By default, all graphs show time history style plots for the entire simulation. Clicking on FFT will cause the currently displayed frame to be redisplayed in the frequency domain (i.e., versus Hz). This is accomplished by performing a Fast Fourier Transform (FFT) on either a portion of the waveform or on the entire waveform padded with zeros as needed. The choice is made depending upon the number of total points and how close the number of points is to a whole power of 2. A boxcar window function is used (i.e., unwindowed). The FFT is computed ignoring the variable sample rate of the time history data in the data file. Thus, the indicated frequencies are, to a small extent, somewhat variable.

You can select the ZOOM option, and enter start and stop values for Hz to redisplay the FFT plot for a closer look at frequency ranges of interest.

When you select either NEXT or PREVIOUS the display is reset to time history format.

The program will not permit you to compute the FFT of an FFT (i.e., a cepstrum). When you already have an FFT plot showing on the screen, the FFT button is disabled.

10.6. HCPY

Clicking on this selection with your mouse will display an information box reminding you of how to obtain a hardcopy.

Hardcopies can only be obtained via sending screen dumps to your printer or by using a screen capture utility (not provided). For example, the above figure was inserted into this manual (a Word for Windows document) by using the PrintScreen key in combination with Microsoft Windows 3.1 to capture the graphics display to the Windows clipboard.

If you choose to send screen dumps directly to your printer, you must first make sure that your printer is properly prepared to print a graphics screen dump, as opposed to a regular text screen dump. This must be done prior to running BBDPLOT. The GRAPHICS utility that ships with DOS is used expressly for this purpose. See your DOS manual for complete details on how to use this utility. The following two examples show how to do this for an EPSON compatible dot matrix computer and HP Laserjet II compatible computer.

At your DOS prompt type either of the following commands:

| | |
|--|--------------------------|
| <code>GRAPHICS <ENTER></code> | ← for dot matrix |
| <code>GRAPHICS LASERJETII <ENTER></code> | ← for laserjet II |

Once you've done this and you are running the BBDPLOT program, just press the PrintScreen key to send the current graphics screen image to your printer. On some computers you may have to hold down the Shift key or Alternate key when you press the PrintScreen key. Execution of the program will be suspended until the screen dump is completed.

If you forget to run the proper GRAPHICS command prior to doing screen dumps, you will get unintelligible images (i.e., garbage) from your printer.

10.7. EXIT

Selecting this option with your mouse will display a Yes/No prompt asking if you are sure you want to exit the program. Simply press the Y or N keys to indicate your choice.

10.8. DATA

Selecting this option will display in a window the contents of the primary BABERDYN printed output file having the same base file name as the plot files being displayed. You can scroll up and down through the file using the UP-ARROW, DOWN-ARROW, PAGE-UP, and PAGE-DOWN keys. Press the ESCAPE key when you are through to delete the box from the display.

10.9. HELP

Selecting this option will display a brief description of each of the 11 frames. Scroll up and down through the list using the UP-ARROW, DOWN-ARROW, PAGE-UP, and PAGE-DOWN keys. Press the ESCAPE key when you are through to delete the box from the display.

11. THEORETICAL MODEL

This section presents the theoretical background and design concepts for BABERDYN. The user will find an overall view of the basic approach of BABERDYN, such as coordinate systems, governing equations, numerical methods, how the program is organized, assumptions, and approximations.

11.1. NOMENCLATURE

| | | |
|-----------------|---|---|
| B | = | total curvature factor = $f_o + f_i - 1$ |
| b_o, b_i | = | amplitude of anomaly on outer race and inner race, respectively (in) |
| C_b, C_c | = | damping coefficient of ball/pocket, and cage/land contact (lbf-sec/in) |
| $(CF)_q$ | = | centrifugal force on rolling element, lb. |
| c_o, c_i | = | number of lobes on outer race and inner race, respectively |
| d | = | ball diameter, in |
| E_B | = | modulus of elasticity for ball, N/cm ² (lbs/in ²) |
| $E(\epsilon_i)$ | = | the complete elliptic integrals of the first order having the modulus $\sin(\epsilon_i)$ |
| F_N | = | ball collision normal force, lb. |
| F_C | = | ball/cage collision force, lb. |
| F_t | = | ball collision tangential force, lb. |
| F_x, F_y, F_z | = | forces parallel to X, Y, and Z, lb. |
| f_o, f_i | = | ratio of transverse radius of ball race to ball diameter |
| K_o, K_i | = | outer and inner race/ball Hertzian deflection constants for ball bearings (lb/in ^{1.5}) |
| k_b | = | ball/race force coefficient |
| K_b, K_c | = | stiffness characteristic of ball/pocket, and cage/land contact |
| $K(\epsilon_i)$ | = | the complete elliptic integrals of the second order having the modulus $\sin(\epsilon_i)$ |
| L_i | = | land inner radius, in. |
| L_o | = | land outer radius, in. |
| M_y, M_x | = | moments about axes parallel to Y and X, lbf-in. |
| M_{Gq} | = | gyroscopic moment acting on ball, lbf-in. |

| | | |
|--------------------|---|---|
| m_B, J_B | = | mass, and mass moment of inertia of ball (slug, slug-in ²) |
| \bar{N} | = | ball collision normal unit vector |
| n | = | number of balls |
| P_h | = | Hertzian contact stress, Mega Pascals (lbs/in ²) |
| P_D | = | mounted diametral clearance in roller bearing, cm (in.) |
| P_o, P_i | = | normal contact force between outer race and ball, inner race and ball, respectively (lb) |
| P_{oq}, P_{iq} | = | dynamic rolling-element loads at outer and inner race contacts, lb. |
| q | = | rolling element position index |
| \bar{R} | = | offset vector of X_C, Y_C, Z_C from X Y Z |
| RB | = | $4(1 - \nu_{Ri}^2) / E_R + 4(1 - \nu_B^2) / E_B$ |
| \bar{R}_{Cb} | = | vector from ball center to contact point on ball expressed in pocket coordinate system |
| \bar{R}_{lp} | = | vector to contact point on cylinder (before deformation), origin of vector is X_p, Y_p, Z_p , expressed in pocket coordinate system |
| \bar{R}_i | = | position vector of i-th ball from X Y Z origin, expressed in X Y Z coordinates |
| \bar{R}_{ip} | = | position vector of i-th ball from X_p, Y_p, Z_p origin, expressed in local pocket X_p, Y_p, Z_p coordinate system |
| R_{LIM} | = | limiting distance before ball hits cage |
| r | = | radius of loci of ball-bearing inner-race curvature centers, in. |
| r_B | = | ball radius, in. |
| r_C | = | cylinder radius of ball pocket, in. |
| r_c^* | = | variable to represent race land contact(s) |
| r_p | = | pitch radius, in. |
| r_{IN} | = | cage inner radius, in. |
| r_o | = | radial distance from cage geometric center to center of ball when ball touches the cone and cylinder simultaneously, in. |
| r_{out} | = | cage outer radius, in. |
| r_p | = | pitch radius, fixed, from bearing to center of ball, in. |
| $\sin(\epsilon_i)$ | = | modules of elliptic integrals |

| | | |
|----------------------------------|---|---|
| \bar{T} | = | ball collision tangential unit vector |
| \bar{V}_L | = | relative velocity of race land, cm/sec (in./sec) |
| \bar{V}_c | = | relative velocity of cage/ball in pocket coordinate system, in/sec |
| X, Y, Z | = | rotating coordinate system, rotating about Z_I at nominal cage speed $\omega_{B/C}$ (Z parallel to Z_I) |
| X_I, Y_I, Z_I | = | inertial, fixed coordinate systems |
| $X_{race}, Y_{race}, Z_{race}$ | = | race fixed coordinate system, rotating about Z_I through λ angle i |
| \dot{X}_{ROLL} | = | ball/race tangential velocity component of roll, in/sec |
| X_C, Y_C, Z_C | = | cage fixed coordinate system |
| X_p, Y_p, Z_p | = | pocket coordinate system. Origin is far away from cage origin. |
| $\bar{x}, \bar{y}, \bar{z}$ | = | linear displacements parallel to X, Y, Z , in. |
| \dot{x}_o, \dot{x}_i | = | ball/race slip velocity at outside, inside races, in/sec |
| α | = | ball pocket cone angle, radians |
| α_q | = | angle between vector of ball's angular velocity about its own center and X -axis, radians |
| $\bar{\alpha}_x, \bar{\alpha}_y$ | = | angular displacements parallel to X and Y , radians |
| β | = | initial contact angle of ball bearing after mounting, radians |
| β_{oq}, β_{iq} | = | dynamic outer and inner race operating contact angles, radians |
| ϕ_o, ϕ_i | = | phase angle shift for outer and inner race anomaly, respectively (rad) |
| γ | = | $\frac{r_B}{r_p} \cos \beta$ |
| γ_i | = | angle rotated by inner race in time t (rad) |
| γ_o | = | angle rotated by outer race in time t (rad) |
| δ_{oq}, δ_{iq} | = | approach of rolling element to outer and inner races, in. |
| μ | = | friction coefficient |
| ψ_i | = | angular position of the i -th ball |
| $\theta_X, \theta_Y, \theta_Z$ | = | Small angles (X_C, Y_C, Z_C is obtained by rotating $X Y Z$ through these angles), radians |
| ν_R | = | Poisson's ratio for race |
| ν_B | = | Poisson's ratio for ball |

| | | |
|------------------------------|---|---|
| ω_B | = | rotation rate of ball, rad/sec |
| $\overline{\omega}_B$ | = | ball spin vector in pocket coordinates $[\overline{\omega}_B] = \omega_B$, rad/sec |
| $\omega_{B/C}$ | = | nominal cage orbital speed, rad/sec |
| ω_i | = | inner race rotational speed, rad/sec |
| ω_o | = | outer race rotational speed, rad/sec |
| ω_{Bq} | = | angular velocity of ball about own center, rad X sec ⁻¹ |
| $\omega_{Soq}, \omega_{Siq}$ | = | angular velocity of spin of ball with respect to outer or inner race, rad X sec ⁻¹ |
| $\omega_{Roq}, \omega_{Riq}$ | = | angular velocity of rolling of ball with respect to outer or inner race, rad X sec ⁻¹ |
| Ω | = | angular velocity of rotating race, rad X sec ⁻¹ |
| ω_{EQ} | = | orbital angular velocity of rolling element, rad X sec ⁻¹ |

Subscripts *o* and *i* refer to conditions at outer and inner race contacts, respectively. Subscript *q* refers to conditions at the *q*th rolling-element position. Other notations are defined in the text.

11.2. QUASI-STATIC BALL LOAD DEFLECTION ANALYSIS

A.B. Jones^[5] and T. Harris^[10] developed methods for computing the outer and inner race loading of each ball as it orbits between the races and the inner race-to-ball and outer race-to-ball contact angle variation with ball position under the influence of external axial, radial and moment loading. The authors have applied the Jones and Harris methods, but with some modifications, to determine the ball-to-race loads and contact angles for use in the subsequent analysis of ball and ball-cage dynamics. Those calculations are performed by the companion quasi-static program BASDREL. The results of the quasi-static analysis actually become part of the BABERDYN input. See the BASDREL manual for a detailed discussion of the quasi-static analysis of ball bearings.

11.3. BALL-CAGE DYNAMICS

The significant forces acting on the balls are:

- ❑ race normal loads due to preloading and external loads
- ❑ centrifugal loads
- ❑ gyroscopic moments
- ❑ cage collision normal loads
- ❑ surface drag forces due to cage pocket tangential forces and race traction forces

The cage collision forces require dynamic modeling and solution of the equations of motion of both the balls and cage. The surface drag forces, similarly, require dynamic solutions as the cage tangential forces and race traction forces are dependent upon the relative velocities between the ball and cage and the ball and raceway when skidding is occurring. Figure 25 illustrates the force diagram of a ball. The equations of motion for the balls are written in local ball pocket coordinate systems and the results are then applied to the cage coordinate system for solution. Ball motions in the *radial* direction are neglected to simplify the model, because these motions are high frequency, low amplitude motions and have no significant effect on ball-to-cage collision forces or cage motions.

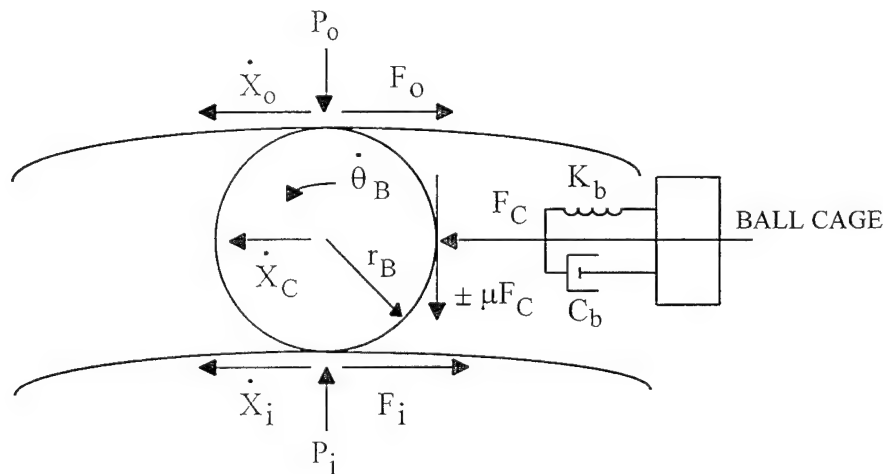


Figure 25. Ball-Bearing Slip Model (View Normal To Ball-Spin Axis).

11.3.1. Ball-To-Race Forces.

Figure 25 illustrates the force system operating on each ball. The raceway radial load on the ball is determined from the quasi static analysis as described in the Quasi-Static Loads Section above. Traction forces are developed at the ball-race interfaces because of slip between the balls and races. There has been a great deal of work to develop models of ball-to-race traction behavior. The various efforts^[13-17] have produced models, or test results, which are limited to a narrow operating range and to specific bearing design parameters. In addition, the

models are complex and require numerical integration over the contact area. The traction forces and moments acting on the balls could be determined by integrating the product of normal stress and traction coefficient over the Hertzian contact region, i.e.:

$$F_i = \iint k_i P_h dx dz$$

This numerical integration would significantly increase the computing time for analysis because of the number of traction contacts in a ball bearing. The author concluded that it is more efficient and accurate to evaluate ball slip forces empirically (see Refs.[9] and [18]).

The ball traction force is a function of ball/race normal load (P_o , P_i), slip velocity (\dot{x}_s) and traction coefficient (k_b), i.e.:

$$\frac{F_{i,o}}{P_{o,i}} = f(k_b, \dot{x}_s)$$

where $F_{i,o}$ is the X-axis component of the pocket collision force as shown in Figure 25.

The balls are assumed to be holonomically constrained to move within the confines of the raceway grooves as discussed by Walters[3]. The traction forces on the ball can be written:

$$F_o = k_b P_o \dot{x}_o / \dot{x}_{ROLL} \quad [1]$$

$$F_i = k_b P_i \dot{x}_i / \dot{x}_{ROLL} \quad [2]$$

Summing forces along the ball orbit path, we obtain:

$$\sum F_x: \pm F_c - F_o - F_i - m_B \ddot{x}_c = 0 \quad [3]$$

and summing moments about the ball center (neglecting out of plane gyroscopic effects), we obtain:

$$\sum M_o: \pm F_c - F_o r_B \mp F_c m r_B - J_B \ddot{\theta}_B = 0 \quad [4]$$

Further, from geometry, the relationship between inner race slip velocity (\dot{x}_i) and outer race slip velocity (\dot{x}_o) and the ball geometric center velocity (\dot{x}_c), we obtain:

$$\dot{x}_i + \dot{x}_o = 2\dot{x}_c \quad [5]$$

$$\dot{x}_o - \dot{x}_i = 2r_B \dot{\theta}_B \quad [6]$$

The slip forces can be evaluated by integrating Eqs. [1] and [2]. Eqs. [3], [4], [5] and [6] will then be used to solve for the ball/cage collision force and the ball shift due to slip and ball rotation, using the total incremental force vector as solved for in Equation [43] in the following section.

11.3.2. Ball and Ball-Cage Dynamics.

Referring to Figure 2 6, a ball bearing is shown with a set of inertial reference axes X_I, Y_I, Z_I and a second coordinate frame X, Y, Z with its Z -axis parallel to Z_I , and with a Z axis rotation rate about the bearing axis of symmetry. The X, Y, Z frame rotation rate is the rotation rate of the ball and cage system for low speed bearings, the cage and ball train nominal rotation rate is a function of bearing geometry and kinematics. The nominal ball-cage rotation rate is:

$$\omega_{B/C} = \frac{1}{2} [\omega_i(1 - \gamma) + \omega_o(1 + \gamma)] \quad [7]$$

where ω_i and ω_o are the inner and outer race rotation rates, respectively, and:

$$\gamma = \frac{r_B}{r_p} \cos \beta \quad [8]$$

where β is the bearing contact angle. At high speed, centrifugal loading of the balls against the outer race will alter the working contact angles at the inner and outer race contacts. Consequently, the true ball cage rotation rate will be different than that predicted by Eq. [7] by a fraction of a percent. The ball cage motions, velocities and accelerations computed in the cage-fixed coordinate system are correct within that rotating coordinate system. There will be a small error of less than 1% in frequencies when cage motions are transformed back into the inertial reference system (X_I, Y_I, Z_I), but this is an insignificant error for practical bearing design. The contact angle used in the calculation of nominal cage rotation rate is the average outer race contact angle. This is based on the implicit assumption of outer race dominance in cage rotation rate. Because of centrifugal forces on the balls, this assumption is a reasonable one as ball slip at the outer race is minimized by the much larger traction forces developed by the high ball-to-outer-race forces (P_o).

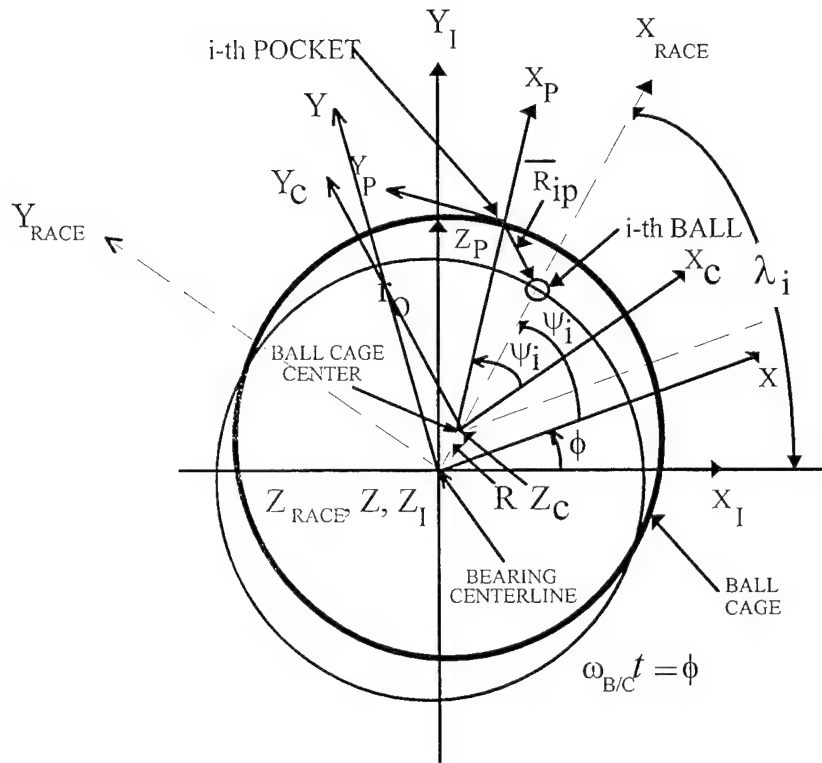


Figure 26. Relationships Of Coordinate Frame Systems.

Using the X, Y, Z ball-cage coordinate set, we can, through small angle transformations, define a cage-fixed coordinate frame. Let $\theta_z, \theta_y, \theta_x$ be sequential rotations about the Z , rotated Y , and rotated X axes, respectively. These rotations bring the new frame parallel to the cage symmetry axis and transverse axes (see Figure 26).

Using small angle approximations, the ball-cage to cage-fixed transformation is:

$$A = \begin{Bmatrix} 1 & \theta_z & -\theta_y \\ -\theta_z & 1 & \theta_x \\ \theta_y & -\theta_x & 1 \end{Bmatrix} \quad [9]$$

The cage center of mass (CM) (cage-fixed coordinate origin) may be offset from the X, Y, Z origin. This offset can be represented by the vector \bar{R} .

11.3.3. Collisions Between Balls and Cage.

Figure 27 illustrates a cross-section of a cylinder/cone pocket, ball-guided design and Figure 28 shows a race-guided cage. Collisions are determined by finding the position (ψ_i) of each of the n balls in its respective cage pocket and, by geometry, determining proximity of the ball pocket.

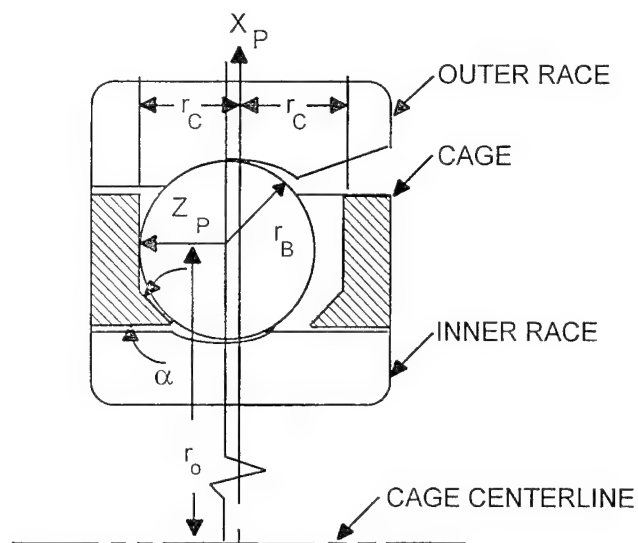


Figure 27. Ball-Guided Cage Pocket Cross Section.

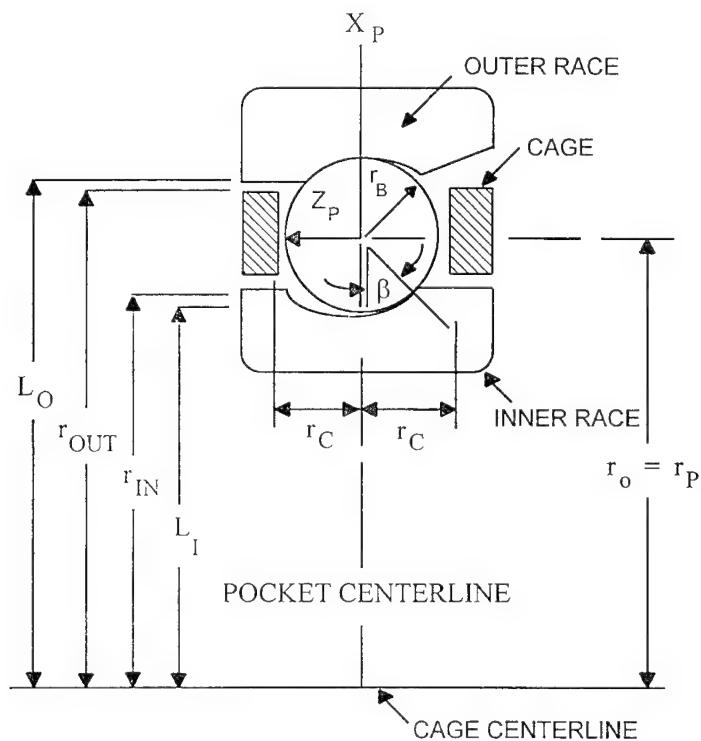


Figure 28. Race-Guided Cage Cross Section.

11.3.4. Ball Guided Designs.

We can define a local pocket coordinate frame X_p, Y_p, Z_p in the i th pocket. From Figure 27, r_0 is the radial distance to the ball center when the ball is simultaneously in contact with the cylindrical and conical portions of the ball guided cage pocket. Once we have determined the ball center position, a positive X_p -axis component will indicate possible cylinder contact, and a negative component will indicate possible cone contact.

The balls are initially fixed in the X, Y, Z frame, the position of the i th ball being:

$$\bar{R}_i = \begin{Bmatrix} r_p \cos \psi_i \\ r_p \sin \psi_i \\ 0 \end{Bmatrix} \quad [10]$$

where ψ_i denotes the angle between the X -axis and the i th ball center line. Translated into the local pocket coordinates, this becomes:

$$\bar{R}_{ip} = [B_i][A](\bar{R}_i - \bar{R}) - \begin{Bmatrix} r_0 \\ 0 \\ 0 \end{Bmatrix} \quad [11]$$

where

$$\bar{R}_{ip} = [B_i] \begin{Bmatrix} R_{ipx} \\ R_{ipy} \\ R_{ipz} \end{Bmatrix}$$

The matrix $[B_i]$ defines the position of the i th pocket in the cage as:

$$[B_i] = \begin{Bmatrix} \cos \psi_i & \sin \psi_i & 0 \\ -\sin \psi_i & \cos \psi_i & 0 \\ 0 & 0 & 1 \end{Bmatrix} \quad [12]$$

Again referring to Figure 27, if R_{ipx} is greater than or equal to zero, cylinder contact is possible. The limiting distance from the X_p -axis for a collision is:

$$R_{LIM} = r_C - r_B \quad [13]$$

$$\Delta R_{LIM} = \sqrt{R_{ipy}^2 + R_{ipz}^2} - R_{LIM} \quad [14]$$

If ΔR_{LIM} is positive, a collision is taking place.

For the computation of forces and moments due to the collision, the ball-to-cage relative velocity is needed in addition to R_{LIM} . The vector from the pocket origin to the contact point is:

$$\overline{R_{hp}} = \begin{Bmatrix} r_{ipx} \\ r_c \cos \theta_p \\ r_c \sin \theta_p \end{Bmatrix} \quad [15]$$

where

$$\theta_p = \tan^{-1} \left(\frac{R_{ipz}}{R_{ipy}} \right) \quad [16]$$

The radius vector from the ball center to the point of contact is:

$$\overline{R_{Ch}} = \begin{Bmatrix} 0 \\ r_B \cos \theta_p \\ r_B \sin \theta_p \end{Bmatrix} \quad [17]$$

and the ball spin vector in pocket coordinates is:

$$\overline{\omega_B} = \begin{Bmatrix} -\omega_{Bo} \sin \beta \\ 0 \\ \omega_{Bo} \cos \beta \end{Bmatrix} \quad [18]$$

where

$$\omega_B = \frac{r_p}{2r_B} (1 - \gamma^2) (\omega_o - \omega_i) \quad [19]$$

Letting ω_c^* be the cage rotation rate relative to the X, Y, Z coordinate frame (in cage-fixed coordinates) and defining R_c as the linear velocity of the cage geometric center in the X, Y, Z frame, we can show that the relative velocity vector between the cage and ball is (in pocket coordinates including ball slip position changes):

$$\bar{V}_c = [B_i] \dot{\bar{R}}_c + [B_i] \bar{\omega}_c^* \times \left(\bar{R}_{hp} + \begin{Bmatrix} r_o \\ 0 \\ 0 \end{Bmatrix} \right) - \bar{\omega}_B \times \bar{R}_{ch} + [B_i][A] \dot{\bar{R}}_i \quad [20]$$

The tangent and normal unit vectors at the point of contact can then be written:

$$\bar{N} = \begin{Bmatrix} 0 \\ \cos \theta_p \\ \sin \theta_p \end{Bmatrix} \quad [21]$$

$$\begin{aligned} \bar{T}' &= \bar{V}_c - (\bar{V}_c \cdot \bar{N}) \bar{N} \\ \bar{T} &= \frac{\bar{T}'}{|\bar{T}'|} \end{aligned} \quad [22]$$

The normal force component is:

$$F_N = K_b \Delta R_{LIM}^{1.5} - C_b (\bar{V}_c \cdot \bar{N}) \quad [23]$$

where K_c and C_c are stiff spring and damper constants, and the tangential force is:

$$F_T = -\mu F_N \quad [24]$$

where μ is the friction coefficient, and the total incremental force vector is:

$$\Delta \bar{F}_i = F_N \bar{N} + F_T \bar{T} \quad [25]$$

K_b can be computed using classical methods[19, 20] and C_b is estimated based on materials characteristics.

If these forces are transformed back into the cage-fixed frame, they may be added to the forces from other pockets as:

$$\bar{F} = \sum_i [B_i]^T \Delta \bar{F}_i + F_{gravity} + F_{bias} \quad [26]$$

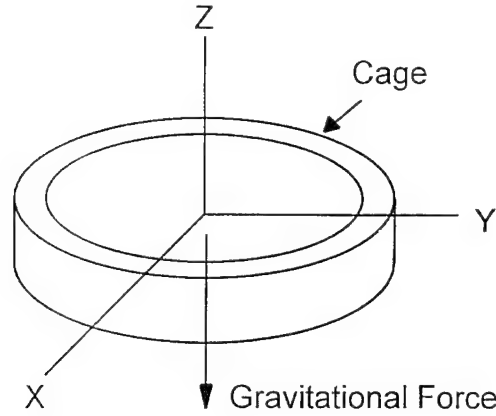


Figure 29. Depiction of Gravitational Force Acting on Cage.

The gravitational load is in the negative Z axis. The bias force is due to cage mass imbalance, or similar. It follows that the incremental moment is:

$$\Delta \bar{M}_i = \left(\bar{R}_{hp} + \begin{Bmatrix} r_o \\ 0 \\ 0 \end{Bmatrix} \right) \times \Delta \bar{F}_i \quad [27]$$

and the total moment on the cage is:

$$\bar{M} = \sum_i [B_i] \Delta \bar{M}_i + \frac{2\pi\nu R^2 UL}{C} + M_{bias} \quad [28]$$

The second term is a moment load produced on the cage by the shearing of the lubricant film between the cage and the guiding race land. This term is due to Pinkus where

ν = absolute (or dynamic) viscosity

R = cage radius

U = relative sliding velocity between cage and land

L = cage thickness

C = radial clearance between cage and land

M_{bias} = bias moment due to dynamic cage imbalance, or similar

If R_{ipx} is less than or equal to zero, cone contact is possible. Identical logic may be followed as in the previous section with the following changes in equations (α is the cone angle as shown in Figure 27):

$$R_{LIM} = r_c - r_b + R_{ipx} \cot \alpha$$

$$\Delta R_{LIM} = \left(\sqrt{R_{ipx}^2 + R_{ipz}^2} - R_{LIM} \right) \sin \alpha \quad [29]$$

$$\bar{R}_{hp} = \begin{Bmatrix} R_{ipx} - r_B \cos \alpha \\ (r_c + R_{ipx} \cot \alpha - r_B (1 - \sin \alpha)) \cos \theta_p \\ (r_c + R_{ipx} \cot \alpha - r_B (1 - \sin \alpha)) \sin \theta_p \end{Bmatrix} \quad [30]$$

$$\bar{N} = \begin{Bmatrix} -\cos \alpha \\ \sin \alpha \cos \theta_p \\ \sin \alpha \sin \theta_p \end{Bmatrix} \quad [31]$$

$$\bar{R}_{ch} = r_B \bar{N} \quad [32]$$

The sum of forces and moments are computed as before.

11.3.5. Race Guided Designs.

Race guided designs result in collisions between the ball and cylindrical portion of the ball pocket or between the cage and race lands (see Figure 28). The equations for ball/cylinder contact are the same as developed above for ball-guided designs. Referring to Figure 28, cage-inner race collision occurs if:

$$\Delta R_{LIM} = R_{ipx} - (r_{IN} - L_I) > 0$$

The inertial position vector to the cage contact point is

$$\bar{R}_1 = \bar{R} + \begin{Bmatrix} r_{IN} \\ 0 \\ r_c^* \end{Bmatrix}_p \quad [33]$$

where the subscript p indicates the coordinate system in which the vector is being measured.

The inertial vector to the inner race contact point is:

$$\bar{R}_2 = \begin{Bmatrix} L_I \\ 0 \\ r_c \end{Bmatrix}_{race} \quad [34]$$

The relative inertial position vector is:

$$\Delta \bar{R} = \bar{R}_1 - \bar{R}_2 = \bar{R} + \begin{Bmatrix} r_{IN} \\ 0 \\ r_c^* \end{Bmatrix}_p - \begin{Bmatrix} L_I \\ 0 \\ r_c \end{Bmatrix}_{race} \quad [35]$$

and by differentiating we obtain:

$$\bar{V}_c = ([B_i] \dot{\bar{R}}_c) + ([B_i] \omega_c^*) \times \begin{Bmatrix} L_I \\ 0 \\ r_c \end{Bmatrix} - [B_i][A] \left[\begin{Bmatrix} 0 \\ 0 \\ \omega_i - \omega_{B/C} \end{Bmatrix} \times \left([B_i]^T \begin{Bmatrix} L_I \\ 0 \\ r_c \end{Bmatrix} \right) \right] \quad [36]$$

The normal unit vector at the cage contact is:

$$\bar{N} = \begin{Bmatrix} 1 \\ 0 \\ 0 \end{Bmatrix} \quad [37]$$

$$\bar{T}' = \bar{V}_c - (\bar{V}_c \cdot \bar{N}) \bar{N} \quad [38]$$

and the tangential unit vector:

$$\bar{T} = \frac{\bar{T}'}{|\bar{T}'|} \quad [39]$$

The normal force component is:

$$F_n = K_c \Delta R_{LIM}^{1.5} - C_c (\bar{V}_c \cdot \bar{N}) \quad [40]$$

where

$$\Delta R_{LIM} = R_{ipx} - (r_{IN} - L_I) \quad [41]$$

The tangential force component is:

$$F_T = -\mu F_n \quad [42]$$

The total incremental force vector is:

$$\Delta \bar{F}_i = F_n \bar{N} + F_T \bar{T} \quad [43]$$

These forces may be added to the forces from ball-pocket contact collision, and then transformed back into the cage-fixed frame and added to other ball-pocket forces.

$$\bar{F} = \sum_i [B_i]^T \bar{F}_i \quad [44]$$

The incremental moment is:

$$\Delta M_i = \begin{Bmatrix} r_{in} \\ 0 \\ r_c^* \end{Bmatrix} \times \Delta \bar{F}_i \quad [45]$$

and the total moment on the cage is:

$$\bar{M} = \sum_i [B_i]^T \Delta \bar{M}_i + M_{viscous} + M_{bias} \quad [46]$$

Again referring to Figure 28, cage-outer race contact occurs if:

$$\Delta R_{LIM} = [R_{ipx} + (L_o - r_{out})] < 0 \quad [47]$$

The inertial position vector to the cage contact point is:

$$\bar{R}_1 = \bar{R} + \begin{Bmatrix} r_{out} \\ 0 \\ r_c^* \end{Bmatrix} \quad [48]$$

The relative inertial position vector is:

$$\Delta \bar{R} = \bar{R}_1 - \bar{R}_2$$

$$\Delta R = \bar{R} + \begin{Bmatrix} r_{out} \\ 0 \\ r_c^* \end{Bmatrix}_p - \begin{Bmatrix} L_o \\ 0 \\ r_c^* \end{Bmatrix}_{race} \quad [49]$$

and by differentiating we obtain:

$$\dot{\bar{V}}_c = [B_i] \dot{\bar{R}}_c + ([B_i] \dot{\bar{\omega}}_c^*) \times \begin{Bmatrix} r_{out} \\ 0 \\ r_c^* \end{Bmatrix} - [B_i][A] \left[\begin{Bmatrix} 0 \\ 0 \\ \omega_o - \omega_{b/c} \end{Bmatrix} \times \left([B_i]^T \begin{Bmatrix} L_o \\ 0 \\ r_c^* \end{Bmatrix} \right) \right] \quad [50]$$

and as before; the normal unit vector is:

$$\bar{N} = \begin{Bmatrix} 1 \\ 0 \\ 0 \end{Bmatrix} \quad [51]$$

$$\bar{T}' = \bar{V}_c - (\bar{V}_c \cdot \bar{N}) \bar{N} \quad [52]$$

and the tangential unit vector:

$$\bar{T} = \frac{\bar{T}'}{|\bar{T}'|} \quad [53]$$

The normal force component is:

$$F_n = K_c \Delta R_{LIM}^{1.5} - C_c (\bar{V}_c \cdot \bar{N}) \quad [54]$$

where

$$\Delta R_{LIM} = R_{ipx} + (L_o - r_{our})$$

The tangential force component is:

$$F_T = \mu F_n \quad [55]$$

The total incremental force vector is:

$$\Delta F_i = F_n \bar{N} + F_T \bar{T}$$

and as before:

$$\bar{F} = \sum_i [B_i]^T \Delta \bar{F}_i + F_{gravity} \quad [56]$$

and the incremental moment is:

$$\Delta \bar{M}_i = \begin{Bmatrix} r_{out} \\ 0 \\ r_c^* \end{Bmatrix} \times \Delta \bar{F}_i \quad [57]$$

These forces may be added to the forces from ball-pocket contact collision and then transformed back into the cage-fixed frame and added to other ball-pocket forces so that:

$$\bar{M} = \sum_i [B_i]^T \Delta \bar{M}_i + \frac{2\pi\nu R^2 UL}{C} + M_{bias} \quad [58]$$

Once the total forces and moment vectors are found, accelerations may be computed. Integration is done in the cage-fixed coordinate frame (X_c, Y_c, Z_c). The basic equation of motion for the cage center of mass is:

$$\bar{F} = m \frac{{}^i d^2 R}{dt^2} \quad [59]$$

where \bar{F} the net force on the cage, m is the mass, R is inertial position of the cage center of mass, and i implies differentiation with respect to the inertial frame. It is convenient to rewrite Equation [59] to perform the integration in the cage-fixed coordinate frame (X_c, Y_c, Z_c). The inertial velocity of the center of mass is:

$$\frac{{}^i d\bar{R}}{dt} \equiv \dot{\bar{R}} \quad [60]$$

Equation [59] can be written as:

$$\bar{F} = m \frac{{}^i d\dot{\bar{R}}}{dt} \quad [61]$$

The derivative in Eq. [61] can be performed in the cage-frame using the familiar rule for differentiating vectors in different coordinate frames:

$$\frac{{}^i d\dot{\bar{R}}}{dt} = \frac{{}^c d\dot{\bar{R}}}{dt} + \omega_c \times \dot{\bar{R}} \quad [62]$$

where c implies differentiation in the cage frame and ω_c is the inertial angular velocity of the cage coordinate frame. Substituting Eq. [61] into [60] yields:

$$\frac{{}^c d\dot{\bar{R}}}{dt} = \frac{\bar{F}}{m} - \bar{\omega}_c \times \dot{\bar{R}} \quad [63]$$

The term on the left is not a true "acceleration," but simply the time derivative of the inertial velocity vector with respect to the cage frame. Equation [62] now represents the basic translational equation of motion. The rotational dynamic equations of motion are now required to complete the full dynamic equations of the cage. The basic Euler equation for a rigid body reference to the center of mass is:

$$\bar{M} = \frac{{}^i d\bar{H}}{dt} \quad [64]$$

where \bar{M} is the net moment exerted on the cage, \bar{H} is the inertial angular momentum of the cage, and i again represents differentiation in the inertial frame. The inertial angular momentum expressed in the cage frame is given by:

$$\bar{H} = [I] \bar{\omega}_c \quad [65]$$

where $\bar{\omega}_c$ is the inertial angular velocity expressed in the cage frame and $[1]$ is the diagonal body-fixed inertial matrix. Again, using the rule for vector differentiation, Equation [64] can be written as:

$$\bar{M} = \frac{{}^i d\bar{H}}{dt} = \frac{{}^c d\bar{H}}{dt} + \bar{\omega}_c \times \bar{H}$$

therefore:

$$\bar{M} = [I] \frac{{}^c d\bar{\omega}_c}{dt} + \bar{\omega}_c \times \bar{H} \quad [66]$$

Rewriting Eq. [66] provides:

$$\frac{{}^c d\bar{\omega}_c}{dt} = [I]^{-1} (\bar{M} - \bar{\omega}_c \times \bar{H}) \quad [67]$$

Equations [63] and [67] now form a complete set of dynamic equations for the cage. The terms on the left side of Equations [62] and [66] represent, for numerical integration purposes, the incremental changes in the inertial vectors \bar{R} and $\bar{\omega}_c$ but expressed in the cage frame. From these incremental changes, the \bar{R} and $\bar{\omega}_c$ vectors can be determined.

The \bar{R} and $\bar{\omega}_c$ inertial vectors are then transformed into the cage frame and integrated to get \bar{R} and $\bar{\theta}$ where:

$$\bar{\theta} = \begin{Bmatrix} \theta_x \\ \theta_y \\ \theta_z \end{Bmatrix} \quad [68]$$

11.3.6 VISCOUS FORCES ON BALL CAGE

Oil lubrication produces viscous drag between the ball cage and the race lands. Similarly, each ball will produce a viscous torque with its surrounding ball pocket. Classical equations for viscous shear forces were used for partially modeling these effects. A moment load is produced on the ball cage by the shearing of the oil film between the cage and the guiding race land(s). This oil shear torque from Pinkus is:

$$\bar{M} = \frac{2\pi\nu R^2 \bar{V}L}{C}$$

where:

$$\nu = \text{Absolute viscosity of the bearing lubricant, N sec cm}^{-2} \text{ (lbf}\cdot\text{s}\cdot\text{in}^{-2}\text{)}$$

| | | |
|-----------|---|--|
| r_{out} | = | Cage outer radius (in) |
| ∇ | = | Sliding velocity vector ($V_{inner/outer \text{ ring}} - V_{cage}$) (in/s) |
| L | = | Width of the cage web (in) |
| C | = | Radial clearance between the cage and guiding land (in). |

When the cage collides with the guiding land, a normal collision reaction force is produced which is a function of the combined cage/race stiffness (K_{CR}) and the damping coefficient C_{CR} . A tangential friction force is also generated which is proportional to the normal collision force (N).

The total moment on the cage during race collision is:

$$\overline{M} = \frac{2\pi\nu R^2 \overline{\nabla} L}{C} + u \overline{N} R$$

where:

| | | |
|----------------|---|---|
| u | - | Coulomb friction coefficient at between the cage and land |
| \overline{N} | - | Normal unit vector acting at the cage/land interface (N) |

Bearing Element Imperfection Torque Noise Calculation

The bearing performance is very sensitive to the various physical dimensions and parameters, such as race out-of-roundness or ball size variation. A mathematical model to predict torque noise caused by bearing element imperfections has been proposed by Ragulskis et al and later refined by Mullin and Speece. During rotation of a bearing, the balls roll along the raceways of the inner and outer rings as shown in Figure 30. In actual bearings, the balls are either climbing over bumps or entering troughs while rolling along the raceway. If assuming that the total energy absorbed in the deformation of a ball and race is equal to the external work done in rotation:

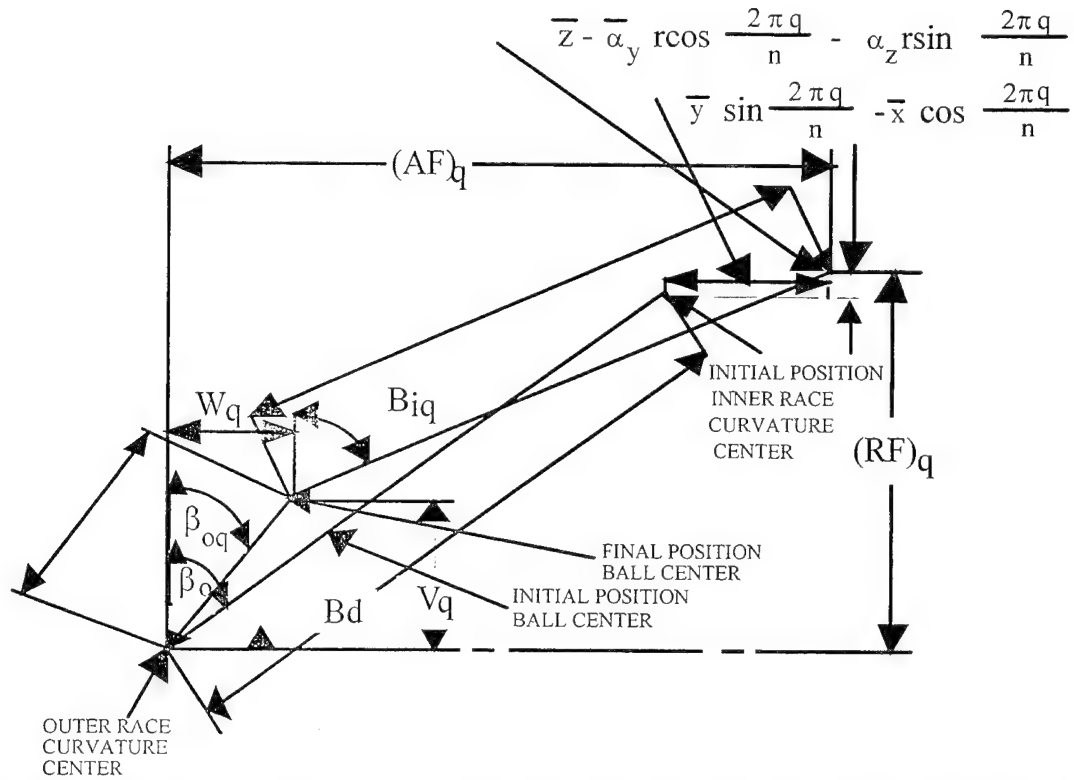


Figure 30. Positions of ball center and raceway groove curvature centers at angular position with and without applied load.

$$\Delta M \, d\gamma = P \, dy + \text{Incremental Spin Torque Work} \quad [69]$$

where:

- γ = Rotating angle (rad)
- y = Height of anomaly (in)
- P = Instantaneous ball load (lb)
- K_n = Hertzian stiffness, lb/in^{1.5}

Based on Mullin and Speece, the incremental spin torque work is small compared to that from the elastic deformation of ball and race and thus can be neglected. Eq. 69 becomes:

$$\Delta M = P \frac{dy}{d\gamma} = P \quad [70]$$

The instantaneous total torque is then obtained by summing over all balls:

$$\Delta M_{\text{Total}} = \sum_{j=1}^{N_{\text{ball}}} \Delta M_j$$

where ΔM_j is ΔM as defined in equation [70] for the j -th ball.

There are two cases to be considered:

Case 1: Outer race rotating and inner race stationary.

From Allan, the rolling distances between races and ball are:

$$(X_o)r = X_o / 2 = r_o \gamma_o / 2$$

$$(X_i)r = X_o r_i / (2 r_p) = r_o r_i \gamma_o / (2 r_p)$$

where

$$\gamma_o = 2\pi \omega_o t$$

Moment for each ball including preload effects:

$$\Delta M_{outer} = K_n [(\delta_o + b_o \sin (A1_o \gamma_o + \phi_o))]^{1.5*} \\ b_o A1_o \cos (A1_o \gamma_o + \phi_o)$$

$$\Delta M_{inner} = K_n [(\delta_o + b_i \sin (A1_i \gamma_o + \phi_i))]^{1.5*} \\ b_i A1_i \cos (A1_i \gamma_o + \phi_i)$$

Case2: Outer race stationary and inner race rotating.

$$(X_o)r = X_i r_o / (2 r_p) = r_o r_i \gamma_i / (2 r_p)$$

$$(X_i)r = X_i / 2 = r_i \gamma_i / 2$$

where

$$\gamma_i = 2\pi \omega_i t$$

Moment for each ball including preload effects:

$$\Delta M_{outer} = K_n [(\delta_o + b_o \sin (A2_o \gamma_i + \phi_o))]^{1.5*} \\ b_o A2_o \cos (A2_o \gamma_i + \phi_o)$$

$$\Delta M_{inner} = K_n [(\delta_o + b_i \sin (A2_i \gamma_i + \phi_i))]^{1.5*} \\ b_i A2_i \cos (A2_i \gamma_i + \phi_i)$$

Finally, the total torque for all balls at their instantaneous position is:

$$M_{total} = (\Delta M_{outer})_j + (\Delta M_{inner})_j$$

Collisions between the cage pockets and the balls were modeled simply as coulomb friction for this study.

From Reference 2, the total incremental force vector on the cage is:

$$\Delta \bar{F}_i = F_N \bar{N} + F_T \bar{T} \quad [71]$$

These forces may be added to the forces from ball-pocket contact collision, and then transformed back into the cage-fixed frame and added to other ball-pocket forces.

$$\bar{F} = \sum_i [B_i]^T \Delta \bar{F}_i \quad [72]$$

and the incremental moment is:

$$\Delta \bar{M}_i = \begin{Bmatrix} r_{IN} \\ 0 \\ \dot{r}_C \end{Bmatrix} \times \Delta \bar{F}_i \quad [73]$$

and the total moment on the cage is:

$$\bar{M} = \sum_i [B_i]^T \Delta \bar{M}_i \quad [74]$$

Once the total force and moment vectors are found, accelerations may be computed. Integration is done in the cage-fixed coordinate frame (X_C, Y_C, Z_C). The basic equation of motion for the cage center of mass is:

$$\bar{F} = m \frac{{}^i d^2 \bar{R}}{dt^2} \quad [75]$$

where \bar{F} is the net force on the cage, m is the mass, \bar{R} is the inertial position of the cage center of mass, and i implies differentiation with respect to the inertial frame. It is convenient to rewrite Eq. [75] to perform the integration in the cage-fixed coordinate frame (X_C, Y_C, Z_C). The inertial velocity of the center of mass is:

$$\frac{{}^i d \bar{R}}{dt} \triangleq \dot{\bar{R}} \quad [76]$$

Equation [76] can then be written as:

$$\bar{F} = m \frac{{}^i d \dot{\bar{R}}}{dt} \quad [77]$$

The derivation in Eq. [77] can be performed in the cage-frame using the familiar rule for differentiating vectors in different coordinate frames:

$$\frac{{}^i d\vec{R}}{dt} = \frac{{}^c d\vec{R}}{dt} + \vec{\omega}_c \times \vec{R} \quad [78]$$

where C implies differentiation in the cage frame and $\vec{\omega}_c$ is the inertial angular velocity of the cage coordinate frame. Substituting Eq. [78] into [79] yields:

$$\frac{{}^c d\vec{R}}{dt} = \frac{\vec{F}}{m} - \vec{\omega}_c \times \vec{R} \quad [79]$$

The term on the left is not a true "acceleration", but simply the time derivative of the inertial velocity vector with respect to the cage frame. Equation [79] now represents the basic translation equation of motion. The rotational dynamic equations of motion are now required to complete the full dynamic equations of the cage. The basic Euler equation for a rigid body reference to the center of mass is:

$$\vec{M} = \frac{{}^i d\vec{H}}{dt} \quad [80]$$

where \vec{M} is the net moment exerted in the cage, \vec{H} is the inertial angular momentum of the cage, and i again represents differentiation in the inertial frame.

The inertial angular momentum expressed in the cage frame is given by:

$$\vec{H} = [\mathbf{I}] \vec{\omega}_c \quad [81]$$

where $\vec{\omega}_c$ is the inertial angular velocity expressed in the cage frame and $[\mathbf{I}]$ is the diagonal body-fixed inertial matrix. Again, using the rule for vector differentiation, Eq. [77] can be written as:

$$\vec{M} = \frac{{}^i d\vec{H}}{dt} = \frac{{}^c d\vec{H}}{dt} + \vec{\omega}_c \times \vec{H}$$

therefore:

$$\vec{M} = [\mathbf{I}] \frac{{}^c d\vec{\omega}_c}{dt} + \vec{\omega}_c \times \vec{H} \quad [82]$$

Rewriting Eq. [82] provides:

$$\frac{{}^c d\vec{\omega}_c}{dt} = [\mathbf{I}]^{-1} (\vec{M} - \vec{\omega}_c \times \vec{H}) \quad [83]$$

Equations [79] and [83] now form a complete set of dynamic equations for the cage. The terms on the left side represent, for numerical integration purposes, the incremental changes in

the inertial vectors \bar{R} and $\bar{\omega}_C$ but expressed in the cage frame. From these incremental changes, the \bar{R} and $\bar{\omega}_C$ vectors can be determined.

The \bar{R} and $\bar{\omega}$ inertial vectors are then transformed into the cage frame and integrated to get \bar{R} and $\bar{\Theta}$ where:

$$\bar{\Theta} = \begin{Bmatrix} \Theta_x \\ \Theta_y \\ \Theta_z \end{Bmatrix} \quad [84]$$

12. UTILIZATION AND INTERPRETATION OF RESULTS

Prior to the development of this rigorous, dynamic analysis rolling element bearing computer program, most bearing dynamics problems were solved through a process of trial and error involving (1) modifying bearing test parts such as balls, or races, or the ball cage, (2) experimentally evaluating the performance results, and (3) making further modifications until the desired results were obtained. Obviously, this is a time consuming and costly process.

The computer program BABERDYN offers a more efficient and scientific technique for designing around ball bearing dynamics problems. By performing parametric, analytical studies, the effects of changing designs can be evaluated easily, rather than by the more costly, time consuming process of modifying hardware and testing for the effects. The BABERDYN computer program can be used to vary selected bearing design parameters individually and collectively, and then to evaluate the predicted effects on bearing performance or operational parameters.

The developers of this computer model have found, from experience in analyzing several bearing designs, that many of the design parameters in ball bearings are interdependent, and evaluating only one variable at a time may not lead to an optimum bearing design or design modification. Instead, the authors have found it more productive to evaluate more than one parameter simultaneously, and to then, through three-dimensional graphical analysis, determine optimization trends for guiding the design process.

Each bearing design application may present different types of undesirable performance or operational behavior that the designer would like to improve upon. Therefore, the first step in utilizing dynamic analysis tools such as BABERDYN is to;

1. Identify the undesirable operational characteristic or failure mechanism that requires correction, then
2. Select one or more design parameters that experience, or intuition, suggest might be influential in altering the undesirable bearing behavior and vary these parameters over an appropriate range, and
3. Evaluate the effects on the undesirable bearing behavior by plotting the predicted performance or operational changes as a function of the variables introduced.

Simultaneous evaluation of the effects on performance of design parameter variation can best be illustrated by an example. Recently, the lead author was asked to analytically determine ways for increasing the life of an experimental, high speed, solid lubricated ball bearing that was experiencing ball cage failures. The bearing utilized a ball cage made from a new graphite-polymide composite material. The failures entailed heavy loss of cage material in the ball pockets, followed by total failure and disintegration of the ball cage. The design parameters of this bearing are summarized in Table 12.

TABLE 12. BASELINE BEARING DESIGN PARAMETERS

| | |
|--------------------------|--|
| Bore | 30.00 mm (1.181 in) |
| Outside diameter | 46.99 mm (1.850 in) |
| Ball diameter | 5.56 mm (0.21875 in) |
| Number of balls | 15 |
| Pitch diameter | 38.48 mm (1.515 in) |
| Contact angle | 18 degrees |
| Inner race curvature | 0.54 ± 0.5 percent |
| Outer race curvature | 0.52 ± 0.5 percent |
| Outer race land diameter | 41.55 mm (1.636 in) |
| Materials: | |
| Races | AMS 6430 (M-50) steel |
| Balls | Silicon nitride or silicon carbide |
| Cage | Woven graphite fibers with polyimide resin and solid-lubricant pigment fillers (gallium/indium/tungsten diselenide or molybdenum disulfide) Density = 1.6 gm/cm ³ (0.056 lb/in ³) |
| Lubricant | Same as lubricant filler in separators |
| Cage outside diameter | 41.45 mm (1.632 in) |
| Cage inside diameter | 37.21 mm (1.465 in) |
| Loads: | |
| Axial | 200 N (45 pounds) |
| Radial | 0 |
| Moment | 0 |

A hypothesis was formulated that failures were due to a combination of:

- ☐ excessive wear of the ball pocket, or
- ☐ overstressing of the ball cage in the pocket which would disintegrate the cage pocket due to compressive structural failure or short term fatigue failure.

Based on these hypotheses, it was concluded that two of the performance characteristics evaluated by BABERDYN could be used to provide insight into which hypothesis was correct.

These were:

- ☐ Ball-to-pocket collision force magnitude
- ☐ Friction power dissipation in the ball pockets which would probably indicate excessive wear of the ball pocket.

In addition, it was hoped that the analysis would indicate what design changes might reduce the severity of the problem (or eliminate it). By selecting the design parameters that yielded reduced ball-to-pocket forces, or reduced friction power dissipation that might produce high wear, the design could be improved if one, or both, of the hypotheses were correct.

The cage-to-ball-pocket force prediction for ball pocket number 1 is shown in Figure 31.

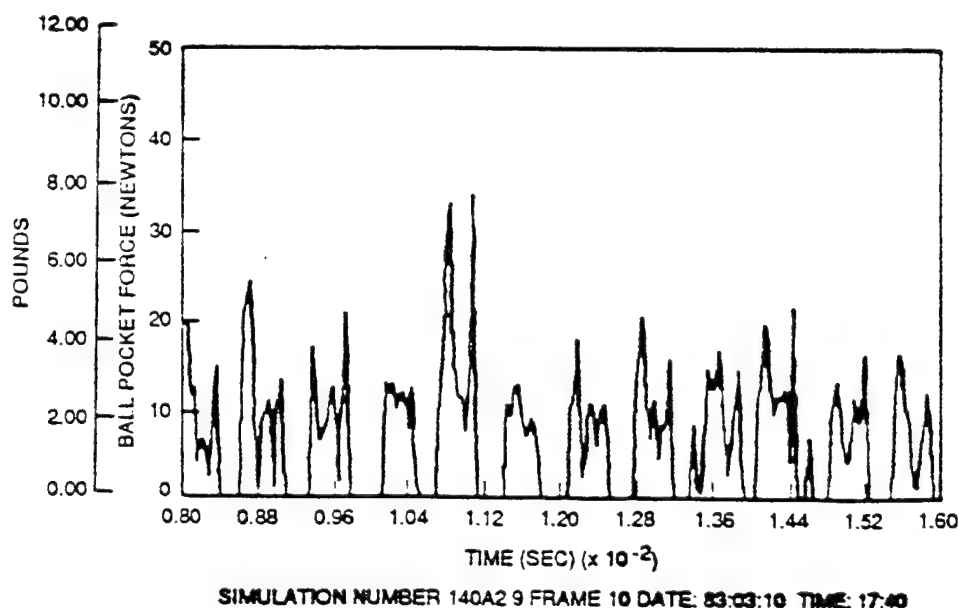


Figure 31. BABERDYN prediction of cage ball-pocket force versus time (pocket No. 1)

Experience has shown that ball pocket clearance and cage-to-race-land clearance have a significant influence on bearing dynamic characteristics. Therefore, these two parameters were selected for analytical exploration. Several dozen computer runs were then made simulating bearing behavior at 24,000 RPM. The goal was to determine if a more optimum choice of ball pocket and/or cage-land clearance might lead to improvement in the bearing cage dynamics and

increase the life of the ball cages that were failing prematurely. A matrix of various ball pocket clearances and cage land clearances was set up, and a number of analytical runs made. BABERDYN produced plots of ball pocket collision force and energy dissipation (which contributes directly to wear).

A number of similar plots were made of ball pocket force, and the peak pocket force from each plot was then plotted on a three-dimensional plot as a function of two variables: ball pocket clearance (B), and cage-to-land clearance (R). Figure 32 is a three-dimensional plot of the results.

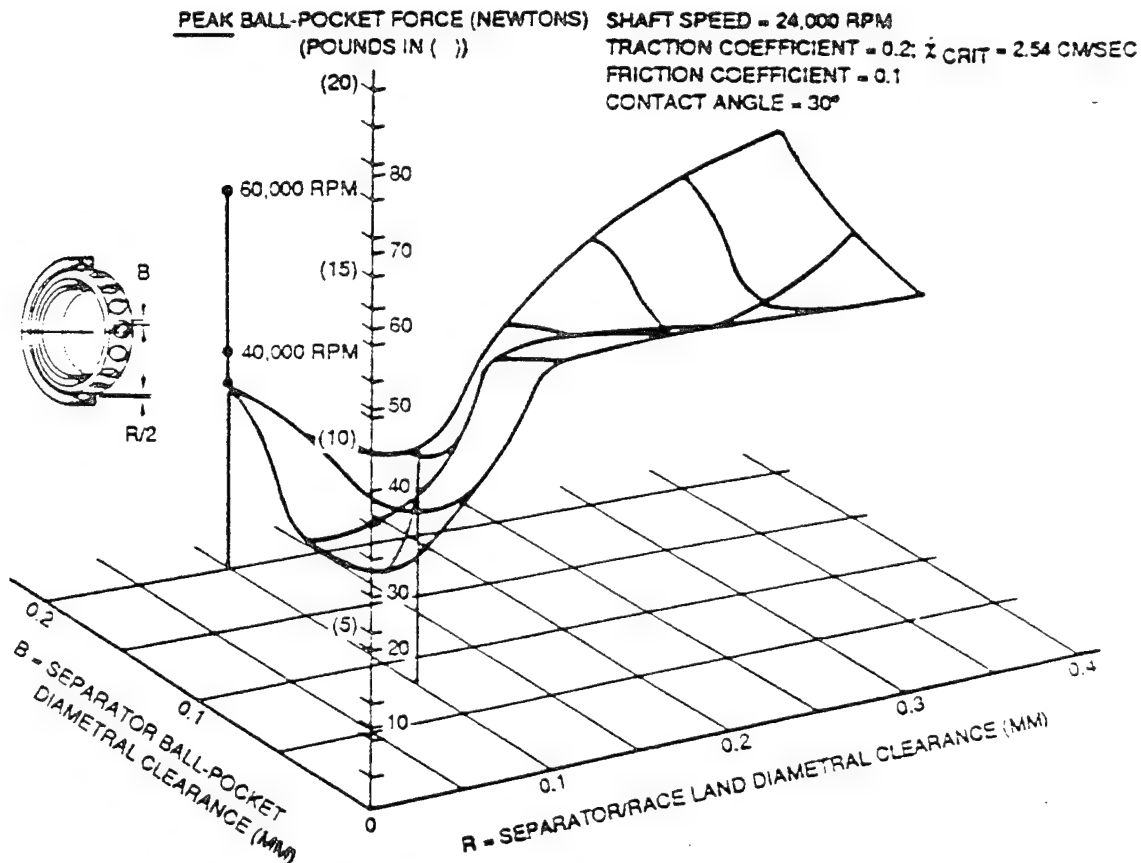


Figure 32. Optimization of ball cage for minimum ball-pocket FORCE.

Examination of Figure 32 shows that large land clearance (R) combined with large ball-pocket clearances (B) tend to produce large ball pocket forces. Small ball-pocket clearances (B) (in the range from 0.1 mm to 0.15 mm) combined with land clearances (R) of 0.1 mm or less appear to be the best design choice for minimum ball-pocket forces. It is also noteworthy that when an optimum race-land clearance (R) of about 0.1 mm is chosen, if non-optimum ball-pocket clearances (B) are used, the ball-pocket forces can still be larger than with the optimum combination of R and B.

Energy dissipation of the pocket-to-ball interface was analyzed similarly. The sum total pocket-to-ball energy dissipation prediction for all ball pockets is shown in Figure 33.

A number of similar plots were made of total ball pocket energy dissipation, and the results for each plot were then plotted in a three-dimensional plot as a function of two variables; ball pocket clearance (B), and cage-to-land clearance (R). Figure 34 is a three dimensional plot of the results.

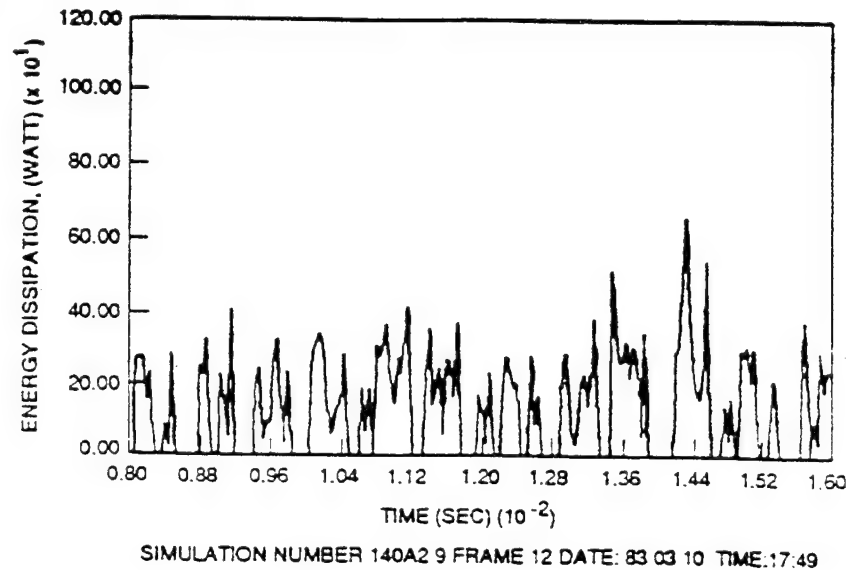


Figure 33. BABERDYN prediction of separator ball-pocket wear energy dissipation versus time.

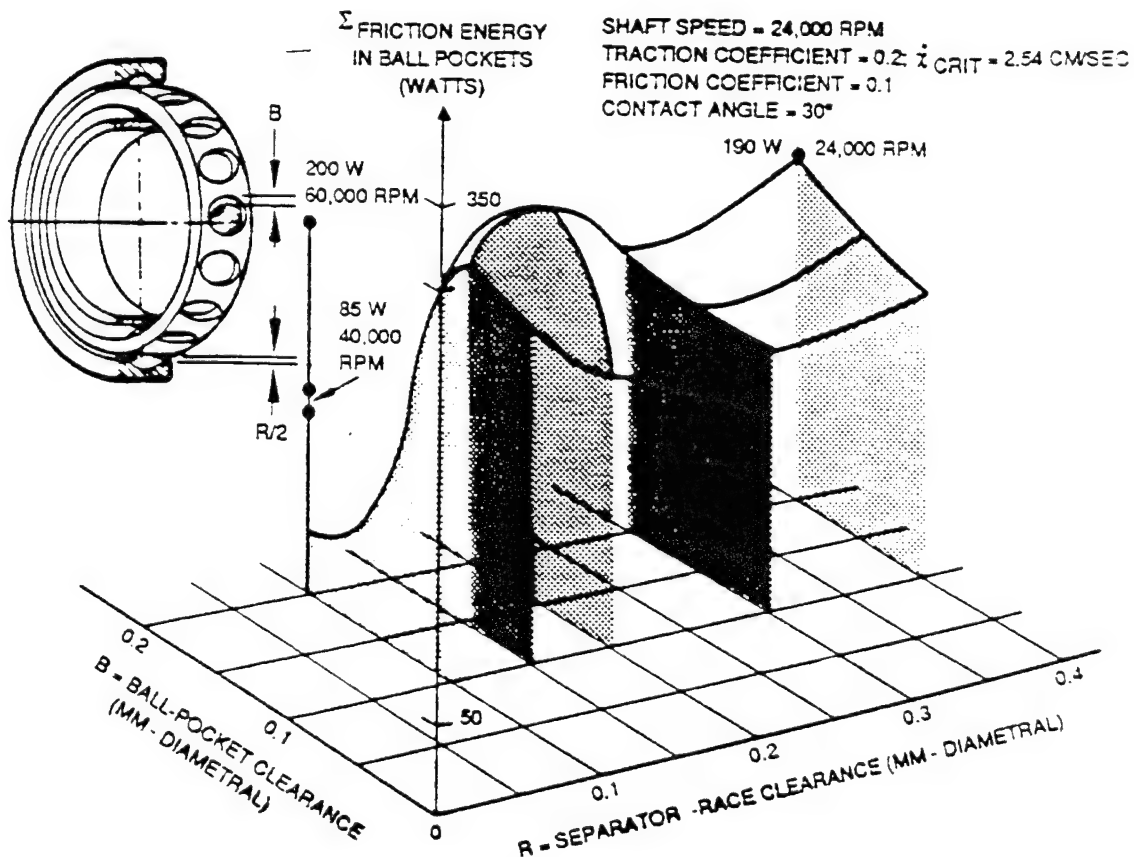


Figure 34. Optimization of ball cage for minimum ball-pocket WEAR.

Figure 34 illustrates that for this particular design, the worst choice for minimizing wear is to make the ball-pocket clearances (B) equal to the race land clearances (R) (i.e., the ratio of $B/R = 1.0$). Designs with large land clearances (R) and ball pocket clearances (B) are also relatively poor, although some reduction in wear energy is possible in certain selected combinations. The best designs have ball pocket clearances somewhat greater than the separator land clearances (i.e., $B/R > 1.0$).

These examples are included only for purpose of illustration. Each design presents a different set of undesirable performance characteristics and the bearing designer can select the most suspect variables and, similarly, explore design changes until trends are detected that drive the design performance in the desired direction.

13. REFERENCES

1. C.R. Meeks, "The Dynamics of Ball Separators in Ball Bearings-Part II: Results of Optimizations Study", ASLE Transactions, Vol 28, No. 3, July 1985.
2. C.R. Meeks, and Karen Ng, "The Dynamics of Ball Separators in Ball Bearings-Part I: Analysis", ASLE Transactions, Vol. 28, No. 3, July 1985.
3. C.R. Meeks, "Computer Simulation of Ball Bearing Dynamics and Correlation with Test Measurement on Ball Separator Motions", AFWAL-TR-86-2054, Air Force Wright Aeronautical Labs, WPAFB, October 1986.
4. C.R. Meeks, "Ball Bearing Dynamic Analysis Using Computer Methods and Correlation with Empirical Data", paper presented at the International Tribology Conference 1987, Melbourne, Australia, Dec. 2-4, 1987.
5. A.B. Jones, "A General Theory for Elastically Constrained Ball and Radial Roller Bearings Under Arbitrary Load and Speed Conditions", ASME Journal of Basic Engineering, pp 309-320, June 1960.
6. C.T. Walter, "The Dynamics of Ball Bearings", J. Lubr. Tech. 93, pp 1-10 1971.
7. P.K. Gupta, "Dynamics of Rolling-Element Bearings, Part III: Ball Bearing Analysis", J. Lubr. Tech. 101, July 1979.
8. J.W. Kannel and S.S. Bupara, "A Simplified Model of Cage Motion in Angular Contact Bearings Operating in the EHD Lubrication Regime", ASME Journal of Lubrication Technology, Vol. 100, 395, July 1978.
9. Dale Schulze, "An Evaluation of the Usefulness of Two Math Models for Predicting Performance of a 100 mm Bore Angular Contact High Speed Thrust Bearing", Tech. Report AFWAL-TR-80-2007, April 1980, WPAFB.
10. T.A. Harris, "Rolling Bearing Analysis", 1st ed., John Wiley & Sons, 1966, pp 203-241
11. R.W. Daniels, "An Introduction to Numerical Methods and Optimization Techniques", North-Holland, 1978, pp 71-112.
12. John R. Rice, "Numerical Methods, Software, and Analysis", 1st ed., McGraw-Hill, 1983, pp 217-264.
13. Arvid Palmgren, "Ball and Roller Bearing Engineering", 3rd ed., SKF Industries, Inc., 1959.

14. R.J. Roark and W.C. Young, "Formulas for Stress and Strain", 5th ed., McGraw-Hill Book Company, Inc., New York 1975.
15. P.K. Gupta, et al, "On the Traction Behavior of Several Lubricants", J. Lubr. Tech. 103/55, January 1981.
16. J.W. Kannel and Scott Barber, "A Technique in Evaluation of Thin Lubricants Under Combined Sliding and Rolling Contact", ASLE Preprint 82-LC-3D-1, 1982
17. F.W. Smith, "Lubricant Behavior in Concentrated Contact-Some Rheological Problems", ASLE Trans, Vol. 3, 1960, pp 18-25.
18. F.W. Smith, "The Effect of Temperature in Concentrated Contact Lubrication", ASLE Trans., Vol. 5, 1962, pp 142-146.
19. J.A. Jeffries, and K.L. Johnson, "Sliding Friction Between Lubricated Rollers", Proc. Instn. Mech. Engineers., London, Vol. 182, Part 1, 1967-68.
20. P.K. Gupta, "Traction Modeling of Military Lubricants", WRDC-TR-89-2064, Wright Patterson Air Force Base, Ohio. Final Report, August 1989.
21. P.K. Gupta, & N. Forster, " Modeling of Wear in Solid Lubricated Ball Bearings," ASLE Transactions, 30, 1, pp 55-62, 1987.

APPENDIX A - LUBRICANT PROPERTIES DATA BASE

This Appendix provides a database of lubricant properties compiled from a variety of published references (1-5), in addition to many oil manufacturing catalogues and brochures. The complete data base, shown in Table A-1, lists the name of the lubricant and its viscosity at two reference temperatures. This Appendix also contains instructions on running the program VISC, a utility provided for computing lubricant viscosity at bearing operating temperatures different from the reference temperatures. Lastly, this Appendix presents a method for performing a manual calculation to obtain the lubricant viscosity pressure coefficient from the viscosity at the operating temperature.

Table A-1. Lubricant Properties Data Base.

| LUBRICANT NAME | KINEMATIC VISCOSITY | | SPECIFIC GRAVITY |
|------------------------------|--------------------------------------|-------------------------------------|------------------|
| | MEDIUM TEMPERATURE 104° F (40° C) | HIGH TEMPERATURE 212° F (100° C) | |
| ANDERSOL L401D | 12.54 | 3.50 | |
| APIEZON C | 102.50 | 10.50 | |
| BARRIERTA 0 FLUID | 27.72 | 4.74 | |
| BARRIERTA 1 EL FLUID | 97.90 | 12.27 | |
| BARRIERTA 1 M1 | 197.29 | 21.90 | |
| BARRIERTA 19 FLUID | 392.41 | 38.42 | |
| BARRIERTA FOY 150 FLUID | 154.20 | 47.26 | |
| BRAYCO 880 | 11.88 | 3.07 | |
| BRAYCO 885 | 13.66 | 3.59 | |
| BRAYCO 899 | 24.86 | 4.95 | |
| BRAYCOTE 814Z | 18.11 | 6.04 | |
| BRAYCOTE 815Z | 43.37 | 9.75 | |
| CORAY 100 | 97.00 | 9.13 | |
| DOW CORNING 200 FLUID | 37.31 | 15.67 | |
| DOW CORNING 710 | 209.00 | 31.09 | |
| DOW CORNING 710 FLUID | 207.23 | 30.94 | |
| DOW CORNING FS-1265 | 161.65 | 28.46 | |
| DOW CORNING MOLYKOTE Q5-0161 | 71.17 | 20.65 | |
| ISOFLEX ALLTIME 28 | 24.31 | 5.08 | |
| KG-80 | 164.00 | 15.30 | 0.878 |
| KRYTOX 143AC | 226.18 | 3.90 | 1.908 |
| MOBIL SHE 61 | 28.61 | 5.50 | |
| MOBIL RL743A | 27.92 | 5.55 | |
| NPE UC4 | 17.42 | 3.98 | |
| NPE UC7 | 36.01 | 6.60 | |
| NPE UC9 | 50.95 | 8.40 | |
| NYE 185 C | 224.50 | 24.20 | |
| NYE 188B | 113.50 | 14.80 | |
| NYE JOJOBA OIL | 24.79 | 6.47 | |
| NYE SYNTHETIC OIL 132 | 16.52 | 3.82 | |
| NYE SYNTHETIC OIL 179A | 29.82 | 5.78 | |
| NYE SYNTHETIC OIL 182 | 67.53 | 10.66 | |
| NYE SYNTHETIC OIL 186 | 112.14 | 15.52 | |
| NYE SYNTHETIC OIL 500R | 48.69 | 8.65 | |
| P10 | 13.08 | 3.48 | |
| PDP | 12.11 | 3.30 | |
| SILICONE FLUID DC510 | 37.24 | 14.81 | |
| SRG-40 | 24.75 | 4.61 | |
| SRG-60 | 83.35 | 10.41 | 0.871 |
| SYNTHETIC OIL 176A | 386.10 | 38.93 | |
| SYNTHETIC OIL 176H | 460.00 | 38.60 | |
| TERRESSO V-78 | 131.29 | 14.19 | |
| VACKOTE 48784 | 92.00 | 10.00 | |
| WINDSOR LUBE 245X | 12.66 | 3.42 | |
| XRL-743A | 29.14 | 5.63 | |

A.1. Viscosity/Temperature Relationship

The procedure to calculate the kinematic viscosity associated with a stated temperature which is different than the reference temperatures reported in the table can be found in ASTM D341-7. For convenience, the applicable formulae to calculate the kinematic viscosity at any temperature are as follows:

$$\begin{aligned}\log(\log(Z)) &= A - B \log(T) \\ Z &= \nu + 0.7 + e^{(-1.47 - 1.84\nu - 0.51\nu^2)} \\ \nu &= (Z - 0.7) - e^{[-0.7487 - 3.295(Z - 0.7) + 0.6119(Z - 0.7)^2 - 0.3193(Z - 0.7)^3]}\end{aligned}$$

where

\log = logarithm to base 10
 ν = kinematic viscosity, centistokes (or mm^2/s)
 T = absolute temperature, K or R
 A = Voghel's law viscosity constant
 B = Voghel's law temperature constant

The procedure to use the above the equations is as follows:

- Insert the second equation into the first to solve for the constants A and B using the known viscosity/temperature points.
- Solve for Z at the desired temperature using the first equation.
- Compute the kinematic viscosity from the value for Z computed in step 2 using the third equation.

A.2. VISC Program

The program VISC was developed to assist users in calculating the fluid kinematic viscosity at operating temperatures different from the reference temperatures appearing in the table. To run VISC make sure the VISC.EXE program file resides in a directory in your DOS PATH. Then simply enter VISC at your DOS prompt and press ENTER. The program does not have any command line parameters. The program will ask whether to use Fahrenheit or Celsius for temperature, and will then ask for you to input the viscosity (always in centistokes) and temperature for two known reference points. After this point the program can be instructed to either compute and print the viscosity at distinct temperatures you input, or create a screen plot (VGA only) of viscosity versus temperature for a temperature range you input.

A.3. Viscosity-Pressure Coefficient

The viscosity-pressure coefficient is the slope of a graph showing the variation in the logarithm of viscosity with pressure. A common unit for viscosity-pressure coefficient is psi^{-1} . Using the values in the data base, the viscosity-pressure coefficient is calculated based on the method of Roelands. The procedure is outlined as follows:

- 1) Find the dynamic viscosity at the bearing operating temperature using the program VISC.
- 2) Compute Z as follows

$$Z = 7.81(H_{40} - H_{100})^{1.5} (0.885 - 0.864H_{40})$$

where

ν_T = absolute viscosity at temperature T at atmospheric pressure.

ν_O = absolute viscosity at operating temperature at atmospheric pressure.

$H_T = \log(\log(\nu_T) + 1.2)$

get ν_{40} and ν_{100} from the data base

- 3) Read off the viscosity-pressure coefficient from the appropriate curve in Figure A-1 taken from reference (6).

A.4. Appendix A - Additional References

- A1. "Instrument Bearing Working Group Lubricant Test Results," IBWG Meeting, Baltimore, 1993.
- A2. Booser, E.R., "CRC Handbook of Lubrication, Volumes I & II," CRC Press, Boca Raton, Florida, 1984.
- A3. McMurtrey, E.R., "Lubrication Handbook for the Space Industry", NASA TM-86556, Alabama, 1985.
- A4. Bhusan, B., "Handbook of Tribology," 1992.
- A5. Blau, P.J., "ASM Handbook of Friction, Lubrication, and Wear Technology," ASM International, 1992.
- A6. Roelands, C.J.A., "Correlational Aspects of the Viscosity-Temperature-Pressure Relationship of Lubricating Oils," Doctoral Thesis, Technische Hogeschool te Delft, Netherlands, 1966.

APPENDIX B - McFRIC BALL/RACE TRACTION ANALYSIS PROGRAM

This Appendix briefly discusses the McFric computer program which computes traction force components and torque in elastohydrodynamically lubricated contacts. In the context of the bearing analysis software described in this manual, the McFric program is useful for predicting ball/race traction curves for bearings for which no test data is available. The program considers the joint effect of 34 different input variables on the elastohydrodynamic and thermal conditions of a rolling/sliding/spinning contact. The McFric program considers the variation of lubricant properties due to temperature and pressure throughout the contact zone, and also plastic deformation due to surface asperities. The primary outputs of the program are data points which define the curve for traction force coefficient for a sliding ball.

The McFric program is available from the Materials Laboratory of the Air Force Wright Aeronautical Laboratories, Wright Patterson Air Force Base. The principle investigator for the effort was J. I. McCool of MRC Bearings-SKF Aerospace. The final report is entitled "Traction Model Development," and the report number is AFWAL-TR-87-4097. The work is unclassified, the program is approved for public release, and distribution is unlimited. To obtain a copy of the program and documentation, contact

Dr. K. J. Eisentraut
Materials Directorate
Wright Laboratory
Wright-Patterson AFB OH 45433-7750
Phone (513)255-4860